

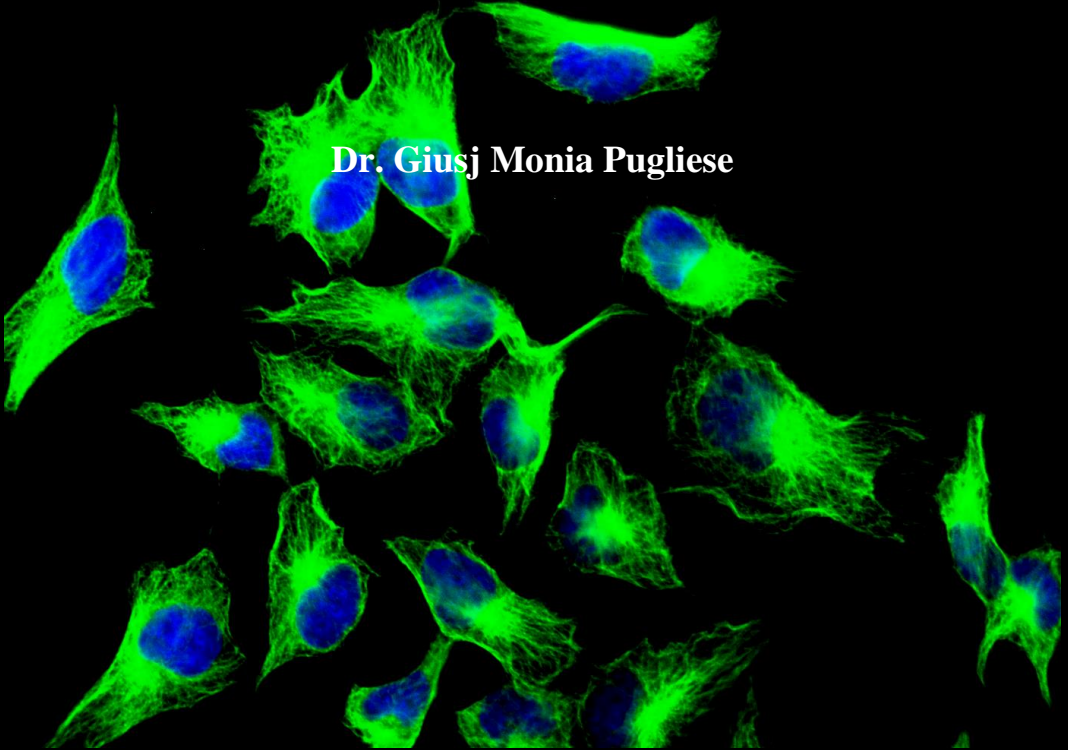


SAPIENZA
UNIVERSITÀ DI ROMA

**DIPARTIMENTO
DI MEDICINA SPERIMENTALE**

**Investigation of the CK2-mediated MUS81
phosphorylation and analysis of its
relevance for chemosensitivity in
BRCA2-deficient human cells**

Dr. Giusj Monia Pugliese



**Ph.D. program "HUMAN BIOLOGY AND MEDICAL GENETICS"
XXXI cycle**

“SAPIENZA” UNIVERSITY OF ROME
Department of Experimental Medicine

Ph.D. program
“HUMAN BIOLOGY AND MEDICAL GENETICS”
XXXI cycle

**Investigation of the CK2-mediated MUS81
phosphorylation and analysis of its relevance for
chemosensitivity in BRCA2-deficient human cells**

Candidate:
Giusj Monia Pugliese

Scientific tutor:

Dottor Pietro Pichierri

Istituto Superiore di Sanità

Director of Doctoral Program:

Prof. Antonio Pizzuti

“Sapienza” University of Rome

Board of examiners:

Prof. Filippo Rosselli

University of Paris-Sud, Paris XI

Prof. Daniela Barilà

University of Tor Vergata, Roma

Academic year 2017-2018

INDEX

<i>ABSTRACT</i>	6
<i>INTRODUCTION</i>	8
<i>1 DNA Replication</i>	8
1.1 Replication fork stalling	13
1.2 Replication fork restart	18
1.3 Repair mechanisms	22
1.3.1 Homologous recombination	27
2 <i>MUS81</i>	37
2.1 Structure and function	37
2.3 Controlling structure-selective endonucleases MUS81 complex	40
2.3.1 MUS81 contributes to DNA damage response	45
2.4 Cell cycle regulation	60
<i>MATERIALS AND METHODS</i>	67
In vitro kinase assay	67
Cell culture, generation of cell lines and RNA interference	67
Chemicals	69
Neutral Comet assay	70
Immunoprecipitation and Western blot analysis	71
PLA (Proximity-Ligation Assay)	72

Antibodies	73
Chromatin fractionation.....	74
Immunofluorescence	74
Cell cycle analysis by flow cytometry	76
Growth Curve.....	76
Chromosomal aberrations.....	77
Clonogenic assays	77
Phosphorylation site prediction	78
Production and purification of GST-fused fragments	78
Phospho-peptide antibody and Dot-blot.....	79
Endonuclease activity assay.....	80
Phosphopeptide enrichment	81
LC-ESI-CID/ETD-MS/MS	82
DNA fibre assay	84
Statistical analysis	85
<i>AIM OF THE WORK</i>.....	86
<i>RESULTS</i>	91
PART I	91
1. MUS81 is phosphorylated at Serine 87 by the protein kinase CK2 both in vitro and in vivo.....	91

2. CK2-mediated phosphorylation ofMUS81 at Serine 87 is an early mitotic event stimulated by mild replication stress and restrained in the MUS81/EME2 complex	100
3. Phosphorylation of MUS81 at Serine 87 by CK2 regulates binding to SLX4.....	109
4. Phosphorylation status of MUS81 at S87 controls unscheduled targeting of HJ-like intermediates in S-phase	116
5. Phosphorylation at Serine 87 induces premature mitotic entry through unscheduled MUS81 function in S-phase	126
6. Regulated phosphorylation of MUS81 at Serine 87 is essential to prevent accumulation of genome instability.	136
PART II	144
1.Regulation of the mitotic function of MUS81 by CK2 sustains viability in cells lacking BRCA2.....	144
2. DNA damage in BRCA2-depleted cells correlates with phosphorylation status of S87-MUS81 and influence cell cycle progression	147
3. The absence of BRCA2 leads to formation of mitotic chromosome bridges in constitutive active MUS81 mutant.....	156
4. Different DNA repair pathways sensitize S87MUS81 phosphorylation mutant in BRCA2 deficient cells.....	162
DISCUSSION	167
ACKNOWLEDGEMENTS	187
REFERENCES	189

ABSTRACT

The to be carefully regulated to avoid unscheduled targeting structure-specific endonuclease MUS81/EME1 plays important roles in the resolution of recombination intermediates, however, its function needs intermediates during DNA replication, which may result in genome instability. Little is known about the regulation of the human MUS81 complex. Hence, we undertook a proteomic analysis to identify regulatory phosphorylation events of MUS81. Our analysis identified several hits and among them we functionally characterized the residue targeted by the pleiotropic kinase CK2. Using biochemical and cell biological approaches, we demonstrated that accurate MUS81 phosphorylation on S87 by CK2 is not required to prevent DNA damage in S-phase but for resolution of branched DNA intermediates in mitosis, which is crucial to facilitate proper DNA segregation under replication stress but contributes modestly to chromosome integrity. However, constitutive S87 MUS81 phosphorylation triggers DNA damage and largely undermines genome integrity in normal cells. Next, using our S87-MUS81 phosphorylation mutant as a tool to

define which function of MUS81, the S-phase-related one or that performed in M-phase, was essential under pathological conditions. As a prototype of pathological condition, we used BRCA2-deficient cells that needs MUS81 to recover from replication stress. Using cell biology approaches to evaluate survival, DNA damage and resolution of mitotic interlinked intermediates, we show that the S87 MUS81 phosphorylation is involved to ensure viability of BRCA2-deficient cells mostly because it is the M-phase function of MUS81 to be essential.

Altogether, our data described a novel regulatory mechanism required to control MUS81 complex function in M-phase in human cells and involved in the viability of BRCA2-deficient cells. As CK2 inhibitors are under evaluation as anti-cancer drugs, our data may be useful to evaluate their use in tumors with signs of BRCAness.

INTRODUCTION

1 DNA Replication

Since the discovery of the DNA structure more than 50 years ago, the remarkable mechanisms that preserve the genetic information encoded by DNA and guarantee its faithful transmission across generations have been the subject of extensive investigation (Ciccia & Elledge, 2010). During every S phase, cells need to duplicate their genomes so that both daughter cells inherit complete copies of genetic information. DNA replication is regulated by recruiting the replication machinery or “replisome” to sites called origins on the chromosome. Replication must be strictly coordinated with the cell cycle to ensure faithful duplication of the genome. The replisome is a molecular machine that replicates the DNA bi-directionally from origins in a semiconservative fashion. The recruitment process is called initiation, whereas subsequent replication of the DNA by the replisome is called elongation. The replisome opens the DNA helix, stabilizes the ssDNA that is formed, and allows enzymes (polymerases) to copy the DNA (Sclafani & Holzen, 2007). The first step in replication initiation is the

assembly of pre-replicative complexes (pre-RCs) at replication origins, a process known as licensing. During licensing, the core replicative helicase component, the hexameric mini-chromosome maintenance 2-7 (MCM) complex, is loaded around double-stranded DNA as an inactive double hexamer (Fig.1). Loading MCM requires several other pre-RC factors: the six-subunit origin recognition complex (ORC; subunits Orc1-6), Cdc6 (cell division control protein 6) and Cdt1. At the G1/S transition, two kinases, CDK and Dbf4-dependent kinase (DDK) activate the MCM helicase, which involves the recruitment of Cdc45 and the heterotetrameric GINS complex to form the CMG complex. The conversion of pre-RCs into bidirectional replisomes requires a host of other factors, including Sld2 (RecQL4 in metazoans), Sld3 (Treslin/TICRR in metazoans), Sld7, Mcm10 and Dpb11 (TopBP1 in metazoans) (Hills & Diffley, 2014). Elongation factors are then recruited, many of them via interactions with the core homo-trimeric sliding clamp PCNA (Rowlands et al., 2017). At each fired origin, two sister replication forks (RFs) are established that move away from the origin as the parental DNA duplex is unwound by the action of DNA helicases. When one RF is terminally blocked

or arrested, firing of dormant or nearby origins ensures that replication is complete (Branzei & Foiani, 2010).

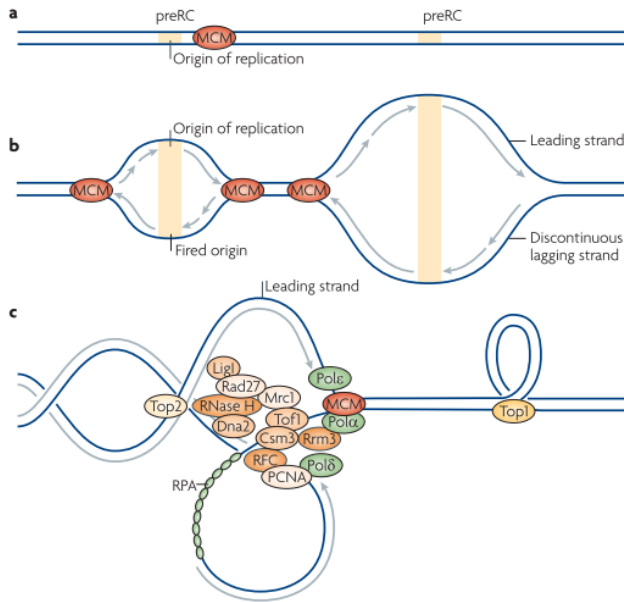


Figure 1 Replication initiation and progression. (a) Replication begins from multiple origins, which are marked by the formation of a pre-replicative complex (preRC). (b) Two replication forks (RFs), which are associated with the replisome that carries out DNA replication, are established at each fired origin. The minichromosome maintenance (MCM) helicase complex is shown ahead of the RFs, unwinding the duplex DNA. Replication is semi discontinuous: DNA synthesis is continuous on the leading strand and discontinuous on the lagging strand, on which primers are elongated to form Okazaki fragments that are processed and ligated to one another.

(c) Numerous proteins are present at the RF. The MCM helicase unwinds the parental duplex, allowing access to the DNA polymerase- α (Pol α) primase, replicative polymerase- δ (Pol δ) and polymerase- ϵ (Pol ϵ) (which elongate the primers) and the replication processivity clamp proliferating cell nuclear antigen (PCNA; also known as Pol30), which is loaded by the clamp loader, the replication factor C (RFC) complex. Replication protein A (RPA) binds single-stranded DNA regions exposed at the RF or during lagging-strand synthesis. The discontinuous fragments synthesized on the lagging strand are processed by Rad27 (FEN1 in humans), Dna2 helicase, RNase H, Pol δ and DNA ligase I (LigI). Several other factors associate with the RF in yeast and are represented: DNA topoisomerases 1 (Top1) and Top2, the checkpoint mediators mediator of replication checkpoint protein 1 (Mrc1), Top1-associated factor 1 (Tof1) and chromosome segregation in meiosis protein 3 (Csm3), and the Rrm3 helicase (Branzei and Foiani, 2010).

Although the bulk of DNA replication is completed during S-phase, it has been known for some time that certain regions of the genome can show a delay in completion of DNA replication. While this was generally assumed to be occurring during the G2 phase, recent data indicate that DNA synthesis can still occur after the cells have initiated the prophase of mitosis. This process, called MiDAS (for mitotic DNA synthesis), appears to be a form of homologous recombination-based DNA repair. MiDAS is more prevalent in aneuploid cancer cells (or

otherwise transformed cells), where it counteracts DNA replication stress that arises at ‘difficult-to-replicate’ loci (Özer & Hickson, 2018), of them the best characterized examples are the ribosomal DNA (rDNA), chromosome fragile sites and telomeres (Gadaleta & Noguchi, 2017). Particularly important are common fragile sites (CFS) because in response to RS, the FANCD2/FANCI protein complex forms “twin foci” (one on each sister chromatid) at CFS loci that can persist into mitosis and their mitotic DNA synthesis requires MUS81-EME1, SLX4, and a non-catalytic subunit of DNA polymerase δ , POLD3 (Pol32 in yeast) (Bhowmick et al., 2016a). The consequences of MiDAS failure and progression through mitosis with unreplicated DNA could be not only the formation of mitotic aberrations such as anaphase bridges, lagging chromatin and chromosome breaks/gaps, but also genomic instability in the next G1 cell cycle of daughter cells, which can acquire an incorrect chromosome number/structure (Özer & Hickson, 2018). Genomic instability refers to a higher rate of chromosomal aberrations, including simple gene mutations, as well as more extensive chromosomal structural and numerical changes (aneuploidy).

Mutations or epigenetic changes in DNA repair and cell cycle checkpoint genes are key drivers of genome instability, particularly in hereditary cancers. For sporadic cancers, an additional pathway for acquiring genomic instability is through the development of oncogene-induced DNA replication stress (Zhang et al., 2018). On this basis, the replication of the genome must be an exact process. Errors that result in under replication or over replication of the genome in any cell cycle have disastrous consequences and can produce a large array of human genetic diseases, including cancer, birth defects, and many developmental abnormalities. Molecular regulatory mechanisms have evolved to ensure that the genome is replicated once and only once and then segregated equally to the resultant daughter cells (Sclafani & Holzen, 2007).

1.1 Replication fork stalling

The replication fork progression is constantly faced with different endogenous or exogenous impediments all along the genome. Exogenous barriers include DNA damage produced by genotoxic components from the environment, radiation, therapeutic treatments and the diet. In contrast, endogenous obstacles come from inherent

DNA structures and composition, protein-DNA complexes, modification of the nucleotide pool, the production of oxidative species, transcription- replication machinery collisions, mutations in tumor suppressor genes and oncogenic protein expression (Branzei & Foiani, 2010). DNA damage can be produced also by chemical agents used in cancer chemotherapy like mitomycin C (MMC), cisplatin, psoralen and methyl-methane sulfonate (MMS), or other one such as the topoisomerase inhibitors camptothecin and etoposide, which induce the formation of single (SSBs) and double (DSBs)-strand breaks, respectively, by trapping covalently linked topoisomerase-DNA cleavage complexes. Other drugs, like hydroxyurea and aphidicolin, impair the progression of replication by depleting deoxyribonucleotide pools or inhibiting DNA polymerase (Mehta & Haber, 2014). These damaged or difficult-to-replicate DNA regions induce replication fork slowing or stalling, also known as “replicative stress”(Zeman & Cimprich, 2014). The stalling of replication forks opens up the risk of fork collapse and damage to DNA. To prevent such adverse effects, cells engage a variety of factors that stabilize the paused forks and aid the timely resumption of elongation (Rowlands

et al., 2017). Replicative stress is mediated by the uncoupling of helicases from DNA replicative polymerases, generating long stretches of single-stranded DNA (ssDNA) (Byun et al., 2005). This situation leads to S-phase checkpoint activation in order to organize replication fork restart (Bournique et al., 2018). The hallmark of DNA damage response (DDR) is the activation of checkpoints to temporarily delay cell cycle progression through inhibition of cyclin-dependent kinase activity, activate DNA repair system or induce cellular apoptosis/senescence. So eukaryotic cells evolved a plethora of enzymatic activities that chemically modify DNA to repair DNA damage including nucleases, helicases, polymerases, topoisomerases, recombinases, ligases, glycosylases, demethylases, kinases and phosphatases. The link between defects in the DDR and cancer pathogenesis has been established via multiple lines of evidence. These include: (i) genetic studies, where defects in tumour suppressor genes that control the DDR (e.g. BRCA1, BRCA2, PALB2, RAD51C, RAD51D, FANC-family genes, MLH1, etc. (Lord & Ashworth, 2012) predispose to familial forms of cancer; (ii) cytogenetic and genomic studies, where the number and type of different DNA mutations and

forms of genomic instability found in human tumours often betray the DNA repair defects that have moulded tumour genomes (Alexandrov et al., 2013); and (iii) functional studies, where experimental induction of specific DNA repair defects causes cancer in animal models (Kersten et al., 2017). The ability of DDR defects to result in disordered, mutated genomes might also be enhanced by commonly occurring defects in gatekeeper tumour suppressor genes such as p53, ATR, ATM, CHK1 and CHK2 (Jackson & Bartek, 2010). In budding yeast, sensing of DNA damage or stalled replication forks relies on the Rad24-dependent loading of the heterotrimeric Rad17-Mec3-Ddc1 (9-1-1 complex in fission yeast and humans) sliding clamp onto DNA. This leads to Mec1 kinase (ATR in humans) activation, followed by the downstream phosphorylation and activation of the primary signalling kinase Rad53. In higher eukaryotes, central component of the DDR is the phosphatidylinositol 3-kinase-like protein kinases (PIKKs) family ATM, ATR and DNA-PK and members of the poly(ADP)ribose polymerase (PARP) family (Ciccia & Elledge, 2010). ATR activation primarily leads to Chk1 kinase activation during the S-phase checkpoint, rather than Rad53 homolog Chk2.

Mec1-dependent activation of Rad53 requires the adaptor Mrc1 (Claspin in humans), which forms a complex to stabilize replication forks at sites of replication stress. Several other proteins function to promote Rad53 activation, including Rad9, Csm3, and Tof1 (Chaudhury & Koepp, 2016). ATM and DNA-PK respond mainly to DSBs, whereas ATR is activated by ssDNA and stalled replication forks. ATM (Ataxia telangiectasia mutated) is 350 kDa oligomeric protein and it exhibits significant homology to phosphoinositide 3-kinases (PIKK). In humans, mutations in ATM cause ataxia telangiectasia, a rare autosomal recessive disorder characterized by genome instability, immunodeficiency and predisposition to cancer (Abraham et al., 2001). These genes normally encode proteins whose function is to induce cell cycle arrest in response to DNA damage; the partial or complete inactivation of these gatekeeper tumour suppressors often allows cells to circumvent cell cycle checkpoints and to continue to proliferate even in the face of persistent DNA damage (Lord & Ashworth, 2012). Similarly, the inactivation of specific tumour suppressor proteins such as ATM, allows cells to proliferate in the face of replication fork stress, i.e. the stalling or slowing of replication forks.

This replication fork stress appears to be a feature of pre-neoplastic lesions and is associated with the activation of oncogenes such as Cyclin E (CCNE1) or Myc.

1.2 Replication fork restart

As mentioned above replication fork stress can also arise through a variety of additional causes, including an excess of naturally occurring secondary structures within the DNA double helix, therapy induced DNA lesions that stall replication forks, nucleotide depletion, collisions between the replication and transcription machinery, or an enhanced incorporation of ribonucleotides into DNA (Zeman & Cimprich, 2014).

Replication checkpoints are involved in modulating the replication fork response to intra-S damage by stabilizing the stalled fork and the association of the replisome with the fork through restraining the activity of recombination enzymes at stalled forks (Branzei & Foiani, 2005). In addition to protecting the stalled forks from collapsing, replication checkpoints are also thought to mediate the damage response that promotes replication resumption following fork

collapse. As a rule of thumb, mechanisms involved in replication fork recovery can be grouped in two: those depending on direct restart of the fork and those being recombination-dependent (Fig.2) (Franchitto & Pichierri, 2014).

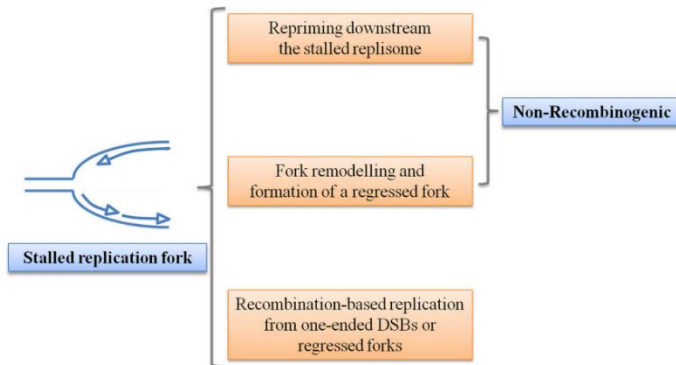


Figure 2 Pathways by which DNA replication can reinitiate after replication fork arrest. Upon stalling of a replication fork, DNA synthesis can be reinitiated through three different mechanisms (from top to bottom): replication can be restarted by repriming downstream of the site of stalling; alternatively, specialized enzymes, such as DNA translocases and helicases, are recruited to remodel the DNA at stalled forks to produce a regressed fork, which is used to protect ssDNA at the site of fork stalling and to restore a functional replication fork; finally, replication can be resumed using recombination from either collapsed forks, after production of one-ended DSBs, or from the regressed replication fork. Perturbation of replication at CFS most probably engages a non- recombinogenic pathway of fork restart (Franchitto & Pichierri, 2014).

The direct restart of the fork has been originally demonstrated in bacteria, and requires the PriA and PriC proteins (Heller & Marians, 2005, 2006).

Even if homologs of PriA and PriC have not been found in eukaryotes, indirect evidence of the presence of a similar mechanisms in higher eukaryotes does exist. Using *Xenopus* extracts, it has been demonstrated that Pol α primase, which is essential for initiation and elongation of DNA synthesis, can be recruited also at ssDNA regions formed after replication fork stalling (Van et al., 2010). Whether the Pol α primase can be recruited at ssDNA regions accumulating after fork arrest also in human cells, is not known, however, a recent paper demonstrated that loss of MCM10 leads to replication stress (Miotto et al., 2014). Interestingly, Pol α primase interacts with MCM10 during initiation and elongation (Zhu et al., 2007).

Recombination-based restart mechanisms are probably most relevant to collapsed forks where the replication machinery has been lost, thus facilitating Holliday junction formation. The recombination factor Rad51 (which catalyzes Holliday junctions) can be recruited to stalled forks (Petermann et al., 2010). Helicases that function in Holliday

junction resolution during recombination, including the RecQ helicase family members Bloom Syndrome protein BLM and the Werner Syndrome protein WRN have demonstrated roles in fork restart (Franchitto et al., 2008). This activity is conserved, as the related protein in budding yeast, Sgs1, is important for recombination-mediated fork restart. Replication fork restart is also linked to Fanconi Anemia (Moldovan & D'Andrea, 2013). Although members of this group are best known for their roles in interstrand crosslink repair, the FANCD1, FANCD2, and FANCD3 proteins have distinct roles in replication fork restart. In particular, FANCD2 is required to stabilize and recruit BLM to stalled forks (Chaudhury et al., 2013; Raghunandan et al., 2015). In addition to recombination factors, conserved scaffold proteins such as Slx4 and Rtt107 that interact with structure-specific nucleases or fork repair proteins are also important for fork restart (Chaudhury & Koepp, 2016; Ohouo et al., 2010). Finally, forks that cannot be recovered may be bypassed by the firing of nearby “back-up” origins, ensuring that chromosome duplication is completed (Jackson, & Blow, 2007; Woodward et al., 2006).

1.3 Repair mechanisms

Despite the complex response initiated by the cell to stabilize and restart a stalled fork, the fork may fail to restart and “collapse”, particularly if replication stress persists or replication stress response components are lost. The physical structure and protein composition of both stalled and collapsed replication forks is still under investigation (Zeman & Cimprich, 2014). To counteract DNA damage, repair mechanisms specific for many types of lesion have evolved. While DNA single strand breaks (SSBs) are repaired by mechanisms of nucleotide excision repair (NER) or base excision repair (BER), or mismatch repair (MMR), DNA double strand breaks (DSBs)s are repaired either by the mechanism of homologous recombination (HR), which utilizes the sister chromatid as a template for a correct replacement of the DNA sequence, or by the mechanism of non-homologous end joining (NHEJ), which is more prone to errors (Friedberg et al., 2006; Hoeijmakers, 2001).

The cellular choice of using HR or NHEJ is largely dependent on the phases of the cell cycle; NHEJ is present throughout the cell cycle, whereas HR predominates in the S and G2 phases, in order to ensure

the high-fidelity preservation of genetic information (Helleday, 2003). If the repairing process does not occur correctly, the DNA injuries result in mutations and chromosomal aberrations which alter the cellular behavior and lead to cancer. Genes that encode for enzymatic or scaffolding proteins involved in the “core” DDR activities are: XPA-XPG, RPA, ERCC1, DNA glycosylase, APE1, DNA polymerase $\beta/\delta/\epsilon$, XRCC1, DNA ligase 1/3, DNA ligase IV, Ku70/80, RAD50/MRE11/NBS1, BRCA1, BRCA2, and RAD51 (Fig. 3) (Davis & Chen, 2013; Fortini et al., 2003; Kowalski et al., 2009; Leng et al., 2012; Stracker and Petrini, 2014; Yang et al., 2013). Furthermore, ubiquitination, sumoylation, acetylation and methylation processes provide an additional layer of complexity targeting stability and efficiency of DDR proteins machinery (Huen & Chen, 2008; Polo & Jackson, 2011).

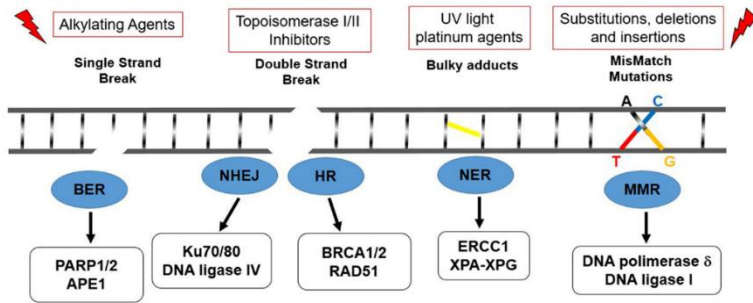


Figure 3 Diagram of targeted DDR pathways. In the lower part of the figure the DDR mechanisms and the related proteins involved are represented. In the upper part of the figure the targeting strategy for the corresponding defective DDR mechanisms are shown (Cerrato, Morra, & Celetti, 2016).

As mentioned above one important DNA repair mechanism to maintain genomic integrity is recombination. It is an important mechanism to repair nicks, gaps, breaks, or stalled forks to prevent chromosome fragility and protect cell health. Damage that results in DSBs can be repaired by various types of end-joining, by annealing of processed ends, or by recombination-based mechanisms using either a sister chromatid or homolog as the template (Jinxue He, Xi Kang, Yuxin Yin, K.S. Clifford Chao, 2016).

There are at least two hypotheses for how a stalled fork may be processed into a DSB. First, it may be an attempt by the cell to resolve

an otherwise irresolvable stalled fork structure using endonucleolytic cleavage and recombination-based restart pathways (Hanada et al., 2007; Petermann et al., 2010; Segurado & Diffley, 2008). This response could be initiated by the formation of vulnerable structures (a reversed fork, stalled fork, or ssDNA), or could be a symptom of the aberrant activation of nucleases in the absence of ATR. Second, persistent ssDNA alone, found at the stalled fork, in gaps left behind the fork, or in structures which arise from these gaps, may also be targeted by endonucleases or prone to passive breakage under prolonged stalling conditions (Lopes et al., 2001; Lopes, Foiani, & Sogo, 2006; Sogo, Lopes, & Foiani, 2002). As noted, recent evidence has also suggested that stalled replication forks can reverse, rewinding the parental DNA and extruding the newly replicated strands in a “chicken foot” structure (Fig. 4b,c) (Zeman & Cimprich, 2014).

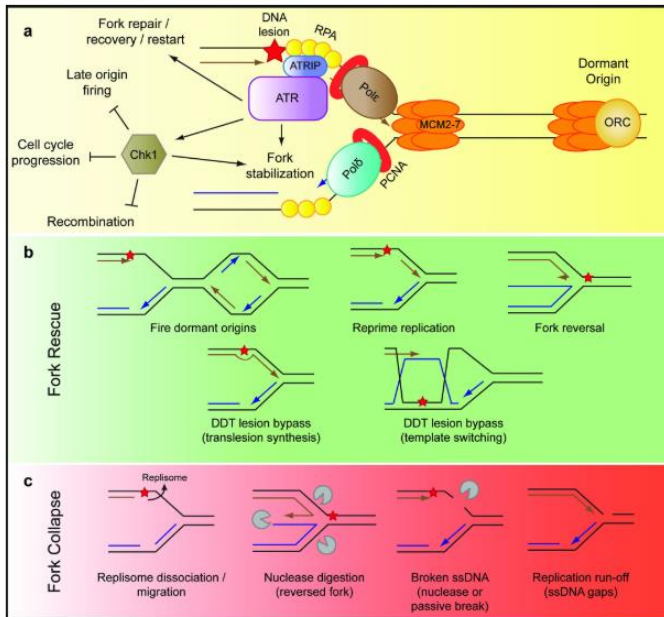


Figure 4 Mechanisms of stalled replication fork restart and collapse (a) The ATR-mediated replication stress response. ATR and its obligate binding partner ATRIP are activated by a primer-template junction at the stalled replication fork, where ATR initiates a signalling cascade primarily mediated by the effector kinase Chk1. This response promotes fork stabilization and restart, while preventing progression through the cell cycle until replication is completed.(b) Mechanisms for the restart / rescue of stalled forks. Replication forks stalled at DNA lesions (shown here on the leading strand, red star) and stabilized by the ATR pathway can restart replication by firing dormant origins, repriming replication, reversing the stalled fork or activating the DNA damage tolerance pathways. Key intermediates in these restart pathways are illustrated. (c) Mechanisms of fork collapse. If stalled forks are not stabilized, or

persist for extended periods of time, replication forks will collapse, preventing replication restart. The mechanism by which a replication fork collapses is still ambiguous, and several possibilities are presented here, including dissociation of replisome components, nuclease digestion of a reversed or stalled fork (middle panels) or replication run-off. (Zeman and Cimprich, 2014).

1.3.1 **Homologous recombination**

Among the DSB- repair pathways, HR- and single-strand annealing (SSA) require extensive resection, whereas non-homologous end-joining (NHEJ) and alternative end-joining/microhomology-mediated end joining (aEJ/MMEJ) require little or no resection (Fig. 5). Elaborate control of DSB end resection appears to be the critical point of DSB pathway choice, this regulation involves extensive chromatin remodelling, histone modifications, the Ku70–80 heterodimer, the checkpoint adaptor Rad9 (yeast) or its homologs 53BP1 (mammals), and RIF1. It appears that control of DSB end resection represents a key difference between DSB repair in yeast and mammalian cells, although the end resection machineries are largely conserved (Heyer et al., 2015). HR is a template-dependent process and in somatic cells there is a significant bias toward the sister chromatid, although there

is evidence for HR between homologs in the G1 phase of the cell cycle. Control of DSB end resection appears to be a critical component and only recently been established by genetic and biochemical approaches that have elucidated a two-step mechanism involving nucleases and helicases. A key conserved target for cell-cycle-dependent kinases in the end-resection machinery was identified as yeast *Sae2* and its mammalian homolog CtIP (Huertas & Jackson, 2009). *Sae2*/CtIP cooperate with the Mre11/Rad50/Xrs2 (mammalian MRE11/ RAD50/NBS1) complex to provide the initial resection of DSBs. It is unclear whether *Sae2*/ CtIP phosphorylation affects the MRE11-associated exo- and endonuclease activities, which differentially affect pathway choice in DSB repair (Cannavo and Cejka, 2014; Lengsfeld et al., 2007; Atsushi et al., 2014). In addition, yeast *Dna2*, a nuclease/helicase that cooperates with *Sgs1* and RPA in long-range resection, is recruited to DSBs in a CDK-phosphorylation-dependent manner (Chen et al., 2015).

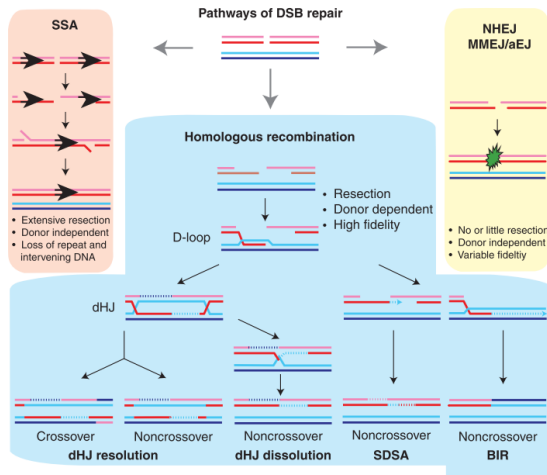


Figure 5 Homologous recombination (HR) and pathway choices. The pathways of double-strand break (DSB) repair include non homologous end joining (NHEJ), alternative end joining (aEJ, also called microhomology-mediated end joining), which are differentiated whether the joint involves no or few nucleotides (1–5 nt) or greater (5–25 nt) homology. Single-strand annealing (SSA) is possible when the DSB is flanked by direct repeat sequences and requires extensive resection. HR includes several sub pathways including break-induced replication (BIR), which leads to loss of heterozygosity, synthesis-dependent strand-annealing (SDSA), which leads to a noncrossover outcome, and the double Holliday junction pathway (dHJ), which through nucleolytic resolution of dHJs generates crossover and non crossover outcomes. Dissolution of dHJs, in contrast, leads exclusively to non crossover products (Heyer et al., 2015).

Three distinct nucleases (MRE11, EXO1, and DNA2), a RecQ helicase (Sgs1 in budding yeast and either BLM or WRN in humans and other mammals), and other several molecular factors are involved. First, this pathway includes the MRN complex.

The MRE11 subunit has 3'-5' exonuclease activity on single or double stranded DNA, and its homodimerization promotes binding to DNA and interaction with RAD50 (Williams et al., 2008). RAD50 stimulates MRE11 DNA binding and nuclease activity and facilitates DNA tethering for the MRN complex (MRE11, EXO1, and DNA2). NBS1 has no known enzymatic activities, but its recruitment to DSBs is essential for activation of ATM and initiation of DDR. NBS1 has a phosphopeptide binding FHA domain and structurally divergent tandem BRCT repeats linking the core MRN activities to proteins phosphorylated in response to DNA damage.

An important protein interacting with NBS1 through the FHA/BRCT domains is CtIP (Sae2 yeast homologous). CtIP plays an essential role in the activation of the MRN complex and the initiation of resection (Makharashvili et al., 2014; Eid et al. 2010). Since the MRN nuclease activity cannot generate the products observed after resection at DSBs,

it is thought that MRN plays a role only in the initial stages of the pathway. Indeed, MRN complex provides the MRE11 nuclease, which cooperates with CtIP to catalyze the first step in DSB processing, short oligonucleotides are removed from the 5' end. The short 3' ssDNA tails formed after MRN-CtIP cleavage are subject to extensive resection in a second step execute via two parallel pathways determining 3'-ssDNA overhang. Single-stranded DNA generated by resection of the ends of a DSB provides a substrate for assembly of the Rad51 filaments needed for strand invasion; Rad51, a DNA-dependent ATPase that forms nucleoprotein filaments with DNA, is a homolog of the bacterial RecA protein. Previous works observed that Single-stranded DNA within the RecA filament has a repeating unit of three nucleotides, which maintains a B-form structure. ATP hydrolysis promotes dissociation of the newly formed heteroduplex DNA and the displaced single strand. It is known that replication protein A (RPA) binds avidly to single-stranded DNA and effectively competes with Rad51, such that a number of proteins termed mediators are necessary to displace RPA to promote Rad51 binding, critical mediators are Rad52 in yeast and BRCA2 in mammalian cells, as Rad51 recruitment

to DSBs, and hence HR, are substantially impaired when these proteins are disrupted (Jasin & Rothstein, 2013).

The resolution of such HR intermediate is carried out by a group of proteins called dissolvases or resolvases, which restore structural and molecular integrity of the DNA sequence, as described earlier on. Since inaccurate recombination or junction resolution may trigger chromosome aberrations, cells often repair DSBs by an alternative “recombination” pathway called single-strand annealing (SSA). This process is based on the RAD52 single-strand annealing activity for re-sealing of the broken DNA-ends and does not require the RAD51 strand-exchange activity.

After replication fork stalling, RAD52 is recruited at perturbed forks to limit accessibility of fork remodeling factors, avoiding excessive fork reversal and inability of RAD51 to subsequently stabilize them. Later, RAD52 may also contribute to stabilization of RAD51 filaments assembled at the reversed replication forks (Malacaria et al., submitted).

In mitotic cell cycles, HR repair template usually comes from the homologous sequence on the sister chromatid. Moreover, molecular

intermediates of the recombination reaction, referred to as joint molecules (JMs), will form between the sister chromatids and link chromosomes, sometimes covalently (Holliday junctions), that can interfere with chromosome segregation. Hence, efficient JM disengagement and completion of HR are critical to prevent chromosome missegregation and thereby aneuploidy (Pfander & Matos, 2017). JMs that have matured to contain single or double Holliday junctions (HJs or dHJs, respectively) must be eliminated prior to mitosis to allow the equal distribution of DNA to the daughter cells (West et al., 2016; Wild & Matos, 2016). These activities can be subdivided into dissolution and resolution mechanisms. Dissolution involves the combined action of a helicase and a topoisomerase, both of which are located in a single protein complex called BTR (BLM-TOPOIII alpha- RMI1-RMI2) in human cells and STR (Sgs1-Top3-Rmi1) in budding yeast. Mechanistically, dissolution works by first converting dHJs to hemicatenanes by the actions of the BLM/Sgs1 helicase and the type IA topoisomerase TOPOIII alpha/Top3, followed by cleaving and resealing these hemicatenane structures by the activity of TOPOIII alpha/Top3 (Cejka, 2010; Chen et al., 2014;

Hickson, 2014). Due to the mechanism employed, STR and BTR are unable to ‘dissolve’ single HJs.

The second principal mechanism of dHJ removal is resolution, which can operate on different JM structures, among them single HJs, and is catalyzed by structure-selective endonucleases, that cut HJs to produce crossover (CO) and non-crossover (NCO) products: MUS81-EME1 (Boddy et al., 2001), SLX4-SLX1 (Wyatt, Sarbajna, Matos, & West, 2013) (Andersen et al., 2009; Fekairi et al., 2010; Wyatt et al., 2013) and GEN1 (Ip et al., 2008) in human cells and Mus81-Mms4 (Schwartz et al., 2012) and Yen1 (Ip et al., 2008) in budding yeast. All three nucleases belong to different protein families and are thought to resolve HJs by distinct – but sometimes cooperating – mechanisms (Pfander & Matos, 2017a).

HJs processing can lead to the incidence of reciprocal genetic exchanges (cross-overs). Hence, if the template used for repair is the homologous chromosome, instead of the sister chromatid, loss of heterozygosity (LOH) can ensue. To suppress crossovers (COs), and the potential for LOH, proliferating cells dissolve most dHJs using the STR/ BTR pathway, which leads to formation of non-crossover

(NCO) recombinants, exclusively (Chen et al., 2001; Symington, 2014).

However, although the resolvases might have been originally considered as backup pathways for BTR, accumulating evidence demonstrating reduced survival of resolvase defective cells indicates that all three pathways are necessary for genome maintenance.

Instead they should be thought of as essential factors that temporally regulated throughout the cell cycle most likely relates to the need to promote NCOs, rather than COs that could lead to a loss of heterozygosity and the ensuing dangerous elimination of tumor-suppressor functions (Fig.6) (West et al., 2016).

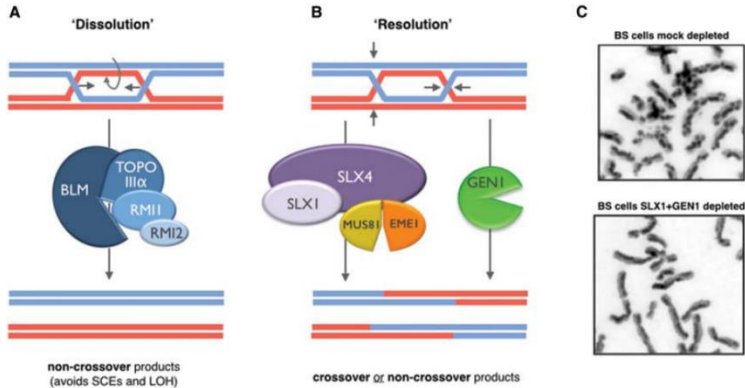


Figure 6 Mechanisms for the processing of recombination intermediates in mitotic human cells. The two mechanisms involve (A) “dissolution” or (B) “resolution.” Dissolution is driven by the convergent migration of two Holliday junctions and topoisomerase- mediated dissolution of the resultant hemicatenane. The reaction involves BLM helicase, Topoisomerase III α , RMI1, and RMI2. Dissolution generates non-crossover products, thereby avoiding sister chromatid exchanges (SCEs) and the possibility for loss of heterozygosity (LOH) when recombination occurs between homologous chromosomes. Nucleolytic resolution is driven by two distinct pathways involving the SLX1-SLX4-MUS81-EME1 complex or GEN1 protein. Both generate crossovers and non-crossovers. (C, top panel) A high frequency of SCEs is observed in cells derived from individuals with Bloom’s syndrome (BS). (Lower panel) The elevated SCE frequency observed in BS cells is largely dependent on the resolution pathways, as observed by depletion of SLX1 and GEN1 (West et al., 2016).

2 MUS81

2.1 Structure and function

The fission yeast and human MMS and UV-sensitive protein 81 (MUS81)–essential meiotic endonuclease 1 (EME1) endonucleases (Boddy et al., 2001), is widely conserved amongst eukaryotes, including *S. cerevisiae* (Interthal & Heyer, 2000), *S. pombe* (Boddy et al., 2000), *Arabidopsis thaliana* (Hartung et al., 2006), mice, and human (Chen et al., 2001), but is absent in eubacteria. It is related to the XPF family of structure-specific endonucleases. XPF family members typically contain a pair of helix-hairpin-helix (HhH) motifs, and a conserved catalytic domain in their C-terminal region with an ERKX₃D active site motif (Fig. 7). In MUS81 the HhH motifs are positioned at either end of the protein, whereas in XPF they occur tandemly at the C-terminal end. The HhH motifs probably promote dimer formation and DNA binding, and are required for nuclease activity. They may also play a role in substrate recognition by engaging the DNA duplexes on either side of a nick or 3'-flap (Newman et al., 2005). Eukaryotic XPFs function as heterodimers with a non-catalytic partner protein (ERCC1 in humans, Rad10 in

budding yeast, and Swi10 in fission yeast) that is important for their stability and nuclease activity, and may also play a part in substrate recognition. Likewise Mus81 has a partner (Eme1 in fission yeast and humans, and Mms4 in budding yeast) that is essential for its endonuclease activity (Abraham et al., 2003; Boddy et al., 2001; Kaliraman et al., 2001; Sancar, 2003). By analogy to XPF-ERCC1 it has been assumed that Mus81-Eme1/Mms4 functions as a heterodimer. However, the individual subunits can self-associate and higher molecular weight complexes have been seen by gel filtration (Blais et al., 2004; Fricke et al., 2005).

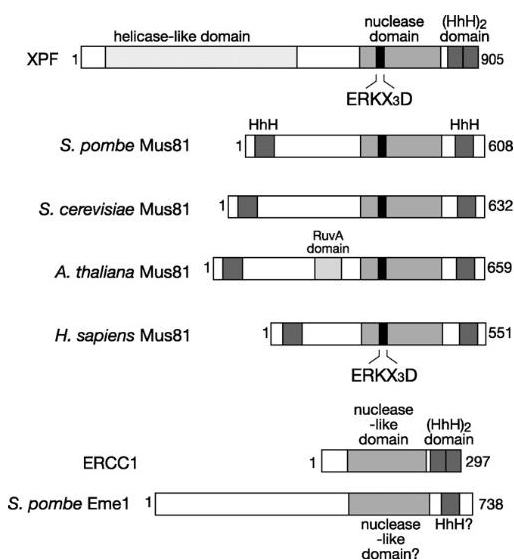


Figure7 The domain structure of Mus81 and Eme1, and their relationship to XPF and ERCC1 (Osman and Whitby 2007).

The *in vitro* substrate specificity of MUS81 complex

Despite their relatedness, biochemical and genetic evidence indicates that MUS81/EME1 and eukaryotic XPF proteins play distinct roles in DNA metabolism (Bastin-Shanower et al, 2003; Boddy et al., 2000). The enzymes have different substrate specificity, and double mutant analysis indicates that they function in separate pathways. Furthermore, whereas XPF exhibits some sequence-dependence for cleavage, the same is not true for MUS8/EME1. The main role of XPF in eukaryotic cells is in nucleotide excision repair where it makes the incision 5' to the DNA lesion. In contrast, several lines of evidence suggest that in mitotic cells MUS81 processes replication and recombination-associated DNA structures that form when RFs stall or collapse (Whitby et al., 2003). *In vitro* MUS81/EME1 has been shown to cleave a number of synthetic DNA structures that are designed to mimic potential *in vivo* substrates.

From such studies, the view has emerged that the preferred substrates for MUS81/EME1 are three- and four- way junctions that, in contrast to eukaryotic XPF's preferred substrates, have an exposed 5'-DNA end, at or close to the junction point, that activates and directs

cleavage (Bastin-Shanower et al., 2003; Fricke et al., 2005; Whitby et al., 2003). Examples of these preferred substrates are nicked HJs, D-loops, RFs with the lagging strand at the junction point, and 3'-flaps (Fig. 8).

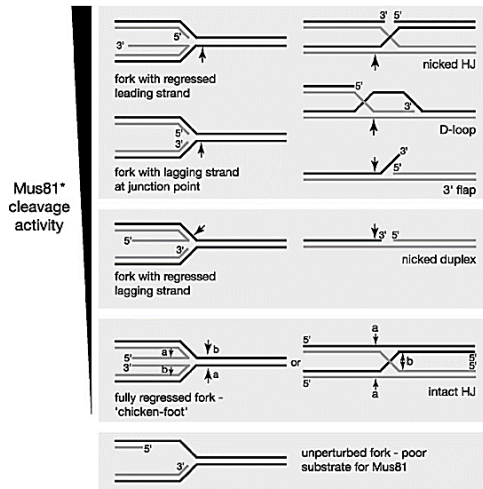


Figure 8 The substrate specificity of Mus81/Eme1. The arrows indicate Mus81 cleavage sites (Osman & Whitby, 2007).

2.3 Controlling structure-selective endonucleases MUS81 complex

In *S. cerevisiae*, a complex of Mus81 and the EME1 orthologue methyl methanesulfonate sensitivity protein 4 (Mms4) is upregulated in mitosis through phosphorylation of Mms4 by the yeast orthologues

of mammalian cyclin-dependent kinase 1 (CDK1) and Polo-like kinase 1 (PLK1), Cdc28 and Cdc5, respectively (Gallo-Fernández et al., 2012; Matos et al., 2011; Szakal & Branzei, 2013) (Fig.9a). In *Schizosaccharomyces pombe*, upregulation of Mus81– Eme1 is instead triggered by DNA damage through a mechanism in which Cdc28-dependent phosphorylation of Eme1 primes the protein for additional phosphorylation by Rad3 (ataxia telangiectasia and Rad3-related protein (ATR) in metazoans) (Dehé et al., 2013) (Fig. 9b). This different mode of regulation may reflect the fact that *S. pombe* lacks a GEN1 nuclease and relies mainly on Mus81– Eme1 for the processing of Holliday junctions (Copsey et al., 2013; Wehrkamp-Richter et al., 2012). In human cells, MUS81–EME1 activity peaks in M phase, and this correlates with the hyper phosphorylation of EME1 by CDK1 and PLK1 and an increased association with the scaffold protein SLX4, which has been shown to stimulate MUS81–EME1 in vitro and coordinates the resolution of Holliday junctions by MUS81–EME1 and SLX1 (Castor et al., 2013; Wyatt et al., 2013) (Fig.9c). Optimal processing of Holliday junctions in meiosis and mitosis is carried out by the MUS81–EME1 and GEN1 resolvases (Blanco & Matos, 2015;

Matos & West, 2014). Upregulation of GEN1 in human cells and its orthologue crossover junction endodeoxyribonuclease 1 (Yen1) in *S. cerevisiae* occurs later in mitosis, at a time that is considered the last point at which Holliday junctions can be resolved before chromosome segregation. Phosphorylation controls both the catalytic activity of Yen1 and its localization, by inactivating its nuclear localization signal and thereby retaining the protein in the cytoplasm. In human cells, control of GEN1 is independent of phosphorylation and instead relies entirely on a nuclear export signal that prevents GEN1 from accessing chromosomes until nuclear envelope breakdown occurs in mitosis (Chan et al., 2014) (Fig.9c).

Of note, Yen1 has an additional function in *S. cerevisiae* — in the response to replication stress — that is distinct from its canonical Holliday junction resolvase activity, although this is still regulated by the cell cycle (Ölmezer et al., 2016). The timely upregulation of Holliday junction resolvases in late G2 and M phase ensures optimal processing of Holliday junctions before chromosome segregation. A current view is that it also provides time for double Holliday junctions to be removed by the combined action of the RecQ-like helicase

Bloom syndrome protein (BLM) in humans (Kowalczykowski, 2015). BLM promotes the partial disassembly of the replisome (Shimura et al., 2008), which may be a prerequisite for MUS81 to process replication intermediates. BLM can also directly associate with MUS81 and enhance its endonucleolytic activity (Ran et al., 2005), thereby potentially contributing directly to the formation of MUS81-mediated DSBs at perturbed replication forks. Another RecQ DNA helicases, WRN (Werner syndrome (WS)) has been proposed to reset reversed forks or other replication intermediates arising after fork stalling, clearing the way to replisome progression once the block is removed (Khakhar et al., 2003). Alternatively, WRN has been implicated in the resolution of recombination intermediates arising after RAD51-dependent strand invasion (Saintigny et al., 2002). Cells mutated in WRN accumulate DNA breaks if challenged with replication-perturbing agents, which is indicative of incorrect handling of stalled forks (Pichierri et al., 2001). In yeasts, mutations of the RecQ helicase Sgs1 or Rqh1 are synthetic lethal with mutations in MUS81 (Boddy et al., 2000; Kaliraman et al., 2001; Mullen et al., 2001).

The observation that mutation in MUS81 reduces viability of RecQ-defective yeasts after fork stalling suggested that these two proteins might function on common substrates in response to replication stress, defining two parallel branches of the replication fork recovery pathway. Franchitto et al. demonstrate that in WRN-deficient cells, the MUS81 endonuclease represents an alternative pathway to ensure recovery of DNA synthesis by recombination-mediated restart of DNA replication (Franchitto et al., 2008).

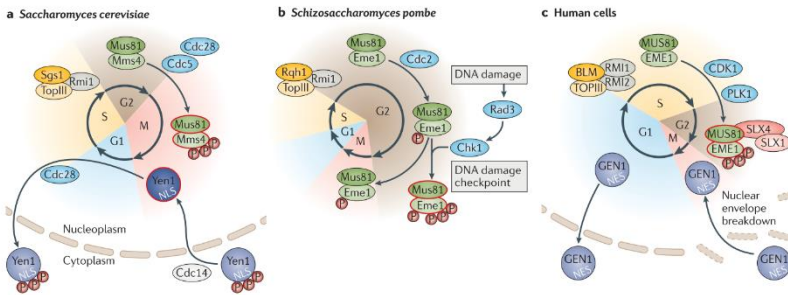


Figure 9 Controlling the processing of Holliday junctions by structure-specific endonucleases. (a) In *Saccharomyces cerevisiae*, efficient processing of Holliday junctions during late G2 and mitosis relies on the timely activation of both MMS and UV-sensitive protein 81 (Mus81)–methane methyl sulfonate-sensitive protein 4 (Mms4) and crossover junction endodeoxyribonuclease 1 (Yen1) through cycles of phosphorylation (P) and dephosphorylation. (b) In contrast to the cell cycle-dependent activation of Mus81–Mms4, upregulation of Mus81–essential meiotic endonuclease

1 (Eme1) activity in *Schizosaccharomyces pombe* occurs in response to DNA damage. Cdc2-mediated phosphorylation primes Eme1 for DNA damage-induced phosphorylation by radiation-sensitive mutant 3 (Rad3). The sequential phosphorylation of Eme1 restricts the catalytic upregulation of Mus81–Eme1 to G2 and only when the DNA damage checkpoint is activated. (c) In human cells, cell cycle-dependent phosphorylation of EME1 by cyclin-dependent kinase 1 (CDK1) and Polo-like kinase 1 (PLK1) correlates with increased Holliday junction resolvase activity of MUS81–EME1 it also promotes interaction of MUS81–EME1 with SLX4–SLX1 Holliday junction resolvase. Control of GEN1 is independent of phosphorylation, but instead relies entirely on a nuclear export signal (NES) that prevents GEN1 from accessing chromosomes until breakdown of the nuclear envelope in mitosis (Dehé and Gaillard, 2017).

2.3.1 MUS81 contributes to DNA damage response

The fact that MUS81–EME1 is upregulated at the onset of mitosis, together with accumulating evidence of the deleterious actions of MUS81 in S phase under specific circumstances, suggests that MUS81 is kept away from replication forks. However, cells that lack functional MUS81 are hypersensitive to DNA-damaging agents that impede replication fork progression (Franchitto et al., 2008). The catalytic activity of MUS81–EME1 can be enhanced by different partners of MUS81, which suggests that a complex regulatory network

exists, that may involve fine-tuning of the nuclease, even in S phase. There is strong evidence that MUS81-dependent enzymes are needed during S phase in human cells. Early reports found that MUS81 levels peak in S phase — with a marked accumulation in the nucleolus — consistent with a role for MUS81 in the maintenance of rDNA loci, which are prone to replication stress (Gao Hui, Xiao-Bo Chen, 2003). Furthermore, MUS81 is needed for replication fork restart following treatment with the replication inhibitors hydroxyurea, camptothecin or aphidicolin (low levels) in human or mouse embryonic stem cells (Hanada et al. 2007; Regairaz et al. 2011; Pepe and West 2014; Fu et al. 2015; Palma, Pugliese et al., 2018).

Despite the evidence that MUS81 has a positive role in DNA replication, very little is known about how its functions in S phase are regulated, and most of what is known relates to negative regulatory processes that prevent the opportunistic action of MUS81 nucleases on replication intermediates. The S phase checkpoint is crucial for preventing any uncontrolled and deleterious action of MUS81 nucleases in response to sustained replication stress. In *S. pombe*, the regulation of Mus81–Eme1 in S phase relies on the phosphorylation

of Mus81 by the kinase checkpoint DNA synthesis protein 1 (Cds1) in response to replication stress (Boddy et al., 2000). Strong activation of Cds1 in response to acute hydroxyurea treatment leads to the dissociation of Mus81 from chromatin and prevents extensive cleavage of replication intermediates and cell death (Froget et al., 2008; Kai et al., 2005). However, Mus81 is necessary for surviving chronic hydroxyurea treatment. Of note, the interaction of Mus81 with the forkhead-associated domain (FHA domain) of Cds1 is conserved in human cells, in which MUS81 interacts with the ATM effector checkpoint kinase 2 (CHK2; also known as CHEK2) (Chen et al., 2001); however, it is unclear whether MUS81 is directly regulated by CHK2 (and object of our laboratory investigation). Identifying which component in the endogenous Mus81–Mms4 complex prevents the efficient processing of these structures may help further the understanding of how Mus81 nucleases are controlled in S phase.

Direct negative regulation of human MUS81 by the checkpoint kinase WEE1, which binds and phosphorylates MUS81, are proposed on the basis that inhibition of WEE1 results in DNA damage that is alleviated by depleting MUS81. A non-mutually exclusive alternative is that

WEE1 curtails replication stress by keeping CDK activity low, thereby preventing uncontrolled firing of replication origins and a shortage of deoxynucleoside triphosphates and replication factors.

Importantly, although depletion of MUS81 prevents DSB formation following depletion of WEE1, it does not prevent the activation of ATR, which suggests that MUS81 acts downstream of replication fork stalling and S phase checkpoint activation (Beck et al., 2012). This is consistent with the deleterious processing of replication intermediates by MUS81–EME1 (Forment et al., 2011; Murfuni et al., 2013) or by MUS81–EME2 and MRE11, which occurs following the inhibition of the ATR effector CHK1.

MUS81–EME2-mediated DNA damage is proposed to result from premature activation of the complex by increased levels of CDK2 (Técher et al., 2016); however, in contrast to the CDK1- and PLK1-mediated upregulation of MUS81–EME1 activity, little is known about the control of MUS81–EME2. What we know is that EME1 interacts with MUS81 throughout the cell cycle, as the interaction between MUS81 and EME2 occurs predominantly during S phase. Preliminary studies in vitro showed that MUS81-EME2 was more

active than MUS81- EME1, and it preferentially cleaved 3'-flaps and RFs, whereas the nicked HJ was the preferred substrate for MUS81- EME1 (Fig.10) (Pepe & West, 2014). Such How the formation of the MUS81-EME2 complex is prevented during G2 and M phase is presently unknown (Pepe & West, 2014) and will be the subject of future study. Moreover, understanding how this complex is regulated is important, given that MUS81–EME2 is the prime culprit responsible for the DNA damage that results from the premature entry into mitosis that is induced by inhibition of WEE1 (Duda et al., 2016).

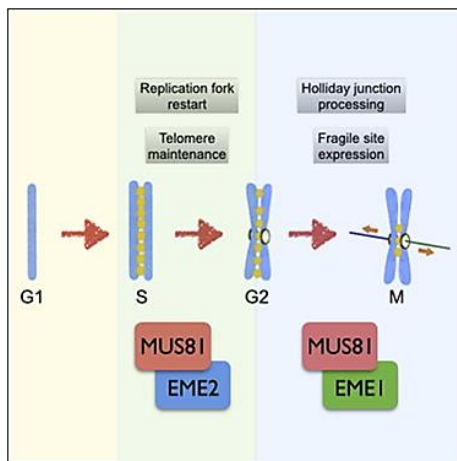


Figure 10 Association of MUS81 with EME1 or EME2 during cell cycle (Pepe and West, 2014).

In addition to preventing catalytic upregulation of MUS81 nucleases, the S phase checkpoint is also needed to prevent their premature association with SLX4, which is present at replication forks (Ohouo et al., 2010; Princz et al., 2015). In human cells, MUS81–EME1 normally associates with SLX4 in late G2 and M phase, following the phosphorylation of EME1 by CDK1 and PLK1 and of SLX4 by CDK1 (Duda, et al., 2016). Increased recruitment of MUS81 to chromatin is seen shortly after inhibition of WEE1 and the resulting formation of DSBs is also reduced by SLX4 depletion (Beck et al., 2012; Duda et al., 2016). The tumour suppressor SLX4 has attracted considerable attention in recent years after it was found to associate in human cells with XPF–ERCC1, MUS81–EME1 and SLX1 (Andersen et al., 2009; Muñoz et al., 2009). SLX4 stimulates the catalytic activity of all three nucleases (Fekairi et al., 2010; Muñoz et al., 2009; Svendsen et al., 2010a) and it has a pivotal role in channelling them into specific genome maintenance pathways and in their timely recruitment to DNA lesions and/or specific genomic loci.

It was recently showed that Human SLX4 provides the scaffold for a tri-nuclease complex called SMX, comprised of SLX1-SLX4,

MUS81-EME1, and XPF-ERCC1. Human SMX is the only known example of a tri-nuclease complex (Wyatt & West, 2017). SMX was found to be a promiscuous endonuclease that cleaves a broad range of DNA secondary structures *in vitro*. It was also shown that SLX4 activates MUS81-EME1 to cleave structures that resemble stalled replication forks (Fig. 11) (Wyatt et al., 2017). Activation involves relaxation of MUS81-EME1's substrate specificity, which is regulated by a helix-hairpin-helix (HhH) domain in the MUS81 N-terminus (MUS81 N-HhH). Intriguingly, MUS81 N-HhH also mediates the interaction with SLX4 via a C-terminal SAP domain (SLX4 SAP) (Nair et al., 2014). Therefore, SMX provides an efficient tool to remove various DNA structures that would otherwise impede DNA replication and/or chromosome segregation. This proposal is supported by data showing that SMX-mediated cleavage of CFSs is necessary for genome stability (Minocherhomji et al., 2015b).

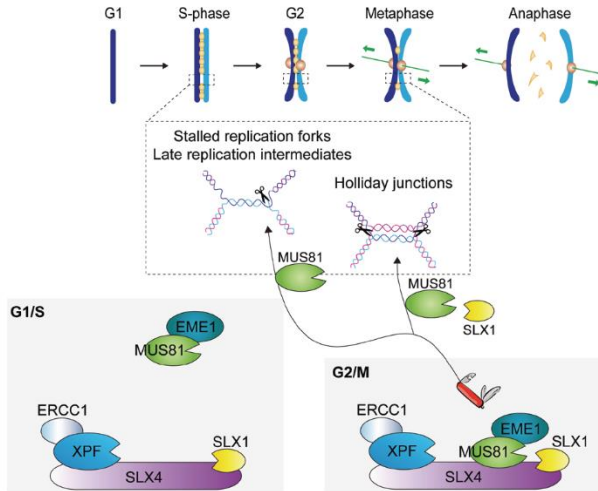


Figure 11 Cell cycle-regulated formation of the SMX tri-nuclease. The MUS81-EME1 subunit is recruited to a sub-complex comprised of SLX1-SLX4 and XPF-ERCC1 at a late phase of the cell-cycle, leading to the formation of SMX. Recombinant SMX cleaves a broad range of branched DNA structures (e.g. stalled replication forks, late replication intermediates, Holliday junctions) that would interfere with replication and/or chromosome segregation in the cell. The nucleases responsible for DNA cleavage depend on the DNA structure: MUS81-EME1 and SLX1 are required for coordinated Holliday junction resolution whereas MUS81-EME1 is activated to cleave replication-related structures (Wyatt & West, 2017).

As mentioned above, DNA damage-induced recruitment of MUS81–EME1 to CFSs, and the activation of the complex by hyperphosphorylation of EME1 at the very late G2-phase of the cell cycle, suggests that cells may be unable to detect replication problems at specific loci and also fail to activate a checkpoint response before entry into mitosis (Dehé et al., 2013; Ying et al., 2013). When cells are treated with mild doses of APH, particular Fanconi anemia proteins, including FANCD2 and FANCI, are specifically recruited to CFS loci in the genome (Chan et al., 2007). DNA replication or repair intermediates at CFSs that escape the attention of MUS81–EME1 during early mitosis manifest as unresolved DNA bridges in anaphase (Ying et al., 2013a). The SNF2-family translocase PICH (also known as ERCC6L) and the BTRR complex colocalize on these bulky bridges and UFBs during anaphase (Baumann et al., 2007; Chan et al., 2007). Failure to separate sister chromatids faithfully during anaphase can result in chromatin segregation defects, and possibly also chromosome-shattering (so called chromothripsis), resulting in an increased incidence of chromosomal rearrangements and micronuclei in subsequent G1 daughter cells (Crasta et al., 2012; Holland &

Cleveland, 2012). Following MUS81 depletion, an increase in the numbers of DAPI-positive chromosome-bulky bridges, micronuclei, and FANCD2-associated UFBs was observed in anaphase, suggesting that failure to cleave the CFS locus leads to an elevation in chromosome nondisjunction events associated with the failed segregation of sister chromatids (Fig. 12). Moreover, an increase in the number of CFS-associated 53BP1 nuclear bodies (Lukas et al., 2011) in newly formed G1 daughter cells is seen in MUS81-depleted cells, representing the transmission of replication errors from the previous cell cycle (Naim et al., 2013; Ying et al., 2013).

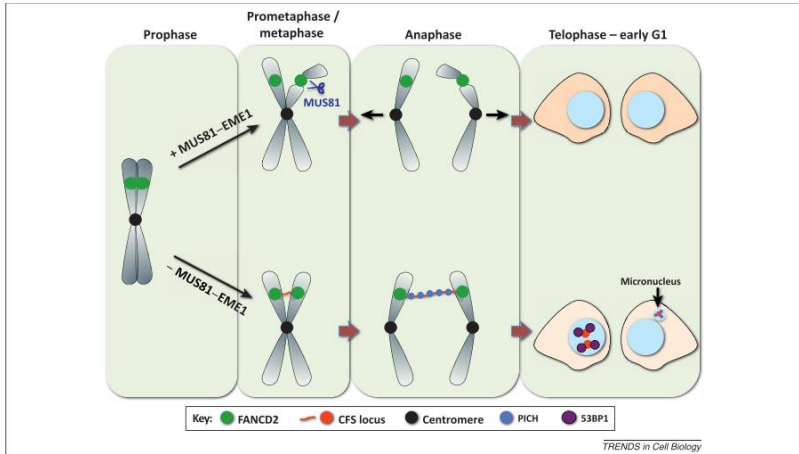


Figure 12 Model representing the molecular events leading up to common fragile site expression. Model showing that MUS81-dependent cleavage is required for the generation of breaks or gaps at common fragile site (CFS) loci, which are marked by the recruitment of a FANCD2 (Fanconi anemia group D2 protein) focus on each segregating sister chromatid in mitosis. FANCD2 foci associate with CFS loci throughout G2 and mitosis. The upper panel (+MUS81-EME1) shows normal cells, and the lower panel (MUS81-EME1) shows the situation in cells lacking MUS81-EME1. Depletion of MUS81 results in a reduction in the incidence of breaks or gaps at CFS loci, promoting the occurrence of CFS-associated sister chromatid non-disjunction. CFS loci that are not cleaved by MUS81 in early mitosis persist as bulky anaphase bridges or ultra-fine anaphase DNA bridges (UFBs) marked by FANCD2 foci at their termini, which are then processed by the Bloom’s syndrome helicase BLM and the PICH (Plk1- interacting checkpoint helicase) translocase in anaphase.

This permits cell division to take place, albeit with structural abnormalities that manifest as an increased frequency of CFS-associated, PICH-positive micronuclei in G1-daughter cells. In addition, the DNA repair factor 53BP1 forms nuclear bodies in G1 cells, potentially 'shielding' CFS regions (Minocherhomji & Hickson, 2014).

Most recently, it was observed that RAD52 is important for homology-directed DNA repair and has been found to promote MUS81 recruitment to persistent replication intermediates, without interfering with the localization of SLX4 (Bhowmick 2016b; Sotiriou et al., 2016). Murfunj et al. demonstrates the cooperation between RAD52 and MUS81 in response to replication stress; briefly RAD52, through its ssDNA annealing activity, produce a D-loop intermediate and possibly helps recruiting MUS81/EME1 complex by protein-protein interaction. The flap intermediate is targeted by MUS81 resulting in DSBs and fork collapse. In the absence of a functional checkpoint (i.e. inactive CHK1), the RAD52-dependent pathway is a favourite way of ensuring proliferation at the expense of genome stability (Murfunj et al., 2013a). Replication fork stalling at genomic regions that are difficult to replicate or contain endogenous DNA lesions is a hallmark of BRCA2 deficiency (Lai et al., 2017). BRCA2 plays essential roles both in the protection of the stalled replication

forks by preventing their nucleolytic degradation (Schlacher et al, 2011) and in fork restart through RAD51-mediated reactions (Roy et al., 2016). Recently, it has been reported that MUS81 facilitates DNA replication not only upon treatment with drugs that interfere with DNA replication (Hanada et al., 2007; Sarbajna et al., 2014; Ying et al., 2013b), but also in the absence of exogenous damage (Fu et al., 2015). Most recently, it was demonstrated on one side a dual cell-cycle dependent role of MUS81 to sustain replication fork progression in BRCA2-deficient cells through mechanisms distinct from the restart of stalled replication forks. Lemaçon and coworkers have shown that MUS81-dependent cleavage of the resected forks is required for fork restart in BRCA2-deficient cells through a break-induced replication (BIR)-like mechanism mediated by POLD3-dependent DNA synthesis. They also proposed that MUS81 acts downstream of MRE11- and EXO1-mediated degradation (Lemaçon et al., 2017a). On the other, Lai and coworkers have demonstrated that loss of MUS81 triggers increased replication stress and reduced survival in BRCA2-deficient cells. These cells progress into mitosis with incompletely replicated DNA, visualized as multiple chromosome interlinks in anaphase.

Moreover, BRCA2-deficient cells rely on MUS81 to continue DNA synthesis during mitosis, the absence of which causes severe chromosome segregation defects and G1 arrest. Moreover, in cells lacking BRCA2, MUS81-dependent nucleolytic cleavage removes DNA bridges caused by under-replicated DNA and provides a mechanism to complete replication in mitosis. MUS81 provides a mechanism of replication stress tolerance that sustains proliferation and survival of BRCA2-deficient cells. In cancer cells lacking BRCA2, dysfunctional checkpoints, including SAC failure, enable mitotic entry and progression with incompletely replicated genomes. Thus, BRCA2-deficient cells rely on MUS81 not only to reduce the replication stress burden during S phase, but also to eliminate the detrimental consequences of under-replicated DNA during mitosis (Fig.13) (Lai et al., 2017). In the second part of my elaborate, I wanted to investigate the role of phosphorylation on S87 residue of MUS81 in BRCA2-deficient cells in sustaining replication fork progression and viability during unchallenged DNA replication.

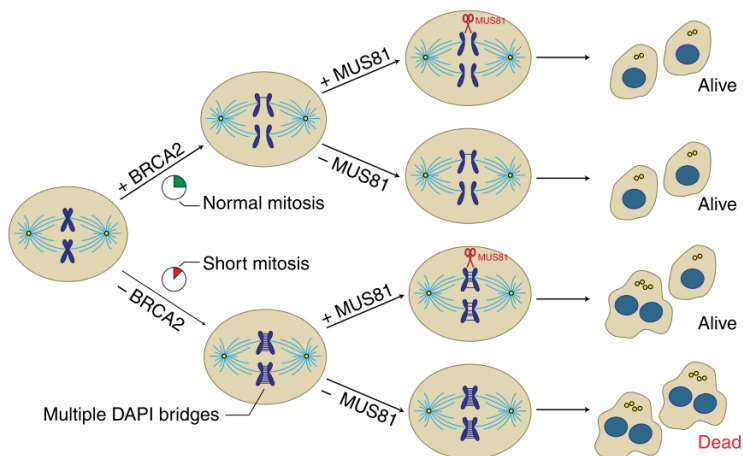


Figure 13 Model for concerted action of MUS81 and BRCA2 during mitosis. BRCA2-proficient cells require MUS81 for cleavage of UFBs formed during mitosis at under-replicated CFS. In cells lacking BRCA2, incomplete DNA replication at multiple sites leads to DAPI-stained bridges detectable in anaphase as chromosome interlinks. MUS81 is required to resolve these bridges and to promote mitotic DNA synthesis, ultimately facilitating chromosome segregation. MUS81 inactivation in BRCA2-deficient cells leads to persistent chromosome interlinks, multinucleation, supernumerary centrosomes and cell death. Blue, sister chromatids; yellow, centrosomes; light blue, microtubules (Lai et al., 2017).

2.4 Cell cycle regulation

Cells need to recruit safely these potentially damaging endonucleases to DNA only at specific time-points of the cell cycle, and regulate their controlled ‘activation’ in response to DNA damage (Minocherhomji & Hickson, 2014).

Budding yeast Mus81 forms a constitutive dimer with Mms4, which is phosphorylated at the G2/M Transition (Ehmsen & Heyer, 2008; Gallo-Fernández, 2012; Matos, 2011; Matos, 2013; Szakal & Branzei, 2013). Phosphorylation of Mms4 in mitosis leads to an upregulation of the catalytic activity of Mus81-Mms4, which is crucial for timely resolution of JMs before chromosome segregation. The mitotic phosphorylation of Mms4 was initially found to require Cyclin-dependent kinase (Cdc28, Cdk1) and the Polo-like kinase Cdc5. Recent work identified a third cell cycle kinase targeting Mms4 – the Dbf4- dependent kinase DDK. Importantly, however, Mus81 activation is diminished in the absence of any of the three cell cycle kinases (Princz et al., 2017).

Following the initial work in yeast, studies carried out in human cells indicate that similar principles operate to regulate MUS81 function

(Duda et al., 2016; Matos et al., 2011; Wyatt et al., 2013). EME1 is phosphorylated in a CDK1-dependent manner at the G2/M transition. Several studies suggest that human cells rely on an alternative molecular strategy to boost the ability of MUS81 to process HJs: CDK1-mediated phosphorylation promotes MUS81-EME1 association with SLX1-SLX4 to form the SLX-MUS complex (Castor et al., 2013; Garner, 2013; Wyatt et al., 2017, 2013) (Fig. 14).

How CDK1 activity enhances the ability of MUS81 to interact with SLX4 has yet to be determined. However, MUS81 and SLX4 are phosphorylated in a CDK1-dependent and cell cycle stage-specific manner, alongside EME1, suggesting that their modification might stabilize the SLX-MUS complex (Duda et al., 2016; Wyatt et al., 2013). Hence, to efficiently resolve replication intermediates during mitosis, MUS81 function is likely to require SLX4 for two reasons: (a) recruitment to sites of stalled replication and (b) modulation of the nuclease activity through relaxation in substrate specificity. It will be interesting to determine if SLX4 also changes the properties of MUS81-EME2 nuclease using *in vitro* approaches and to investigate whether anti-EME1 or EME2 immunoprecipitates display different

profiles of RF cleavage throughout the cell cycle (Pfander & Matos, 2017a).

Another cell cycle kinase, WEE1, has also been implicated in the regulation of MUS81 in human cells. However, in contrast to CDK1 and PLK1, WEE1 was found to suppress MUS81 function (Beck et al., 2012; Domínguez-kelly et al., 2011; Duda et al., 2016) and prevents excessive origin firing and replication stress by limiting CDK2 activity during S-phase, which may lead to formation of aberrant replication intermediates that become MUS81 targets (Beck et al., 2012; Domínguez-kelly et al., 2011). Recent work revealed another key role of WEE1 in suppressing MUS81 function. By restraining CDK1 activity in S-phase, WEE1 indirectly prevents unscheduled SLX4 phosphorylation and premature SLX-MUS complex formation. This precludes widespread recruitment of MUS81 nuclease to replication intermediates and, ultimately, avoids chromosome pulverization. Consistent with this notion, inhibition of CDK1 restores bulk DNA replication and suppresses the shredding of chromosomes caused by WEE1 inhibition. One surprising finding arising from the analysis of chromosome breakage upon inhibition of

WEE1 was its exquisite dependency on EME2, making us think that MUS81-EME2 requires especially tight control (Duda et al., 2016).

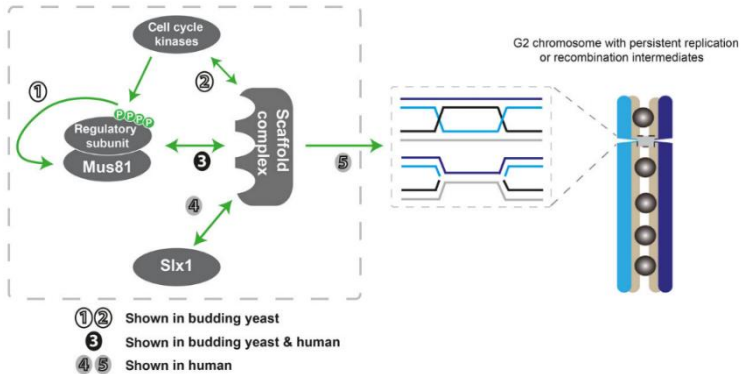


Figure 14 Mechanisms of Mus81 regulation. In budding yeast, cell cycle kinases phosphorylate Mms4 to enhance the nuclease activity of Mus81-Mms4 (1). The scaffold protein Rtt107 indirectly enhances Mus81 activity by promoting Mms4 phosphorylation (2). It is unknown if the Slx4 scaffold regulates Mus81 activity through direct binding (3) or through spatial coordination of the activities of Mus81 and Slx1 (4). Dpb11 and Rtt107 may regulate Mus81 recruitment to substrates (5). In human cells, binding to the SLX4 scaffold relaxes and enhances the nuclease activity of MUS81 in vitro (3), coordinates MUS81 and SLX1 for Holliday junction resolution (4), interacts with TOPBP1 and is required for substrate targeting in vivo (5). The regulatory subunit EME1 (if EME2 is also phosphorylated in vivo is unknown) is phosphorylated in a cell cycle stage-specific manner (1), but the role of this modification is unknown (Pfander and Matos 2017).

Additional factors operate downstream of or in parallel to SLX4 in controlling MUS81. SMC2, which is required for chromosome condensation, WAPL and PLK1, which are necessary for the release of sister- chromatid arm cohesion in early mitosis, were shown to promote MUS81 recruitment to sites of stalled replication, without interfering with the recruitment of SLX4.

Precisely how these factors contribute to MUS81 recruitment remains unclear (Minocherhomji et al., 2015).

Despite the many results obtained about the cell cycle control of the MUS81 nuclease it will be extremely interesting to learn more about how cells control MUS81 function. This led us to a question: Does MUS81 phosphorylation control its function? It is likely that the MUS81 undergoes cell-cycle-specific phosphorylation events that may contribute to tightly regulate its function together with the observed modification of the EME1/2 subunit.

In fact, although signs of phosphorylation induced changes in the electrophoretic mobility of EME1 and EME2 are apparent (Pepe & West, 2014a), little if any information exist on phosphorylation of the MUS81 subunit and its possible functional relevance.

However, phosphorylation of the invariant subunit of the two MUS81/EME complexes could be a more efficient way to regulate activity of the holoenzyme, as well as association with proteins that can influence its biological activity under normal or pathological conditions (Fekairi et al., 2010; Franchitto et al., 2008; Pepe & West, 2014a; Sarbajna & West, 2014). In addition to mentioned kinases an attractive one for the regulation of MUS81 complex is the pleiotropic CK2 (Franchin et al., 2017; Meggio & Pinna, 2003). Indeed, CK2 is important to regulate mitotic progression, is activated by CDK1 and phosphorylates several repair/recombination enzymes, such as MDC1, MRE11 and RAD51 (Chapman & Jackson, 2008; Kim, 2005; Meggio & Pinna, 2003; Spycher et al., 2008; Strauss et al., 2018). Protein kinase CK2 is a serine/threonine kinase highly conserved throughout evolution and is ubiquitously expressed in eukaryotic cells. Traditionally, CK2 is described as a constitutively active tetrameric enzyme composed of two catalytic α and/or α' subunits and two regulatory β subunits. CK2 is involved in various intracellular processes ranging from regulation of transcription and DNA replication to proliferation, survival and differentiation. Evidence that

CK2 plays a role in cell-cycle regulation in mammalian cells comes from findings that CK2 is associated with the mitotic spindle and centrosomes and interacts with and/or phosphorylates numerous cell-cycle regulatory proteins including Pin1, topoisomerase II, cdc34 and CDK1 (Yde et al. , 2008).

MATERIALS AND METHODS

In vitro kinase assay

For in vitro kinase assays, 300ng or 2 μ g (MS/MS) of the indicated GST-fused MUS81 fragments were incubated with recombinant purified CK2 (NEB), kinase in the presence of 32P-ATP, or ATP, and in kinase-specific reaction buffer prepared according to the manufacturers' directions. After washing, GST-fragments were released and analysed as previously reported (Ammazzalorso et al., 2010). Caseins (Sigma-Aldrich) were used as positive control in the CK2 kinase assay. For the full-length assay, 200ng of full-length MUS81 immunopurified from HEK293T cells (Origene) was incubated with 200ng of CK2 kinase. Phosphorylation was analysed by SDS-PAGE and WB.

Cell culture, generation of cell lines and RNA interference

The SV40-transformed MRC5 fibroblast cell line (MRC5SV40) was a generous gift from Dr. P. Kannouche (IGR, Villejuif, France). HEK293T cells line were obtained from American Type Culture Collection (VA, USA). The cells were maintained in Dulbecco's

modified Eagle's medium (DMEM; Life Technologies) supplemented with 10% FBS (Boehringer Mannheim) and incubated at 37 °C in a humidified 5% CO₂ atmosphere. Cell line were routinely tested for mycoplasma contamination and maintained in cultures for no more than one month.

To obtain the MRC5shMUS81 cells or the shMUS81-HEK293T cells, a retroviral plasmid containing an MUS81-targeting shRNA sequence (Origene cod. TR303095, sequence #1) was nucleofected using the Neon system (Life technologies). Three days after nucleofection, cells were subjected to selection with 500ng/ml puromycin and resistant clones expanded, tested for MUS81 depletion and phenotype before further use. To complement MRC5 shMUS81 cells with the wildtype MUS81 or its phosphomutants, the wild type form of MUS81 ORF cloned into the pCMVTag2B plasmid was subjected to SDM (Quickchange II XL – Stratagene) to introduce the S87A or S87D mutations. After the first round of mutagenesis, all MUS81 ORFs were made RNAi-resistant by SDM, sequence-verified and cloned into pEF1a-IRES-NEO vector by the Gibson Assembly protocol (NEB).

Sequence-verified plasmids were then transfected into MRC5 shMUS81 cells by the Neon nucleofector (Life technologies) in order to obtain cell lines stably expressing MUS81 and its mutant forms. Cell colonies were selected by 1mg/ml G418 antibiotic (Santa Cruz Biotechnologies). RNA interference against MUS81 was performed as previously reported (Ivana Murfuni et al., 2013a). For BRCA2 interference were used . In all experiments, cells were transfected using Lullaby (OZ Biosciences). RNA interference against EME2 was performed with siRNA-SMART pool, 10nmol (197342) from Dharmacon and against BRCA2 with siRNA-FlexiTube, 5nmol (1027417) from Qiagen. The efficiency of protein depletion was monitored by western blotting 48-72h after transfection.

Chemicals

Hydroxyurea (Sigma-Aldrich) was used at 2 mM, the DNA replication inhibitor aphidicolin (APH) (Sigma-Aldrich) was used at 0.2 μ M (low dose) or 1.5 μ M (intermediate dose). The CK2 inhibitor CX4925 (Selleck chemicals) was used at 25 μ M, the CDK1 inhibitor (RO-3306, Sigma-Aldrich) at 9 μ M and WEE1 inhibitor (MK-1775, Selleck chemicals) was used at 500 μ M. The L67 inhibitor of human

DNA ligase I and II (Axon Medchem) was used at 0.5 μ M. Nocodazole (Sigma- Aldrich) was used at 0.5 μ g/ μ l and Thymidine (Sigma-Aldrich) at 2 mM. 5-Bromo-2'-Deoxyuridine (BrdU, Sigma-Aldrich) was used at 30 μ M.

Neutral Comet assay

DNA breakage induction was evaluated by Comet assay (single cell gel electrophoresis) in non-denaturing conditions as described in Murfuni et al. Briefly, dust-free frosted-end microscope slides were kept in methanol overnight to remove fatty residues. Slides were then dipped into molten Low Melting Point (LMP) agarose at 0.5% and left to dry. Cell pellets were resuspended in PBS and kept on ice to inhibit DNA repair. Cell suspensions were rapidly mixed with LMP agarose at 0.5% kept at 37 °C and an aliquot was pipetted onto agarose-covered surface of the slide. Agarose embedded cells were lysed by submerging slides in lysis solution (30 mM EDTA, 0,1% SDS) and incubated at 4 °C, 1 h in the dark. After lysis, slides were washed in TBE 1X running buffer (Tris 90 mM; boric acid 90 mM; EDTA 4 mM) for 1 min. Electrophoresis was performed for 20 min in TBE 1X

buffer at 0.5 V/cm. Slides were subsequently washed in distilled H₂O and finally dehydrated in ice cold methanol. Nuclei were stained with GelRed (1:1000) and visualized with a fluorescence microscope (Zeiss), using a 60X objective, connected to a CCD camera for image acquisition. At least 300 comets per cell line were analyzed using CometAssay IV software (Perceptive instruments) and data from tail moments processed using Prism software. Apoptotic cells (smaller Comethhead and extremely larger Cometail) were excluded from the analysis to avoid artificial enhancement of the tail moment. A minimum of 200 cells was analyzed for each experimental point.

Immunoprecipitation and Western blot analysis

Immunoprecipitation experiments are performed using 2.5 × 10⁶ cells. The cell pellets were resuspended in lysis co-IP buffer (1% Triton X-100, 0.5% Na-deoxycolate, 150 mM NaCl, 1 mM EGTA, 20 mM Tris/HCl pH 8.0), freshly supplemented with protease inhibitor cocktail and benzonase was used for cells lysis. After centrifugation, for each IP sample, lysate was incubated with 20 µl anti-FLAG M2 magnetic beads (Sigma) or cMYC-tagged proteins were purified with Myc-TRAP MA magnetic agarose beads (Chromotek) at 4°C

overnight. The IP reaction was washed three times with the co-IP buffer, incubated in 2× sample loading buffer (100 mM Tris/HCl pH 6.8, 100 mM DTT, 4% SDS, 0.2% bromophenol blue and 20% glycerol) for 10 min at 90°C, then subjected to Western blot using standard methods. Blots were incubated with primary antibodies and were developed using Westernbright ECL (Advasta) according to the manufacturer's instructions. Quantification was performed on scanned images of blots using Image Lab software.

PLA (Proximity-Ligation Assay)

The in-situ proximity-ligation assay (PLA; mouse/rabbit red starter Duolink kit from Sigma-Aldrich) was used as indicated by the manufacturer. Images were acquired with Eclipse 80i Nikon Fluorescence Microscope, equipped with a VideoConfocal (ViCo) system. For each point, at least 500 nuclei were examined and foci were scored at 40×. Parallel samples incubated with only one primary antibody confirmed that the observed fluorescence was not attributable to artefacts. Only nuclei showing more than four bright foci were counted as positive.

Antibodies

The primary antibodies used were: anti-MUS81 (1:1000; Santa Cruz Biotechnologies), anti-DDK (Flag Origene, WB 1:1000, IF 1:200), anti-cMYC (1:1000; Abcam), , anti-CK2 (1:1000; Cell signaling technologies), anti-RxxpS/T (1:1000; Cell signaling technologies), anti-SLX4 (WB 1:1000, IF 1:200, Novus biologicals), anti-pS10H3 (1:1000, Santa Cruz Biotechnologies), anti- H3(1:1000, Santa Cruz Biotechnologies), anti-EME1 (1:1000, Santa Cruz Biotechnologies), anti-EME2 (1:500, Invitrogen), anti-Cyclin A (WB: 1:1000, IF: 1:100, Santa Cruz Biotechnologies), anti 53BP1 (1:400, Millipore), anti-BrdU (1:50, Becton Dickinson), anti-pS139H2A.X (1:1000, Millipore), anti- γ -Tubulin (1:200, Sigma-Aldrich), anti-pS87MUS81 (WB 1:1000, IF 1:200, Abgent), BLM (sc-7790, Santa Cruz Biotechnology, IF 1:50), anti-BRCA2 (1:1000, Bethyl) and anti-Lamin B1 (1:10000; Abcam). HRP-conjugated matched secondary antibodies were from Jackson Immunoresearch and were used at 1:40000.

Chromatin fractionation

Cells (4×10^6 cells/ml) were resuspended in buffer A (10 mM HEPES, [pH 7.9], 10 mM KCl, 1.5 mM MgCl₂, 0.34 M sucrose, 10% glycerol, 1 mM DTT, 50 mM sodium fluoride, protease inhibitors [Roche]). Triton X-100 (0.1%) was added, and the cells were incubated for 5 min on ice. Nuclei were collected in pellet by low-speed centrifugation (4 min, $1,300 \times g$, 4°C) and washed once in buffer A. Nuclei were then lysed in buffer B (3 mM EDTA, 0.2 mM EGTA, 1 mM DTT, protease inhibitors). Insoluble chromatin was collected by centrifugation (4 min, $1,700 \times g$, 4°C), washed once in buffer B + 50mM NaCl, and centrifuged again under the same conditions. The final chromatin pellet was resuspended in 2X Laemmli buffer and sonicated for 15 s in a Tekmar CV26 sonicator using a microtip at 25% amplitude.

Immunofluorescence

Immunofluorescence microscopy was performed on cells grown on 35-mm cover-slips and harvested at the indicated times after treatments. For IF, after further washing with PBS, cells were fixed with 4% PFA/PBS at RT for 10 min and were permeabilized with 0,5% Triton-X 100. After blocking in 3% BSA for 15 min, staining

was performed with the indicated antibody. Nocodazole-treated cells were blocked and fixed with PTEMF buffer (29). After blocking, coverslips were incubated for 1 h at RT with the indicated antibodies. For detection of anti-BrdU, after permeabilization with 0,4% Triton-X 100/PBS, cells were denatured in HCl 2,5N for 45' at RT. Alexa Fluor® 488 conjugated-goat anti mouse, Alexa Fluor® 594 conjugated-goat anti rabbit and Alexa Fluor® 488 conjugated-goat anti donkey secondary antibodies (Life Technologies) were used at 1:200. Nuclei were stained with 4',6-diamidino-2-phenylindole (DAPI 1:4000, Serva). Coverslips were observed at 40× objective with the Eclipse 80i Nikon Fluorescence Microscope, equipped with a VideoConfocal (ViCo) system. Images were processed by using Photoshop (Adobe) program to adjust contrast and brightness. For each time point at least 200 nuclei were examined. Parallel samples incubated with either the appropriate normal serum or only with the secondary antibody confirmed that the observed fluorescence pattern was not attributable to artefacts. Experiments for labeling cellular DNA with EdU (5-ethynyl-2'-deoxyuridine). EdU was added to the culture media (10µM), for 30 min. Detection of EdU was performed

used Click-iT EdU imaging Kits (Invitrogen). For UFBs-immunofluorescence analyses, cells grown on coverslips were fixed with PTEMF buffer (20 mM PIPES pH 6.8, 0.2% Triton X-100, 1 mM MgCl₂, 10 mM EGTA and 4% PFA) for 20 min. Cells were then processed as described above.

Cell cycle analysis by flow cytometry

Cells were processed for flow cytometry as follows: for each point, 10⁶ cells were collected, and after two washes in PBS, fixed in 70% cold ethanol. Then, cells were washed in PBS/BSA 1% and then resuspended in 0.5µg/ml propidium iodide and 0.1mg/ml RNase before analysis. Data were analysed with CellQuest and ModFit LT 4.1. software. Bivariate flow cytometry was performed for anti-BrdU and anti-γ-H2AX staining as indicated in the Anti-BrdU data-sheet (Becton Dickinson).

Growth Curve

The cells were seeded at 1.8 x 10⁴ cells per plate. After trypsinization, cells were counted through electronic counting cells (BioRad) for the following 6 days. The growth curve of the cell cultures was expressed as number of cells as a function of time.

Chromosomal aberrations

MRC5 SV40 cells were treated with Aph (low doses) at 37°C for 18h. Cell cultures were incubated with colcemid (0.2 µg/ml) at 37 °C for 3h until harvesting. Cell suspension was dropped onto cold, wet slides to make chromosome preparations. The slides were air dried overnight, then for each condition of treatment, the number of breaks and gaps was observed on Giemsa-stained metaphases. For each time point, at least 50 chromosomes were examined by two independent investigators and chromosomal damage was scored at 100×magnification with an Olympus fluorescence microscope. For each time point at least 100 chromosomes were examined by two independent investigators and chromosomal damage scored at 100×.

Clonogenic assays

Cells were plated at densities between 800 and 1000 cells per well in 6-well plates. Colonies were fixed in methanol-acetic acid 3:1 and stained with 5mg/ml⁻¹ GIEMSA (Sigma). Cell survival was expressed relative to control cells.

Phosphorylation site prediction

For the prediction of MUS81 phosphorylation sites, the MUS81 protein sequence was scanned using the GPS 2.0 software (<http://gps.biocuckoo.org/download.php>) with a medium threshold that consist in a < 6% of false identification rate (Xue et al., 2008).

Production and purification of GST-fused fragments

The different fragments of MUS81 were amplified by PCR from the pCMV-Tag2B-MUS81 plasmid (Stratagene) containing the full-length MUS81 ORF. PCR-amplified DNA was cloned into the GST-pGEX-2TK plasmid (Stratagene). GST-MUS81 fragments were expressed into *E. coli* BL21PlysS at 30°C for 4h. Bacterial pellets were lysed in BER reagent (Pierce) supplemented with DNase and Lysozyme, as indicated by the manufacturer, and purified by incubation with GSH-magnetic beads (Promega) after extensive washings, as reported previously (Pichierri et al, 2012). Quantification of the magnetic-beads-bound fragments was performed after SDS-PAGE and Coomassie staining against serial dilutions of purified BSA. Magnetic beads-bound GST-MUS81 fragments were then used as substrates for *in vitro* kinase assays.

Phospho-peptide antibody and Dot-blot

Phosphopeptide antibodies were raised in rabbit against the KLH-conjugated phosphopeptide (NH₂)-DGLCRMLDERLQRHRTpSGGD-(COOH) for S87 phospho-specific antibody (Abgent). Antibodies were affinity purified using phosphopeptide columns and contaminating non-phosphospecific antibody was affinity depleted by passing through a column cross-linked with non-phosphopeptide (NH₂)-DGLCRMLDERLQRHRTSGGD-(COOH). The eluted phospho-specific MUS81 antibodies were then enriched by dialysis against TBS containing 50% glycerol and tested by the vendor. The delivered antibody showed a 100-fold higher affinity for the phosphorylated peptide as evaluated by the vendor using an ELISA plate assay. To evaluate the ability of the pS87-WRN antibody to discriminate between unphosphorylated and phosphorylated peptide containing S87 in our hands, peptides were subjected to kinase assays and spotted onto a nitrocellulose strip. After incubation for 1 h at room temperature to ensure that the blots are dry, the strip was blocked with 5% dry milk in TBS (50 mM Tris, 0.5 M NaCl, 0.05% Tween-20, pH

7.4) for 1 h at room temperature and incubate with 100ng/ml of the rabbit anti-pS87-MUS81 primary antibody for 1hr at RT in 5% NFDM-TBS. After extensive washing, blot was detected with enhanced chemiluminescent reagents and images acquired through the ChemiDoc system (Bio-Rad).

Endonuclease activity assay

The functional activity of MUS81 was determined by performing an incision assay on a synthetic substrate mimicking a nicked Holliday Junction (nHJ). The DNA substrate was built by annealing five oligomers purchased from Thermo Fisher Scientific Inc., Waltham, MA. One of them was 5' end labelled with 6-carboxyfluorescein (6-FAM). Oligomer sequences and the substrate structure are in Figure S8. FLAG-tagged MUS81 mutants were affinity purified from cleared lysates by using anti-FLAG M2 magnetic beads (Sigma-Aldrich) according to the CoIP protocol indicate in the standard Methods. Beads were extensively washed and the immunopurified FLAG-MUS81 complexes were mixed with 50 nM of DNA substrate in 10 μ l of reaction buffer (25mM Hepes, 100mM NaCl, 3mM Mg(OAc)₂, 1mM DTT, 100 μ g/ml BSA). After 90 min of incubation at 30°C, DNA

products were deproteinized for 30 min at 37°C by addition of 10 μ l stop buffer (2 mg/ml proteinase K and 0,1% SDS). Reaction products were separated by a 15% native PAGE, at 400V for 2h at 4°C. Fluorescent bands were visualized by Typhoon 9200 Gel Imager (GE Healthcare, Uppsala, Sweden) and quantified using the public domain ImageJ software (available on line at: <http://rsb.info.nih.gov/ij/>). Data analysis was performed by Kaleidagraph (Synergy software).

Phosphopeptide enrichment

Purification of phosphopeptides was then performed according to Thingholm et al. (Thingholm et al, 2006). Briefly, tryptic peptides were diluted 5-fold in dihydroxybenzoic acid (DHB) buffer [350 mg/mL DHB, 80% (v/v) ACN, 2% (v/v) TFA] and applied to TiO₂ beads (200 μ g) pre-equilibrated in 50% ACN. The sample was then washed once in DHB buffer, before being washed two times with wash buffer [80% ACN (v/v), 2% TFA (v/v)] to remove the DHB. The sample was finally eluted with 25 μ L of 2.5% ammonium hydroxide solution (pH \geq 10.5) and immediately neutralized with 2.5 μ L of formic acid. All buffers used ultrapure water and were made fresh on the day of experimentation.

LC-ESI-CID/ETD-MS/MS

The TiO₂-enriched samples were analyzed using a split-free nano-flow liquid chromatography system (EASY-nLC II, Proxeon, Odense, Denmark) coupled to a 3D-ion trap (model AmaZon ETD, Bruker Daltonik, Germany) equipped with an online ESI nano-sprayer (the spray capillary was a fused silica capillary, 0.090mm o.d., 0.020mm i.d.). A sample volume of 15 μ L was loaded by the autosampler onto a homemade 2 cm fused silica precolumn (100 μ m I.D.; 375 μ m O.D.; Reprosil C18-AQ, 5 μ m, Dr. Maisch GmbH, Ammerbuch-Entringen, Germany). Sequential elution of peptides was accomplished using a flow rate of 300 nL/min and a linear gradient from Solution A (2% acetonitrile; 0.1% formic acid) to 50% of Solution B (98% acetonitrile; 0.1% formic acid) in 40 min over the precolumn in-line with a homemade 15 cm resolving column (75 μ m I.D.; 375 μ m O.D.; Reprosil C18-AQ, 3 μ m, Dr. Maisch GmbH, Ammerbuch-Entringen, Germany). To identify phosphorylation sites, two types of peptide fragmentation were carried out in parallel in the mass spectrometer: (i) Collision Induced Dissociation (CID); (ii) Electron Transfer Dissociation (ETD). When CID was used a MS2

was automatically performed on the three most intense MS ions, and MS3 was triggered if one of the top three MS2 peaks corresponded with neutral loss of 98.0, 49.0, 32.7 m/z. For ETD experiments the reaction time was set to 100 ms using a reactant ICC of 500000 allowing a maximum accumulation time for the reactant ion of 10 ms. Acquired MS/MS spectra were processed in DataAnalysis 4.0, and submitted to Mascot search program (in-house version 2.5, Matrix Science, London, UK). The following parameters were adopted for database searches: SwissProt database (release date 12/06/2015); taxonomy=homo sapiens; peptide mass tolerance of ± 0.3 Da; fragment mass tolerance of ± 0.3 for CID ions and of ± 1.3 Da for ETD ions; enzyme specificity trypsin with 1 missed cleavages considered; fixed modifications: carbamidomethyl (C); variable modifications: oxidation (M), phosphorylation (STY). Phosphopeptide identifications were accepted if the Mascot score was over the 95% confidence limit based on the “identity” score of each peptide. A delta ion score was calculated of all phosphopeptides containing more than one serine, threonine or tyrosine residues by taking the difference between the two top-ranking Mascot ion scores. Phosphorylation site

assignments with a delta score > 5 were automatically accepted. All fragmentation spectra with delta score ≤ 5 were manually inspected as to whether the phosphorylation sites were unambiguously determined or not.

DNA fibre assay

The efficiency of replication recovery was measured using the DNA fibre assay. First, DNA replication sites were labelled with 25 mM IdU (15 min), then cells were washed twice with PBS and incubated for other 15 min in fresh medium with 50 mM CldU. For immunodetection of labelled tracts, the following primary antibodies were used: rat anti-CldU/BrdU (Abcam) and mouse anti-IdU/BrdU (Becton Dickinson). Images were acquired randomly from fields with untangled fibres using the Eclipse 80i Nikon Fluorescence Microscope, equipped with a VideoConfocal (ViCo) system. The lengths of labelled tracts were measured using the Image-Pro-Plus 6.0 software. A minimum of 100 individual fibres were analysed for each experiment and each experiment was repeated three times. In dot plots, the mean of at least three independent experiments are presented. The value of the IdU tract length is reported in micrometers.

Statistical analysis

All the data are presented as means of at least three independent experiments. Statistical comparisons were made by Student's t test or by Anova, as indicated. $P < 0.5$ was considered significant.

AIM OF THE WORK

Replication stress represents a major source of genome instability stemming from slow rates of DNA synthesis, aberrant origin firing and frequent stalling of replication forks. Treatment with agents that interfere with DNA replication (for example, hydroxyurea, aphidicolin), as well as oncogene overexpression are known to trigger replication stress. Hence, cells are equipped with pathways that recognize and process branched DNA structures. Structure-specific endonucleases (SSEs) have key roles in DNA replication, recombination and repair, and emerging roles in transcription. These enzymes have specificity for DNA secondary structure rather than for sequence, and therefore their activity must be precisely controlled to ensure genome stability. Recombinogenic and non-recombinogenic pathways ensure replication recovery failure to protect or process stalled forks appropriately for replication restart results in accumulations of DNA double-strand breaks (DSBs) and chromosomal rearrangements. Among these, HR was believed to play an important role in the recovery of stalled or broken replication forks (RFs) during DNA replication and contributes to tolerance of DNA

damage. In addition, HR provides critical support for the correct segregation of homologous chromosomes during the first meiotic division. In all these events, a major step is the formation of Holliday junctions (HJs), four-way branched DNA intermediates, which must be resolved to separate repaired chromosome. One of these pathways utilizes the structure-selective endonuclease MUS81, which was thought to facilitate the resolution of replication and recombination intermediates. Many of our knowledge about the MUS81 nuclease has been obtained during the last years, but new studies indicate a growing importance about how cells control MUS81 function during cell cycle and its correlation with the subunits EME1/2. Several *in vivo* and *in vitro* studies have indicated that the primary role for MUS81 is to resolve HJs.

The regulatory circuit of MUS81 described in this elaborate is quite different from previous work in budding or fission yeast, where the control of the Mus81-Mms4(Eme1) endonuclease activity takes place mainly through cell cycle regulated phosphorylation of Mms4(Eme1). In fact, not only little is known about the regulation of the human MUS81 complex but we also have no evidence of a specific regulation

on MUS81 and how deregulated activation affects chromosome integrity. Analysis by MS/MS identified several phosphorylated residues, including S87, which reveals itself very intriguing also because lie within a putative CK2 consensus sequence. During my doctoral work, I investigate what is the phospho-regulatory mechanism controlling the MUS81 function in human cells. To functionally analyse the role of MUS81 S87 phosphorylation, we generated MUS81 knock-down cells stably expressing RNAi-resistant wild-type, unphosphorylable (S87A) or phosphomimetic (S87D) MUS81 forms. Functional analysis on cells expressing S87A or S87D forms of MUS81 revealed that phosphorylation at S87 is cell cycle (at G2/M) and mild replication stress (low doses of Aphidicolin) dependent and is sufficient to modulate the biological function of the MUS81 complex. Using phosphomutants, we also demonstrate that abrogation of phosphorylation at S87 of MUS81 is sufficient to prevent formation of DSBs after replication stress, phenocopying depletion of MUS81. Indeed, and in line with a role in mitosis, phosphorylation at Serine 87 is suppressed in S-phase and mainly detected in the MUS81 molecules associated with EME1.

Activation of MUS81 in mitotic cells has been linked to association of the MUS81/EME1 complex with the SLX4 scaffolding protein. SLX4 is indeed necessary to support MUS81 function at demised replication forks; we also investigate on modulation of the MUS81/SLX4 interaction by phosphorylation at S87.

Our findings involve CK2-dependent phosphorylation of MUS81 as crucial in the activation of endonucleolytic cleavage under replication stress. CK2 has been recently shown to phosphorylate RAD51 (Yata et al., 2012) thus its activity could be crucial for replication recovery under stressed conditions. Interestingly, CK2 has been found overexpressed in many human cancers (Ruzzene & Pinna, 2010).

Thus, it is tempting to speculate that the hyperactivation of CK2 in such tumours could be results in a higher phospho-activation of MUS81 resulting in more genome instability and contributing to enhance aggressiveness.

In the last part of my doctoral studies I started to investigate if our S87-MUS81 phosphorylation mutant could be a useful tool to define which function of MUS81, the S-phase-related one or that performed in M-phase, was essential under pathological conditions. As a

prototype of pathological condition, we used cells lacking BRCA2 that needs MUS81 to recover from replication stress. Using cell biology approaches to evaluate survival, DNA damage and resolution of mitotic interlinked intermediates, we show that the S87 MUS81 phosphorylation is involved to ensure viability of BRCA2-deficient cells mostly because it is the M-phase function of MUS81 to be essential.

Moreover, we show that the resistance of phosphomimic mutant of MUS81 to Olaparib treatment in cells lacking BRCA2 could be used as a potential target for the development of drugs that could selectively eliminate BRCA2-compromised cells and tumours.

Altogether, our data described a novel regulatory mechanism required to control MUS81 complex function in M-phase in human cells and involved in the viability of BRCA2-deficient cells. As CK2 inhibitors are under evaluation as anti-cancer drugs, our data may be useful to evaluate their use in tumors with signs of BRCAness.

RESULTS

PART I

1. MUS81 is phosphorylated at Serine 87 by the protein kinase CK2 both in vitro and in vivo

The human MUS81 contains an N-terminal unstructured region and a HhH domain that are essential to associate with SLX4, a crucial step for the biological function of the complex in mitosis (Dehé & Gaillard, 2017). Hence, seeking for regulatory events modulating the MUS81 complex, we scanned the N terminal sequence of MUS81 comprising amino acids 1–200, which includes the SLX4 binding region, for the presence of putative phosphorylation sites of mitotic kinases. As shown in Table 1, bioinformatics analysis retrieved several CDKs, PLK1 and CK2 putative phosphorylation sites that score over the specificity threshold of the software. As CK2 was not previously associated to MUS81 regulation and its pharmacological inhibition interfered with the formation of MUS81-dependent DSBs in checkpoint-deficient cells (Forment et al., 2011; Murfunj et al., 2013) (Fig. 16), we decided to focus on this kinase. Hence, to test whether

CK2 could phosphorylate MUS81 in vitro, we performed a radioactive kinase assay. As substrates, we used two different fragments comprising residues 1–206 or 76–206 of MUS81, fused to GST and purified from bacteria (Fig. 15A). Our kinase assays showed that CK2 efficiently phosphorylates the N-terminal MUS81 fragments (Fig. 15B). To confirm phosphorylation and identify phosphoresidues, we incubated the fragment 76–206 of MUS81 with recombinant CK2 and analysed the product of the reaction by MS/MS after affinity-purification of the phosphorylated peptides. From the CK2-modified fragment, we identified three different peptides containing phosphorylated residues (Fig. 15C). Among the three identified residues, S87 was the most promising because it is very close to the SLX4-interacting region of MUS81 (Nair et al., 2014). Hence, to functionally characterize this phosphorylation event, we generated a phosphospecific antibody that recognizes the MUS81 protein modified at S87. Dot blot assay confirmed that the anti-pS87MUS81 antibody efficiently recognizes the modified peptide or the peptide

incubated with recombinant CK2, while it showed no antibody reaction with the peptide incubated with recombinant PLK1 (Fig.17A).

Phosphorylation of MUS81 was also confirmed using a commercial phosphomotif antibody that recognizes a sequence (RXXpS/T) very similar to that surrounding S87 (RHRTpS) (Fig. 17B). Finally, co-immunoprecipitation experiments revealed interaction between the catalytic subunit of the CK2 holoenzyme, CK2 α , and MUS81, supporting the possible physiological relevance of S87 modification (Fig. 17C). Next, we performed *in vivo* experiments to test the ability of the anti-pS87MUS81 antibody to detect MUS81 phosphorylation. To this aim, HEK293T cells stably expressing a shRNA sequence against MUS81 (HEK293TshMUS81) were transiently transfected with empty vector or with plasmids expressing the wild-type, the unphosphorylatable (S87A) or the phosphomimetic (S87D) FLAG-tagged RNAi-resistant form of MUS81 protein. After anti-FLAG immunoprecipitation, the presence of MUS81 phosphorylation was analysed by western blotting. As shown in Fig. 18A S87 phosphorylation was detected only in the wild-type protein,

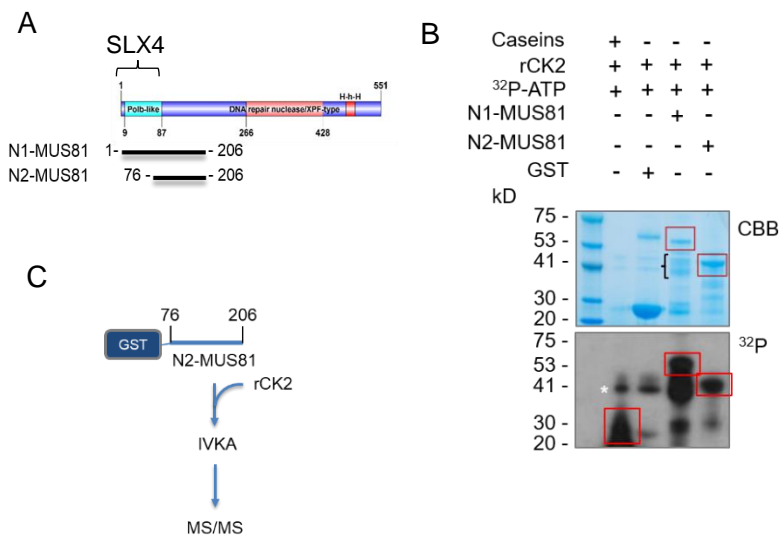
confirming S87 modification *in vivo* and the specificity of the antibody. This result was further corroborated by immunofluorescence in MRC5SV40 cells stably expressing the shMUS81 construct (shMUS81), and shMUS81 cells complemented with the FLAG-tagged-RNAi-resistant form of wild-type MUS81 or each of the two phosphorylation mutants and enriched in mitosis using nocodazole (Fig. 18B). Our analysis revealed the presence of nuclear staining in MUS81WT cells, which was not detectable in shMUS81 cells or in cells expressing the MUS81 mutant forms (MUS81S87A and MUS81S87D; Fig. 18B). Similarly, evaluation of MUS81 S87 phosphorylation by Western blotting in transiently expressing cells enriched in M-phase by nocodazole treatment confirmed that the anti-pS87 antibody efficiently recognised the MUS81 wild-type but not the phosphorylation mutant forms (Fig. 18C). Interestingly, pharmacological inhibition of CK2 substantially reduced S87 phosphorylation as evaluated by IP/WB or immunofluorescence analysis (Fig. 19A and B), proving that S87 residue of MUS81 is an *in vivo* substrate of the protein kinase CK2.

Altogether, our findings show that MUS81 is phosphorylated by CK2

on S87 both in vitro and in vivo, and that S87 phosphorylation is already detectable during unperturbed cell growth.

Table 1. Putative phosphorylation sites identified in the N-terminal MUS81 region

Kinase	Residue	Sequence	Score	Cut-off
CK2	S87	RLQRHRTSGGDHAPD	4,938	3,923
	S95	GGDHAPDPSGGENSP	4,819	3,923
	S97	DHAPDPSGGENSPAP	4,65	3,923
	T159	PNGHHFLTKEELLQR	5,231	3,923
CDKs	S95	GGDHAPDPSGGENSP	4,475	1,649
	S101	DSPSGENSPAQGR	4,205	1,649
PLK1	S101	DSPSGENSPAQGR	3,571	3,462
	S115	LAEVQDSSMPVPAQP	3,578	3,462



Mass spectrometry data

Residue position	Residue type	Sequence	m/z	Kinase
87	Ser	TSpGGDHAPDPSGGENSPAPQGR	734,25	CK2
114	Ser	LAEVQDSpSMoxPVPAQPK	598,30	CK2
87+95	Ser	HRTSpGGDHAPDSpSGGENSPAPQR	858,67	CK2

Figure 15 CK2 phosphorylates MUS81 in vitro. (A) Schematic representation of the N-terminal MUS81 fragments. (B) GST-fused N-terminal MUS81 fragments purified from bacteria were incubated with recombinant CK2 and subjected to in vitro radioactive kinase assay. Caseins were used as positive control. Red boxes indicate position of the fragments. Parenthesis indicates N1-MUS81 degradation products. Asterisk denotes residual co-purifying autophosphorylated CK2. (C) MS/MS analyses of in vitro phosphorylated N2-MUS81. Inset summarizes the identified phosphopeptides and residues.

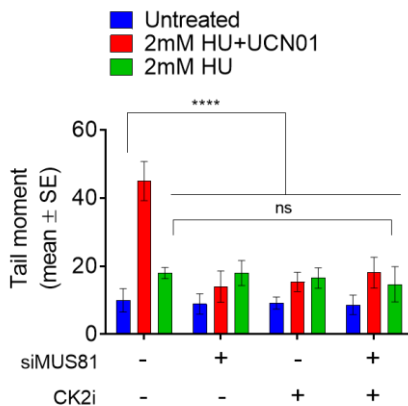


Figure 16 CK2 inhibition suppresses MUS81-dependent DSBs. Cells were treated as indicated for 6 h, in the presence or not of CK2 inhibitor (CK2i), before being analyzed for the presence of DSBs by neutral Comet assays. The CHK1 inhibitor UCN01 was used at 400 nM. Data are presented as mean tail moment \pm SE from three independent experiments. Error bars represent standard errors. **** = $p > 0.001$; Student's t-test.

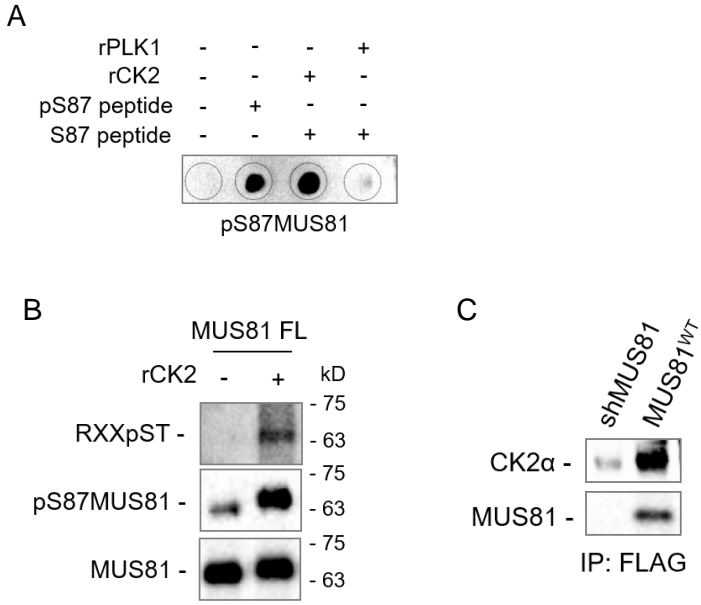


Figure 17 CK2 phosphorylates full-length MUS81 on S87 and they form a complex. (A) Fifty nanograms of peptide or phosphopeptide used as antigen to generate the polyclonal rabbit anti-pS87MUS81 was incubated with the indicated recombinant kinase and ATP. Reaction products were spotted onto a nitrocellulose strip and subjected to WB using the pS87MUS81 antibody. (B) Immunopurified MUS81 Full-Length (FL) protein was incubated with recombinant CK2 kinase and ATP. Phosphorylation was analyzed after WB with anti-pS87MUS81 or anti-RXXpST antibodies. (C) MUS81 was immunoprecipitated from MRC5 shMUS81 complemented or not with RNAi resistant FLAG-MUS81wt protein after synchronization with Nocodazole for 16h. The presence of CK2 in the MUS81 IP was revealed by WB by using anti-CK2α subunit antibody.

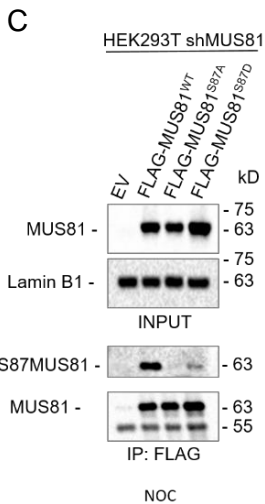
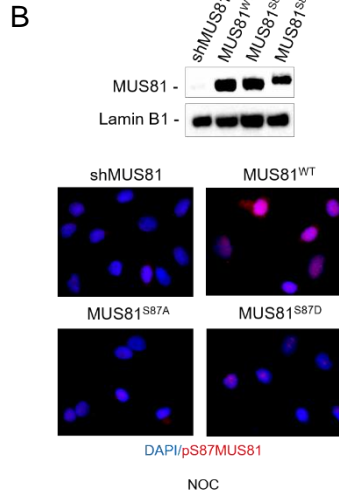
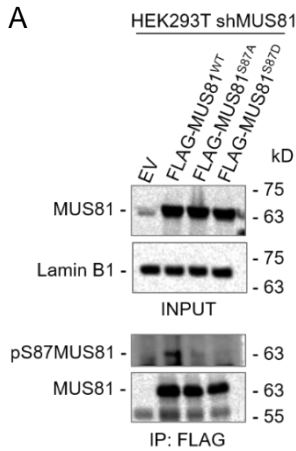


Figure 18 The anti-pS87MUS81 antibody can detect S87-phosphorylated MUS81 in cells. (A) HEK293T shMUS81 were transiently transfected with empty vector or with plasmids expressing the wild-type, the unphosphorylatable S87A or the phosphomimetic S87D FLAG-tagged RNAi resistant MUS81 proteins. After anti-FLAG immunoprecipitation, the anti-pS87MUS81 antibody signal was revealed by WB only in the wild type protein. MUS81 expression and Lamin B1 housekeeping protein were shown in the input as control. EV=Empty Vector. (B) Immunofluorescence experiments performed in MRC5SV40 shMUS81 cells stably complemented with the

Figure 18 The anti-pS87MUS81 antibody can detect S87-phosphorylated MUS81 in cells. (A) HEK293T shMUS81 were transiently transfected with empty vector or with plasmids expressing the wild-type, the unphosphorylatable S87A or the phosphomimetic S87D FLAG-tagged RNAi resistant MUS81 proteins. After anti-FLAG immunoprecipitation, the anti-pS87MUS81 antibody signal was revealed by WB only in the wild type protein. MUS81 expression and Lamin B1 housekeeping protein were shown in the input as control. EV=Empty Vector. (B) Immunofluorescence experiments performed in MRC5SV40 shMUS81 cells stably complemented with the

FLAG-tagged form of MUS81 wild-type or the S87A/S87D phosphorylation mutants. MUS81 expression and Lamin B1 as loading control were revealed by WB. The representative images showed pS87MUS81 antibody signal (red staining) in NOC synchronized cells. Nuclei were depicted with DAPI staining (blue). (C) Anti-FLAG immunoprecipitation performed as described in (A) with HEK293T cells treated with NOC.

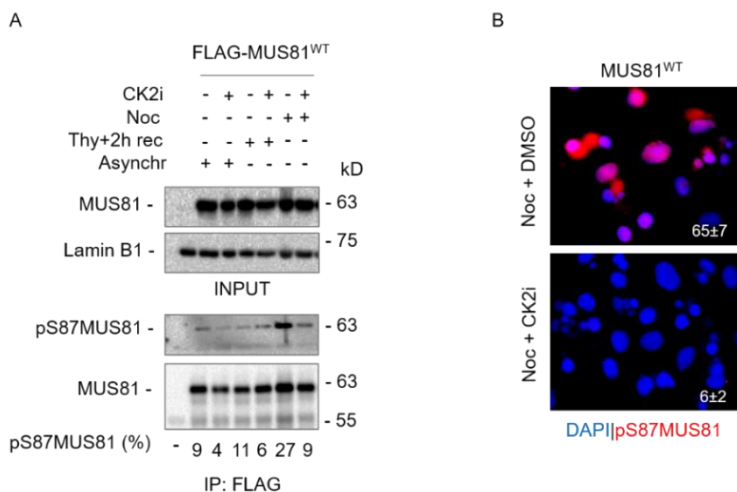


Figure 19 CK2 inhibition abrogated S87 MUS81 phosphorylation in vivo. (A) After transient transfection, FLAG-MUS81wt was immunoprecipitated from HEK293T shMUS81 cells treated as indicated. Cells were accumulated in S-phase by using a double-thymidine block (Thy+2h rec) or in mitosis upon Noc treatment. The CK2 inhibitor was used at 25µM added for the last 6 hours. The anti-pS87MUS81 signal was expressed as normalized percentage of the total immunoprecipitated MUS81.

(B) Representative images of immunofluorescence experiments performed to detect MUS81 S87-phosphorylation upon CK2 inhibition in MRC5 shMUS81 cells stably complemented with MUS81wt. Cells were synchronized by NOC treatment and the last 6 hours we added DMSO or 25 μ M CK2 inhibitor. Representative images were shown. The mean percentage of pS87MUS81 positive cells is indicated in the images \pm SE.

2. CK2-mediated phosphorylation ofMUS81 at Serine 87 is an early mitotic event stimulated by mild replication stress and restrained in the MUS81/EME2 complex

It is still poorly defined whether each of the two MUS81/EMEs complexes shows any cell-cycle specificity (Duda et al., 2016; Matos & West, 2014; Pepe & West, 2014; Pfander & Matos, 2017a). Hence, we analysed if modification by CK2 was cell cycle-dependent. To this aim, HEK293TshMUS81 cells, transiently expressing the wild-type form of MUS81, were synchronized and S87 phosphorylation was determined. Phosphorylation was evaluated by IP/WB using the anti-pS87MUS81 antibody from cells enriched in S-phase after release from a double-thymidine block or in mitosis using Nocodazole (Noc; Fig. 20A). Although MUS81 was found phosphorylated at S87 already in asynchronous cells, the level of phosphorylation was substantially

reduced in S-phase enriched cells, but it was increased in mitotic cells (Fig. 20B). To evaluate phosphorylation in a more physiological context, we performed anti-pS87MUS81 immunofluorescence in asynchronous cultures exposed to a short EdU pulse to label S-phase cells or, as a control, in Noc-arrested cultures. Dual EdU/pS87MUS81 immunostaining revealed that CK2-dependent phosphorylation is absent in S-phase cells, while it is easily detected after Noc treatment (Fig. 20C). Although the most relevant function of theMUS81 complex is the resolution of recombination intermediates in late G2/M, it may also process perturbed or collapsed replication forks (Sarbjana & West, 2014). Thus, we analysed if phosphorylation of S87 might be a common readout of the MUS81 complex activation. To this end, we treated HEK293TshMUS81 cells expressing the wild-type FLAG-MUS81 protein with two doses of aphidicolin (Aph), which partially arrest replication or perturb common fragile sites (CFS), or with hydroxyurea (HU). Phosphorylation was then assessed in anti-FLAG IP by WB using the anti-pS87MUS81 antibody. All these treatments have been reported to stimulate the function of both the MUS81 complexes, however, prolonged treatment with HU leads to a

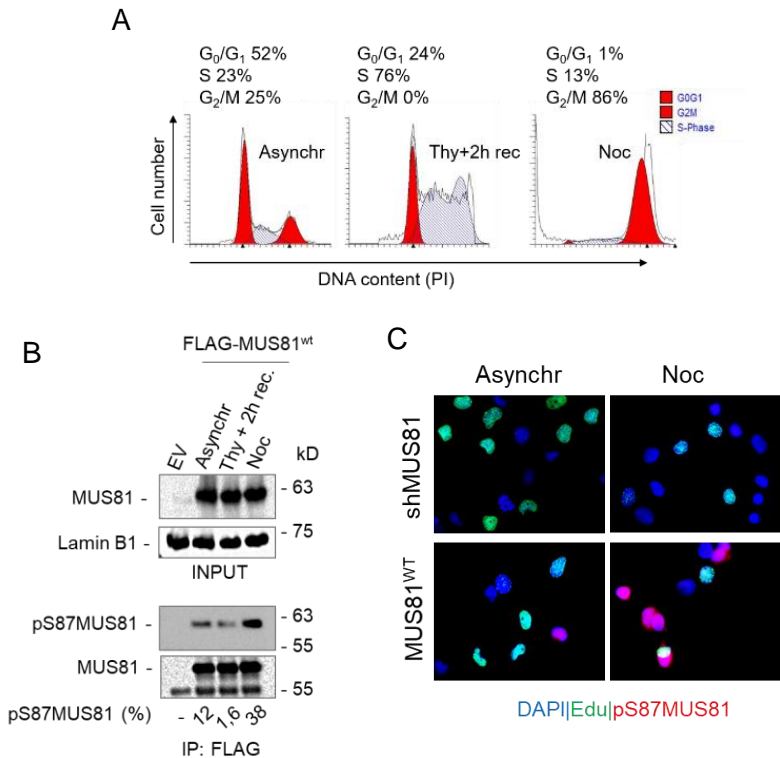
complete arrest of S-phase progression and formation of MUS81-dependent DSBs (Fugger et al., 2015; Hanada et al., 2007; Naim et al., 2013; Ying et al., 2013c). Consistently, Aph treatment accumulated cells in S-phase but did not completely arrest cell cycle progression, while 24 h of HU blocked cells in G1/S phase (Fig. 21). As expected, phosphorylation of S87 was increased in Noc-treated cells, but it was also stimulated by Aph treatments (Fig. 20D). In contrast, and despite the reported formation of DSBs by MUS81, phosphorylation of S87 was barely detectable in cells treated with HU (Fig. 20D). To confirm that treatment with Aph stimulated phosphorylation of MUS81 at S87, we performed anti-pS87MUS81/EdU immunofluorescence in shMUS81 cells complemented with the wild-type form of MUS81 (Fig. 20E). Treatment with a low-dose Aph increased the number of nuclei positive to anti-pS87MUS81 immunostaining and the large majority of cells staining positive for pS87 were EdU-negative. This indicates that a mild replication stress induces a CK2-dependent phosphorylation of MUS81 most likely in G2/M phase. Although it is widely accepted that the MUS81 complex carries out its primary function in late G2 and mitosis, it is still unclear

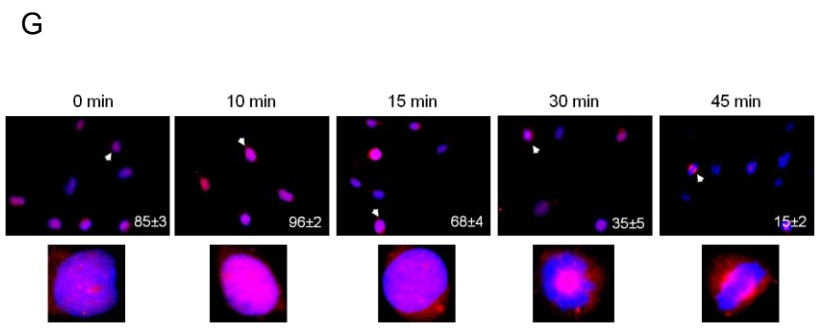
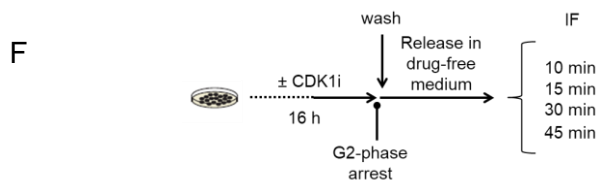
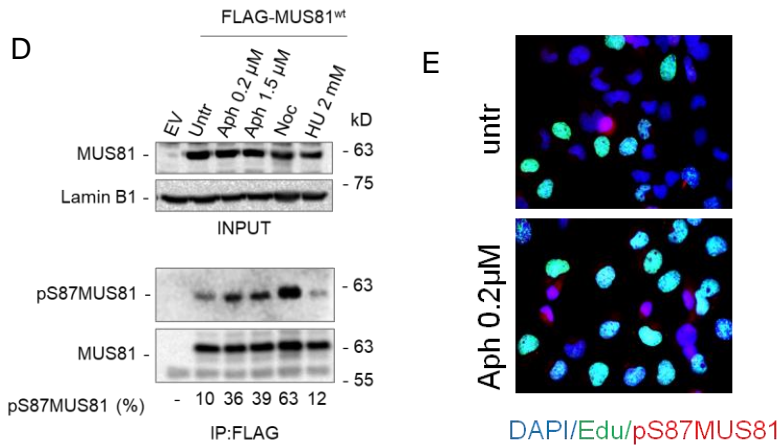
if it is active throughout all this period. Our data suggest that phosphorylation at S87 can be used as diagnostic sign of MUS81 complex function. Hence, we performed immunofluorescence to follow MUS81 modification over time after release from a G2-arrest induced by CDK1 inhibition (Minocherhomji et al., 2015a), as outlined in the experimental scheme (Fig. 20F). Cells released in late G2/M were subjected to anti-pS87MUS81 immunofluorescence at different time-points. Cells blocked in late-G2 showed high levels of pS87MUS81 immunostaining, which increased during the early time-point after release in mitosis (Fig. 20G). Anti-pS87MUS81 nuclear staining declined thereafter in concomitance with appearance of metaphase cells, as evaluated by DAPI staining (Fig. 20G). Interestingly, pS87MUS81 nuclear immunostaining was always confined to cells with morphological features of late G2/prophase, even at later post-release time-points, when population was enriched of metaphase and anaphase cells (30 and 45 min; Fig. 20G). Of note, in several late mitotic cells, pS87MUS81 immunostaining was apparently accumulated at centrosomal regions (see 45 min) as indicated by anti-tubulin co-staining (Fig. 20H). In human cells,

MUS81 exists as an heteroduplex in association with EME1 or EME2 (Ciccia et al., 2007). Although there are conflicting results about the cell cycle-dependent association with EME2(Duda, et al., 2016; Pepe & West, 2014b), EME1 is found throughout the cell cycle, even if its function predominates in G2/M (Pepe & West, 2014b).

Since phosphorylation of S87 is stimulated in early mitosis and is absent in S-phase synchronized cells, we investigated if it was confined to the MUS81/EME1 complex. To this end, we transiently expressed FLAG-MUS81 and Myc-EME2 or Myc-EME1 in HEK293T cells, and immunopurified the fraction of MUS81 associated with EME2 or EME1 by anti-Myc immunoprecipitation. We analysed S87 MUS81 phosphorylation in asynchronous cells or in cells accumulated in M-phase with Noc. As shown in Fig. 22, S87 MUS81 phosphorylation was detectable in both the MUS81 complexes but with different levels. In theMUS81/EME1 complex, S87MUS81 phosphorylation was enhanced by nocodazole treatment by about 3-fold over the basal level while, in the MUS81/EME2 complex phosphorylation was similar in asynchronous cells but did not change after nocodazole treatment. Collectively, these results

demonstrate that CK2 phosphorylates MUS81 at S87 in early mitosis, and that this phosphorylation is stimulated in the presence of mild replication stress. Furthermore, they suggest that phosphorylation of S87 is prevented in S-phase and mainly concerns the MUS81/EME1 complex.





H

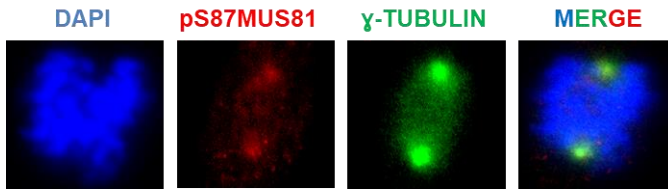


Figure 20 Phosphorylation of MUS81 on S87 is cell cycle-dependent and confined in early mitosis. (A) Flow cytometry analysis of HEK293T shMUS81 cells transiently expressing the wild-type form of FLAG-MUS81 after synchronization in S-phase (Thy+2h rec) or in mitosis (Noc). (B) After transient transfection, FLAG-MUS81wt was immunoprecipitated from asynchronous (asynchr), S-phase or M-phase synchronized HEK293T shMUS81. Phosphorylation was analyzed by WB by using the anti-pS87MUS81 antibody, and the anti-pS87MUS81 signal was expressed as normalized percentage of the total immunoprecipitated MUS81. EV = Empty Vector (C) Anti-pS87MUS81 immunofluorescence staining (red) was performed in MRC5SV40 shMUS81 and FLAG-MUS81wt stably complemented cells previously exposed to short EdU pulse to mark S-phase cells (green). Nuclei were depicted by DAPI staining (blue). (D) After transient transfection, FLAG-MUS81wt was immunoprecipitated from asynchronous HEK293T shMUS81 cells treated as indicated. anti-pS87MUS81 signal was expressed as normalized percentage of the total immunoprecipitated MUS81. EV = Empty Vector. (E) Immunofluorescence experiments were performed to detect S87MUS81-phosphorylation upon mild replication stress induced by low dose of Aphidicolin. MRC5 shMUS81 cells

complemented with MUS81 wt were exposed to short EdU pulse and then stained with anti-pS87 antibody (red) and DAPI (blue). Representative images were shown. (F) Experimental scheme used to study S87 MUS81 phosphorylation over time, from G₂-phase arrested cells to late mitosis. MRC5 shMUS81 cells complemented with MUS81 wt were arrested in G₂-phase by treatment with CDKi (RO-3306). Cells were immunostained for anti-pS87MUS81 at indicated post-release time points. (G) Representative images of anti-pS87MUS81 immunostaining (red). The mean percentage of pS87MUS81 positive cells is indicated in the images \pm SE. At least 200 anaphase, 100 metaphase and 50 prophase cells were analysed in three replicates. Arrowheads indicate the positive cells enlarged in the insets. (H) Representative images of anti-pS87 MUS81 antibody (red) co-localization with α -Tubulin antibody (green) in metaphase cells. Nuclei were depicted with DAPI.

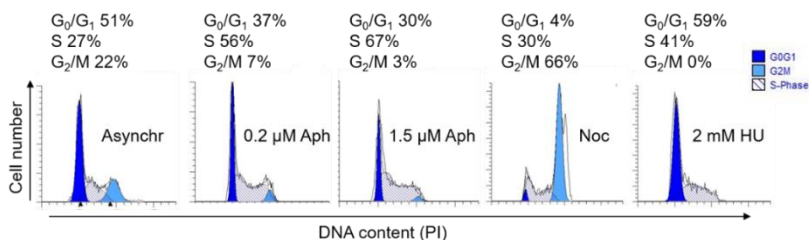


Figure 21 Cell cycle analysis of the population of HEK293T shMUS81 cells transfected with FLAG-MUS81. Flow cytometry profile of cells treated as indicated. The percentages of cells in each different phase of the cell cycle are shown in the panel.

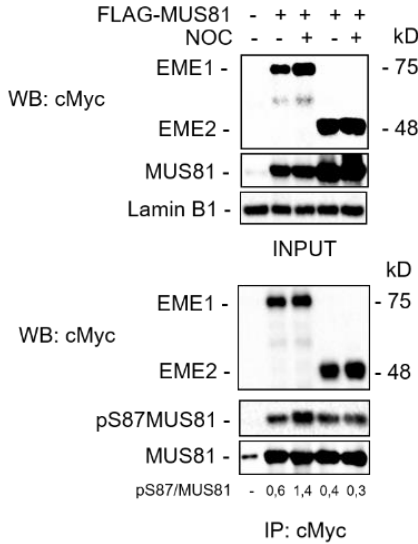


Figure 22 MUS81 phosphorylated at S87 privileges interaction with EME1. HEK293T shMUS81 cells were transfected with cMYC plasmid alone (control) or together with FLAGMUS81wt and cMYC-EME1 or cMYC-EME2. After treatment with Noc for 16h, cMYC-EME1 and EME2 were immunoprecipitated using anti-cMYC magnetic beads.

The presence of MUS81 and its phosphorylation status at S87 were analysed by WB. The fraction of pS87 MUS81 associated to EME1 or EME2 was normalized on the total immunoprecipitated MUS81.

3. Phosphorylation of MUS81 at Serine 87 by CK2 regulates binding to SLX4

Association of the MUS81 complex with SLX4 is essential for some of its function (Dehé & Gaillard, 2017), and given that the SLX4-binding region is close to S87, we asked whether phosphorylation could influence this interaction. To this aim, we performed co-immunoprecipitation experiments in shMUS81 cells complemented

with the wild-type form of wild-type MUS81 or each of the two-phosphorylation mutants. Of note, in our cell model, the level of SLX4 apparently decreased in Noc-treated cells (Fig. 23A, input). This unexpected decrease seems cell-line specific as it was not observed in HEK293T cells (Fig. 19) and may be correlated with proteosomal degradation as it can be reduced by MG132 (data not shown). In asynchronous wild-type or MUS81S87A cells, little SLX4 was found in a complex with MUS81 (Fig. 23A, IP). However, a 2-fold higher amount of SLX4 co-immunoprecipitated with MUS81 in MUS81S87D cells (Fig. 23A). In Noc-treated cells, association of MUS81 with SLX4 was more affected by loss of S87 phosphorylation. Indeed, the unphosphorylatable MUS81 mutant (MUS81S87A) co-immunoprecipitated less SLX4 than the wild-type or the phosphomimic form (MUS81S87D; Fig. 23A). Interestingly, while the amount of SLX4 associated with MUS81 was increased by Noc treatment in wild-type cells, no modulation was detected in the MUS81S87A or in the MUS81S87D mutant (Fig. 23A). In contrast, MUS81 immunoprecipitated similar amounts of EME1 independently on the phosphorylation status of S87 (Fig. 23A). To further confirm

that phosphorylation of S87 affected the interaction of MUS81 with SLX4, we analysed protein-protein interaction at the single cell level by the proximity-ligation assay (PLA). Interestingly, and consistently with biochemical assays, association of MUS81 with SLX4 was enhanced in MUS81S87D cells, while it was only barely detectable in wild-type cells or in cells expressing the unphosphorylatable protein, as evaluated by the number of PLA-positive cells (Fig. 23B and C). Of note, association of MUS81 with SLX4 is strongly enhanced in the presence of the phosphomimic mutant (MUS81S87D) also in cells enriched in S-phase by a thymidine block (Fig. 23B and C), even if their association should be actively prevented at this stage to avoid targeting of replication intermediates (Duda, et al., 2016).

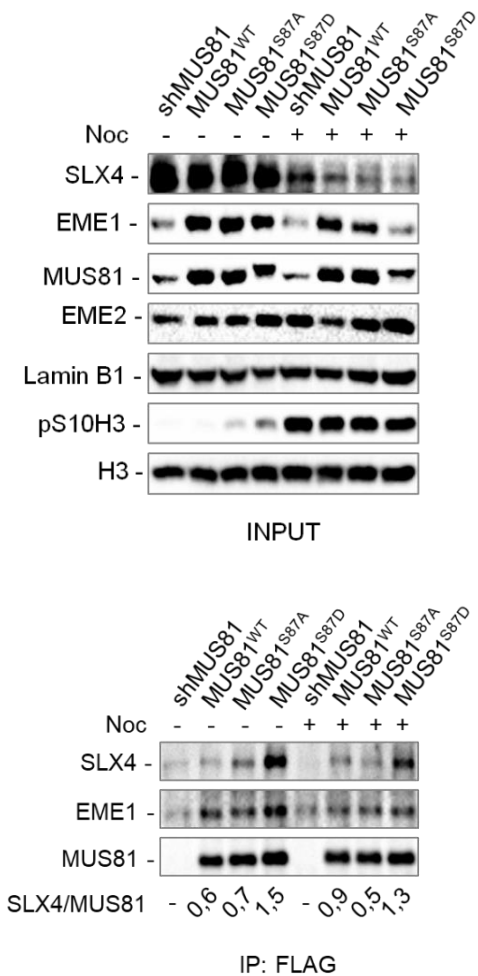
To test if enhanced association between MUS81 and SLX4 might correlate with an increased association with chromatin, we performed cellular fractionation experiments in cells treated with Noc or exposed to HU for 24 h, a condition in which we observed little if any S87 phosphorylation (Fig. 20D). Western blotting analysis of the chromatin fraction with an anti-MUS81 antibody showed no substantial difference in the two phosphorylation mutants, as compared to the

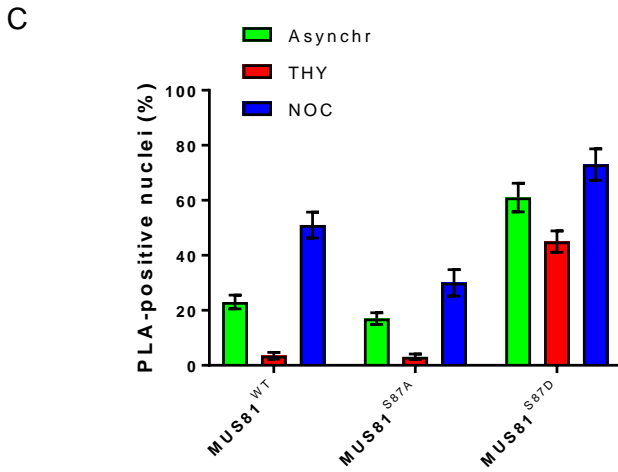
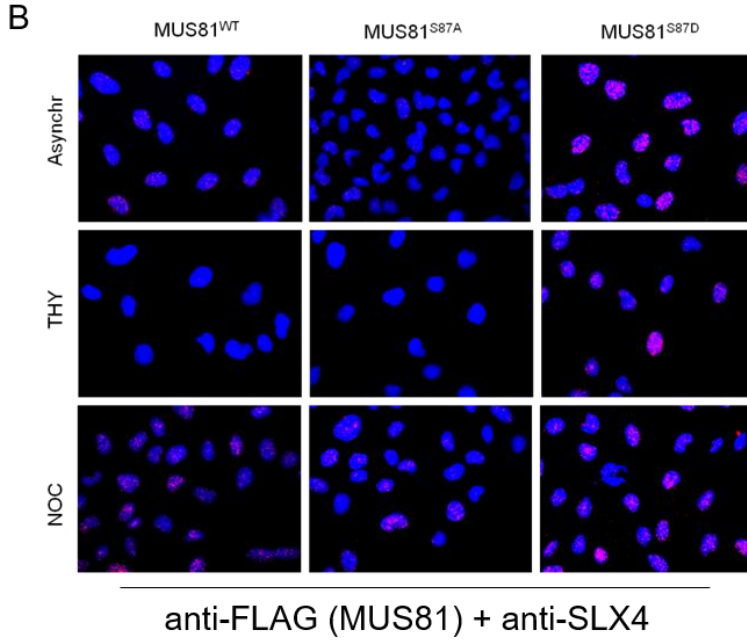
wild-type (Fig. 23D). In a similar way, the fraction of chromatin-associated SLX4 did not vary among the different MUS81 forms, however, the amount of EME1 in chromatin was substantially elevated in asynchronous or Noc-arrested cells expressing the phosphomimetic mutant (Fig. 23D). In contrast, expression of the unphosphorylatable MUS81 mutant enhanced the level of chromatin associated EME1 and EME2 in cells treated with 24h HU, and also increased the amount of EME2 in asynchronous, untreated, cells (Fig. 23D). As our results indicate that a mutation mimicking constitutive S87 MUS81 phosphorylation stimulates association with SLX4 but not chromatin recruitment, we decided to analyse if this interaction might be required for subsequent phosphorylation of MUS81 by CK2.

Hence, we analysed S87 phosphorylation by anti-pS87MUS81 IF in cells transfected or not with siRNAs against SLX4 and accumulated in mitosis with Noc. Depletion of SLX4 did not prevent S87 MUS81 phosphorylation, which is indistinguishable from wild-type cells (Fig. 23E). Therefore, our data indicate that phosphorylation of S87 by CK2 is important to stabilize or stimulate the MUS81-SLX4 interaction.

Moreover, they suggest that phosphorylation takes place before formation of the MUS81/EME1/SLX4 complex.

A





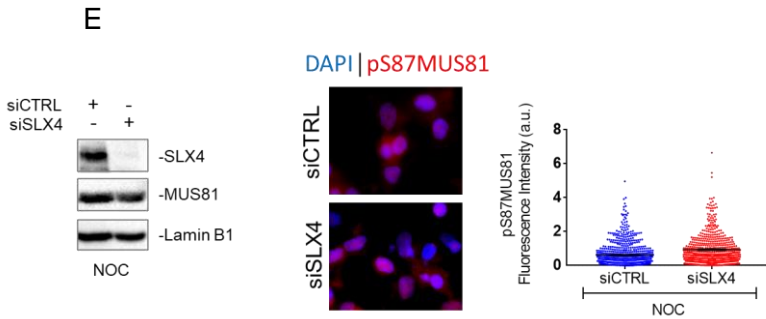
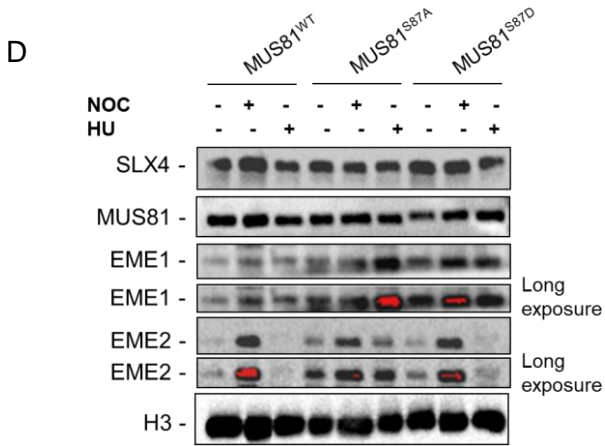


Figure 23 S87-MUS81 phosphorylation regulates SLX4 binding. (A) MUS81 was immunoprecipitated from asynchronous or M-phase synchronized cells expressing MUS81wt or its phosphorylation mutants. The fraction of SLX4 associated to MUS81 was normalized on the total immunoprecipitated MUS81. (B) Interaction of MUS81 and SLX4 was analysed by PLA in asynchronous, THY and NOC-synchronized cells. Representative images of PLA fields are shown. MUS81-SLX4 interaction resulted in red nuclear dots. The mean percentage of PLA-positive cells is represented in the graph in (C). (D) Chromatin fraction was prepared from cells

expressing MUS81wt or its phosphorylation mutants, and treated as indicated. The presence of MUS81 and the indicated proteins in chromatin was assessed by WB. Histone H3 was used as loading control protein. Blots are representative of two different biological replicates. (E)MUS81 phosphorylation was evaluated by anti-pS87MUS81 immunofluorescence on cells transfected siCTRL or siSLX4 and accumulated in M-phase with Noc. The WB shows actual depletion levels, and images are representative of IF. The dispersion graph shows quantification of pS87MUS81 antibody signal intensities.

4. Phosphorylation status of MUS81 at S87 controls unscheduled targeting of HJ-like intermediates in S-phase

By regulating interaction with SLX4, phosphorylation of MUS81 S87 by CK2 may have functional implications. Hence, we used cells expressing the S87 MUS81 phosphomutants as a very specific tool to analyse the phenotypic consequences of a deregulatedMUS81-EME1 function, bypassing the need to interfere with cell-cycle kinases. Our analysis of cell growth evidenced a substantial delay in the proliferation of MUS81S87D cells, while cells expressing the related unphosphorylable MUS81 mutant did not show any apparent defect as compared to the wild-type (Fig. 24A). Delayed proliferation rate of MUS81S87D cells did not correlate with substantial cell cycle defects (Fig. 26A).

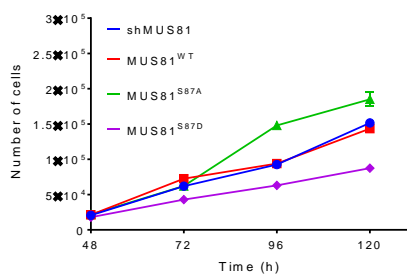
Thus, we analysed if it could derive from accumulation of spontaneous DNA damage by doing immunofluorescence against γ -H2AX or 53BP1. MUS81 deficiency or expression of wild-type MUS81 resulted in low level of γ -H2AX-positive cells (<2%) (Fig. 4B). Very few nuclei were positive for γ -H2AX also in MUS81S87A cells, however, their number was increased of about 10-fold in the phosphomimic S87D mutant (Fig. 24B). Interestingly, in the S87D MUS81 mutant, almost the totality of the γ -H2AX-positive cells were also Cyclin A-positive (i.e. in S or G2 phase) and the large part (60%) were in S-phase (EdU-positive) (Fig. 24C and D). Similarly, the portion of 53BP1-foci/Cyclin A double-positive cells in the population was increased by expression of the phosphomimic MUS81 mutant as compared to MUS81S87A or wild type cells (Fig. 24E).

Flow cytometry analysis of the γ -H2AX-positive population confirmed that DNA damage arises mostly in S-phase or in G2/M cells (Fig. 26B). The higher load of DNA damage in cells expressing the phosphomimic S87D MUS81 protein prompted us to analyse if this could derive from unscheduled targeting of intermediates during DNA replication. We recently demonstrated that ectopic expression of a

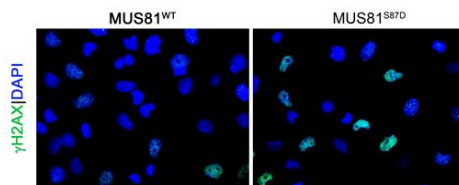
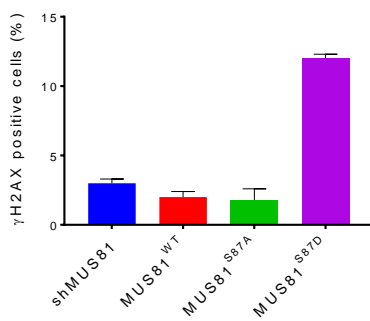
GFP RuvA fusion protein is sufficient to interfere with formation of DSBs by structure-specific endonucleases in human cells during S-phase (Malacaria, 2017). Hence, we ectopically expressed GFP-RuvA in wild-type or in MUS81S87D cells and analysed the presence of DNA damage by neutral Comet assay. As shown in Fig. 25A, the amount of spontaneous DSBs detected in wild-type cells did not decrease upon expression of RuvA. However, expression of RuvA significantly decreased the accumulation of DSBs in MUS81S87D cells. Similarly, when we analysed the formation of 53BP1 foci after ectopic RuvA expression, we observed a substantial reduction of the 53BP1 focus-forming activity especially in cells expressing the S87D MUS81 mutant (Fig. 25B and C). To determine if the incidental cleavage of HJ-like intermediates triggered by deregulated phosphorylation of MUS81 at S87 might correlate also with increased enzymatic activity, we immunopurified FLAG-MUS81 complexes from cells transiently over-expressing the wild-type form of MUS81 or its phosphorylation mutants and assessed the associated endonuclease activity after incubation of anti-FLAG immunoprecipitates with a model nicked HJ, one of the preferred *in vitro* MUS81 substrates (Fig. 27A).

As shown in Fig. 27B, wild type MUS81 apparently cleaved the substrate with comparable efficiency between asynchronous and M-phase enriched cells, while the MUS81-S87D mutant seemed to increase its activity in nocodazole-treated cells. In contrast, the unphosphorylatable MUS81 mutant showed always very little activity. Of note, and in agreement with our PLA and the CoIP data (see Fig. 23), less SLX4 was found associated with the unphosphorylatable MUS81 mutant (Fig. 27C). Surprisingly, loss of S87 phosphorylation MUS81 increased the ability of the protein to immunoprecipitates EME2 although the amount of EME1 was unchanged. Collectively our findings indicate that deregulated MUS81 phosphorylation at S87 and subsequent MUS81-EME1-SLX4 association is sufficient to induce DNA damage in S-phase because of incidental cleavage of HJlike intermediates, which is not correlated with enhanced enzymatic activity.

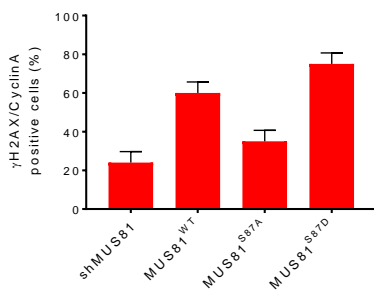
A



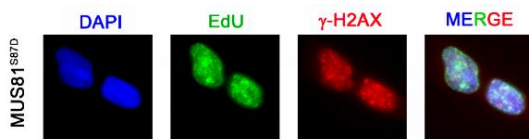
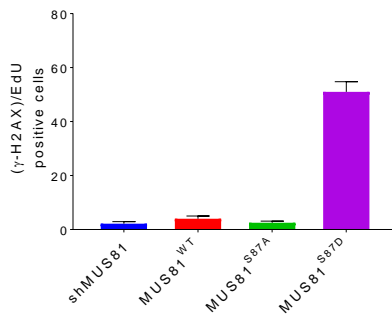
B



C



D



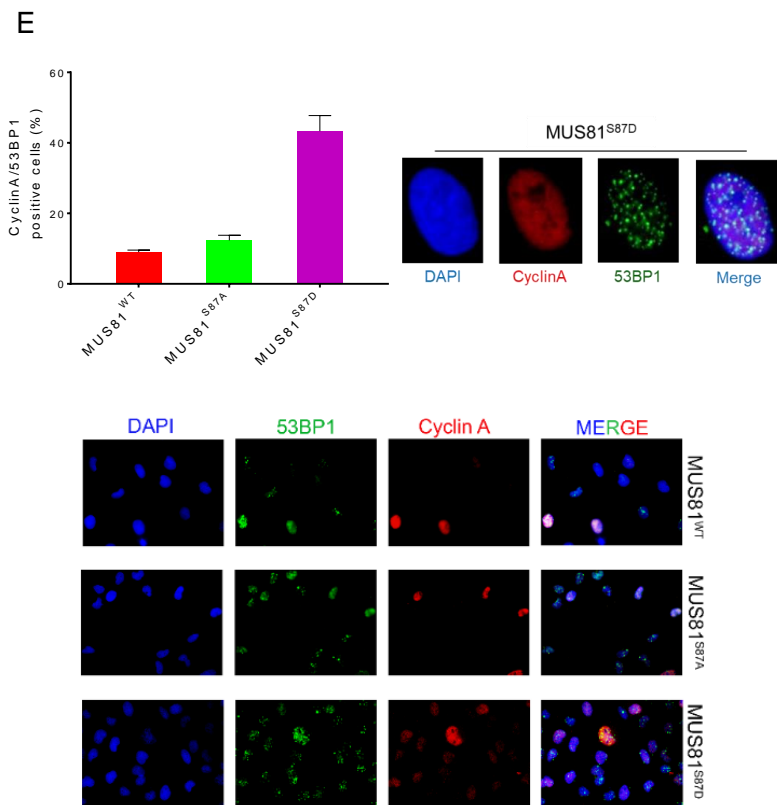


Figure 24 Constitutive phosphorylation of MUS81 at S87 affects cell growth and induces DNA damage. (A) Growth curve in shMUS81 cells stably expressing the wild-type form of MUS81 and its S87 phosphorylation mutants. Each point represents the average number of counts from two independent experiments. (B) Accumulation of spontaneous damage in MUS81 phosphorylation mutants. Untreated cells were immunostained with γ -H2AX antibody, the graph represents the analysis of γ -H2AX positive cells. Representative images of fluorescence fields are shown (γ -H2AX

antibody: green; nuclear DNA: blue). (C) DNA damage, in S/G2-phase cells, was detected by double IF using anti-Cyclin A and γ -H2AX antibodies. (D) Analysis of the level of DNA damage during replication. Cells in S-phase were labelled by an EdU pulse and the graph shows the percentage of EdU (green) and anti- γ -H2AX (red) positive cells. Nuclear DNA was counterstained by DAPI (blue). (E) Analysis of 53BP1 foci formation in Cyclin A positive cells. Representative image of fluorescence cells stained with anti-53BP1 (green) and anti-Cyclin A (red) antibodies. Nuclear DNA was counterstained by DAPI. The graph shows quantification of the 53BP1-positive Cyclin A-cells. Data are mean values from three independent experiments. Statistical analysis was performed by Student's t-test. Significance is reported compared to the wild-type: ***P < 0.01; *P < 0.05.

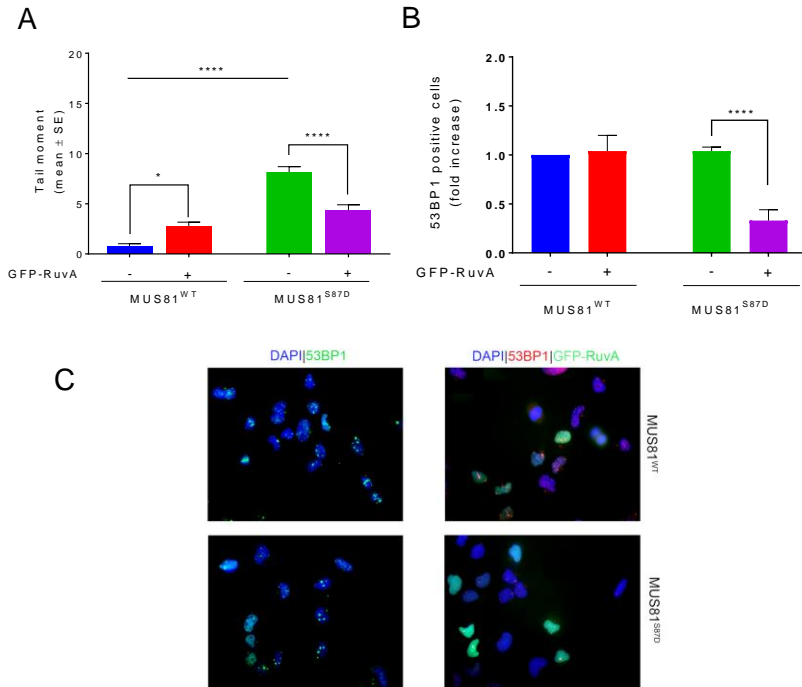
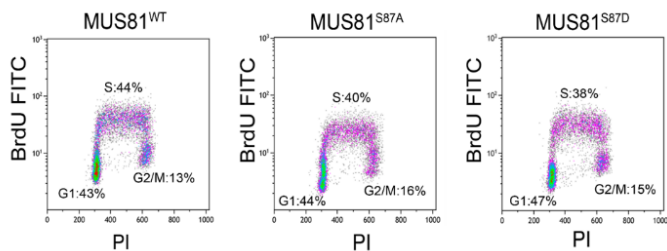
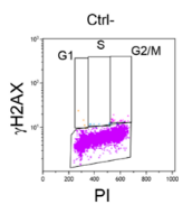


Figure 25 Ectopic GFP-RuvA expression reduces formation of DSBs and 53BP1 foci in constitutive-active MUS81 mutant. (A) MRC5 shMUS81 cells, stably expressing WT or S87D phosphomimetic MUS81 were transfected or not with GFP-RuvA. DSBs were evaluated 48h after transfection by neutral Comet assay. (B) The presence of 53BP1 nuclear foci was evaluated by IF 48 h after transfection. The graph shows the fold increase of 53BP1 foci-positive cells over the untransfected cells. Data are presented as mean \pm standard error (SE) from three independent experiments. * $P \leq 0.5$; **** $P \leq 0.001$, ANOVA test. (C) Representative microscopy fields are presented: 53BP1 antibody (green or red), GFP-RuvA and nuclear DNA was counterstained by DAPI (blue).

A



B



Genotype	γ -H2AX-positive cells (%)			
	G1	S	G2/M	Total
shMUS81	1,14	0,5	1,12	2,76
shMUS81 ^{WT}	0,95	0,78	1,77	3,50
shMUS81 ^{S87A}	0,51	0,54	1,01	2,06
shMUS81 ^{S87D}	0,70	1,14	2,80	4,64

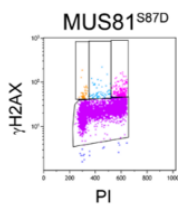
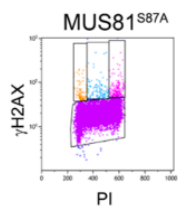
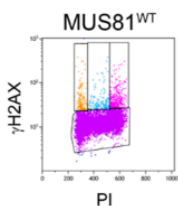
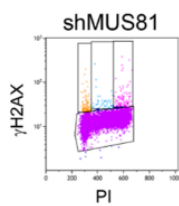


Figure 26 Flow cytometry analysis of cell cycle progression and DNA damage. (A) Asynchronously proliferating MRC5 cells were treated with a 1 h 5-Bromo-2'-Deoxyuridine (BrdU) pulse, stained for BrdU and analyzed by quantitative flow cytometry. Density plots depict mean BrdU intensities. PI staining was used to determine DNA content. (B) Asynchronously proliferating MRC5 cells were stained for γ -H2AX and analyzed by quantitative flow cytometry. Dot plots depict mean γ -H2AX intensities versus total nuclear DNA (PI intensities). The table shows the percentage of γ -H2AX-positive cells in each phase of cell cycle from a representative experiment.

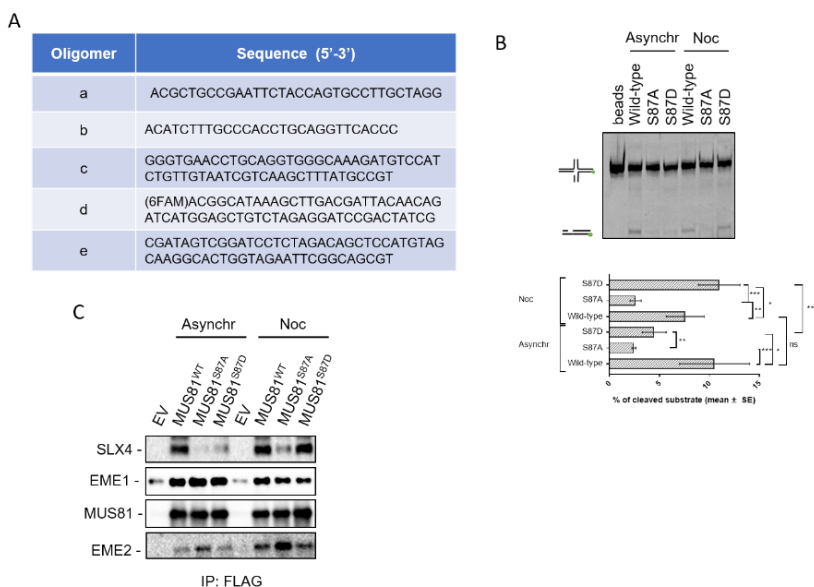


Figure 27 Phosphorylation status of S87 affects MUS81 catalytic activity. (A) Oligomer sequences used to build the synthetic nicked-Holliday Junction (nHJ) substrate. One oligonucleotide (d) is 5' 6-FAM end-labelled. (B) FLAG-MUS81wt,

FLAG-MUS81S87A and FLAG-MUS81S87D immunoprecipitated from asynchronous and Noc-treated cells were incubated with the indicated nHJ substrate (50nM). 5' end fluorescent label is indicated as a green dot. Reaction was performed at 30°C for 90 min and the DNA substrates were analyzed by neutral PAGE. The unbound anti-FLAG beads (1st lane) were used as negative control. Quantification of cleaved products, expressed as percentage of the total substrate, is reported in the graph at the bottom of the panel. (C) The same FLAG-MUS81 immunoprecipitates used in the nuclease assay were analysed by Western blotting for the indicated proteins.

5. Phosphorylation at Serine 87 induces premature mitotic entry through unscheduled MUS81 function in S-phase

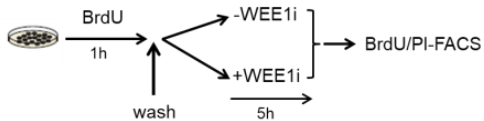
Recent data evidenced that inhibition of WEE1 leads to premature activation of the MUS81 complex, because it releases CDK1 inhibition and stimulates phosphorylation of SLX4, licensing the formation of the MUS81/SLX4 complex in S-phase, and inducing uncontrolled progression in mitosis of unreplicated cells (Duda, et al., 2016). We show that phosphorylation of MUS81 at S87 is crucial to MUS81-EME1 activation. Hence, we analysed if abrogation of S87 phosphorylation could revert the effect of WEE1 inhibition. To analyse premature mitotic entry from S-phase, we pulse-labelled a

subset of replicating cells with BrdU, chased them in BrdU free medium in the presence or absence of WEE1 inhibitor, and analysed progression of the BrdU-positive population through the cell cycle by bivariate flow cytometry (Fig. 28). Under unchallenged conditions, no substantial difference in the progression of the labelled S-phase population was observed in wild-type and MUS81S87A cells. However, a higher percentage of BrdU-labeled G1 cells (G1*), a sign of a faster transit through the cell cycle, was observed in MUS81S87D cells after 5 h of chase as compared with the wild-type ones (Fig. 28B and C). As expected, in wild-type cells, inhibition of WEE1 (WEE1i) resulted in a faster progression from S-phase to mitosis, resulting in a strong increase of BrdU-positive cells in the subsequent G1- phase. In contrast, and interestingly, expression of the unphosphorylable S87A-MUS81 protein completely reverted the effect of WEE1i on cell cycle. Surprisingly, a reduction of the number of BrdU-positive G1 cells after WEE1 inhibition was also observed in cells expressing the phosphomimetic S87D-MUS81 mutant. Consistent results were also obtained by analysing progression of a BrdU-pulse labelled population to mitosis by anti-pS10H3/BrdU double immunofluorescence (Fig. 28D).

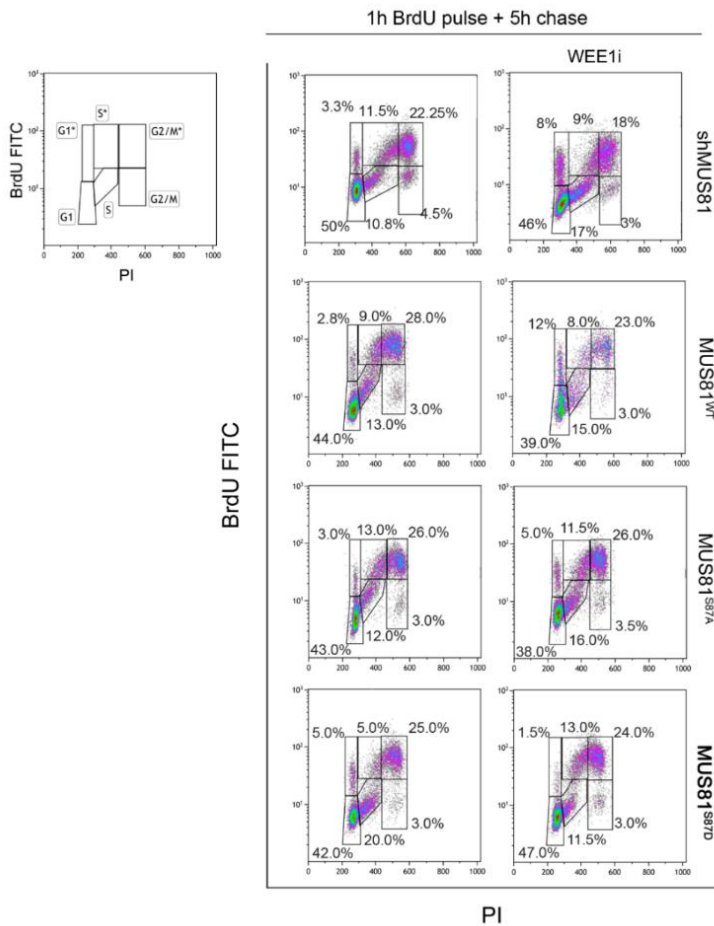
Indeed, treatment of wild-type cells with WEE1i greatly increased the number of BrdU-positive cells accumulated in mitosis by Noc, while expression of the S87A-MUS81 mutant reverted the phenotype. Of note, inhibition of WEE1 failed to increase the fraction of BrdU-positive mitosis detected in MUS81S87D cells. Inhibition of CDK1 can prevent unscheduled activation of MUS81 by WEE1i (Duda, et al., 2016). As shown in Fig. 29A, inhibition of CDK1 reverted the progression of BrdU-labelled S-phase cells to G2/M and the subsequent G1, which is stimulated by WEE1 inhibition, irrespective of the presence of a mutant MUS81 protein. Suppression of the WEE1i-induced premature mitotic entry is also obtained with EME2 or SLX4 depletion (Duda, et al., 2016). In wild type cells, depletion of EME2 reduced the unscheduled progression from S to G2/M and G1, which is stimulated by WEE1 inhibition, but only partially (Fig. 29B and C). Of note, depletion of EME2 reduced the limited progression from S to G2/M and G1 observed in the S87A-MUS81 mutant, while was largely ineffective in modulating the phenotype of the S87D-MUS81 mutant, either in the absence or in the presence of WEE1i. A consistent effect was observed when we analysed the S-M progression

by anti-pS10H3/BrdU double immunofluorescence (Fig. 29D). Depletion of EME2 reduced the premature S-M transit induced by WEE1i in wild-type cells, while it minimally affects the MUS81S87D phenotype. As expected, depletion of SLX4 completely reverts premature SM transit independently on the deregulated S87 phosphorylation of MUS81 (Fig. 29D). These results indicate that phosphorylation of MUS81 by CK2 is absolutely required for the pathological S/M transit associated to WEE1 inhibition and deregulated phosphorylation of SLX4. Moreover, they suggest that the presence of a constitutively-activeMUS81 complex and WEE1 inhibition does not synergize, but rather result in an apparent slow-down of the cell cycle.

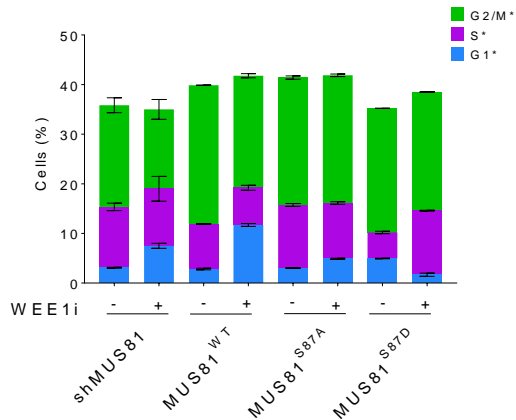
A



B



C



D

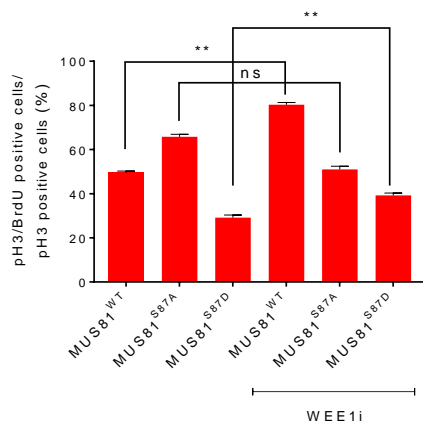
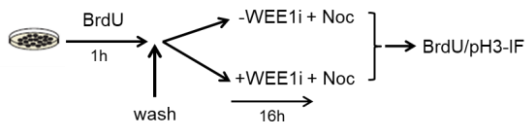
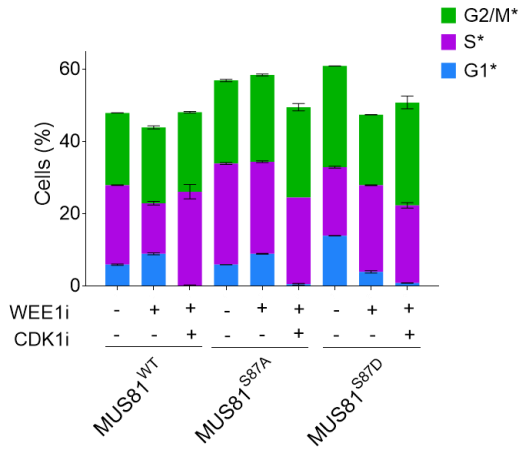
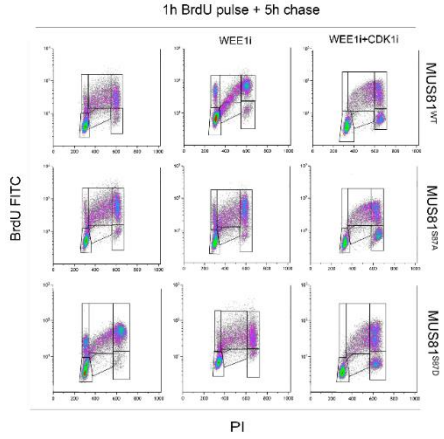
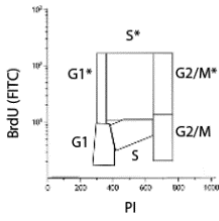
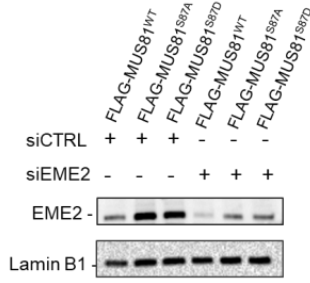


Figure 28 Premature mitotic entry mediated by unscheduled MUS81 function in S-phase depends on phosphorylation at S87. (A) Experimental workflow. (B) S-phase cells were pulse-labelled with BrdU and released in free medium for 5 h, in the presence or not of the WEE1 inhibitor MK-1775 (WEE1i). Progression of S-phase cells through the cell cycle was analysed by bivariate flow cytometry. The scheme indicates how each population was assigned. The star (*) denotes S-labeled, BrdU-positive, populations. Density plots depict mean BrdU intensities versus total nuclear DNA intensities (PI). The percentage of cells found in each phase of cell cycle is indicated. (C) The graph shows the percentage of cells in G2/M*, S* and G1* phase treated or not with WEE1i inhibitor MK-1775, relative to scatterplots in (B). (D) Immunofluorescence analysis of S-M progression. S-phase cells were labelled with a 1 h BrdU pulse, and released in nocodazole to accumulate mitosis. Cells accumulated in mitosis for 16 h, in presence or not of WEE1i, and immunostained using anti-BrdU and pS10H3 antibodies. Data are presented as mean \pm standard error (SE) from three independent experiments. **P < 0.1; ns = not significant, ANOVA test.

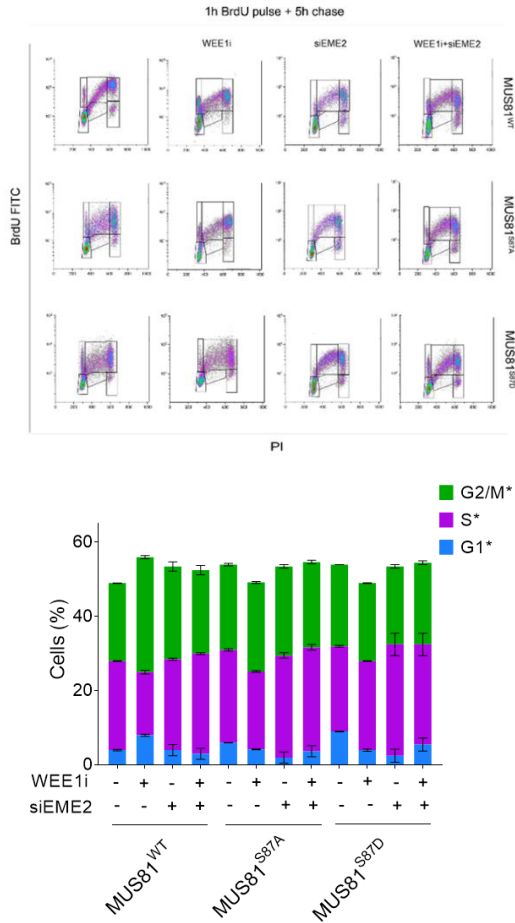
A



B



C



D

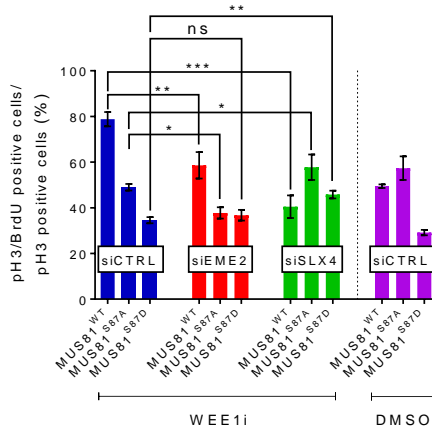


Figure 29 Progression analysis of the BrdU-positive cells through the cell cycle by bivariate flow cytometry. In A) Asynchronously proliferating MRC5SV40 complemented with MUS81WT and S87 phosphorylation mutant cells were treated with a 1h 5-Bromo-2'-Deoxyuridine (BrdU) pulse, release in free medium for 5h, treated or not with WEE1 inhibitor MK-1775 (500nM) and CDK1 inhibitor as indicated and stained for BrdU. The graph shows the analysis by quantitative flow cytometry. Scatterplots depict mean BrdU intensities versus total nuclear PI intensities. The graph shows the percentage of cells in G2/M*, S* and G1* phase treated or not with WEE1i and CDK1i, relative to scatterplots. (B) Western blot of EME2 interference in MRC5SV40 complemented with MUS81WT and S87 phosphorylation mutant cells. Lamin B1 was used as loading control. (C) Analysis by quantitative flow cytometry performed as in (A) with cells treated with WEE1i and/or transfected with siEME2. The graph shows the percentage of cells in G2/M*, S* and G1* phase treated or not with WEE1i and with siEME2, relative to scatterplots.

(D) Immunofluorescence analysis of S-M progression. S-phase cells were labelled with a 1h BrdU pulse and released in nocodazole to accumulate mitosis. Cells accumulated in mitosis for 16h, in presence or not of WEE1i, and immunostained using anti-BrdU and pS10H3 antibodies. Data are presented as mean \pm standard error (SE) from three independent experiments.

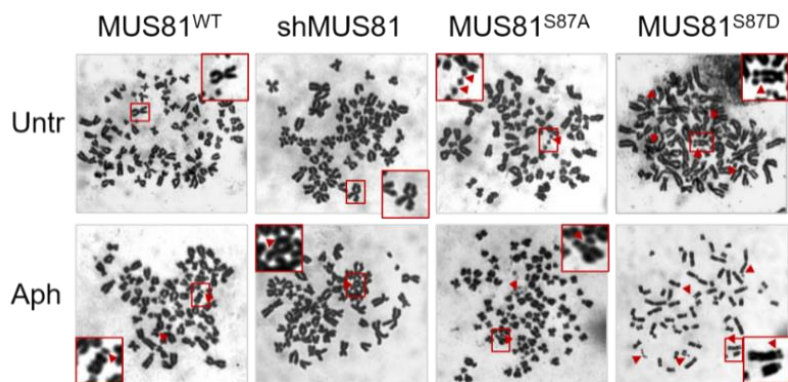
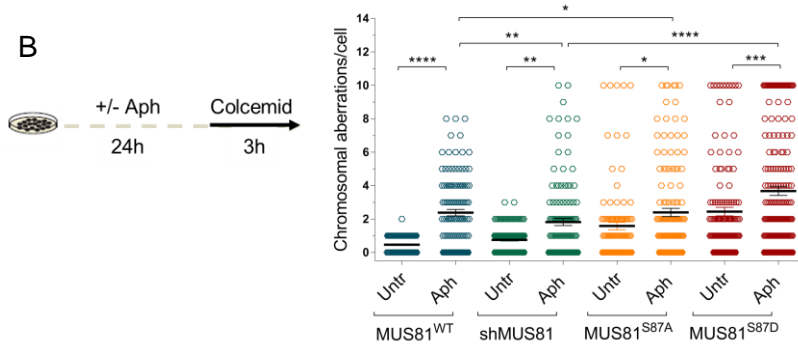
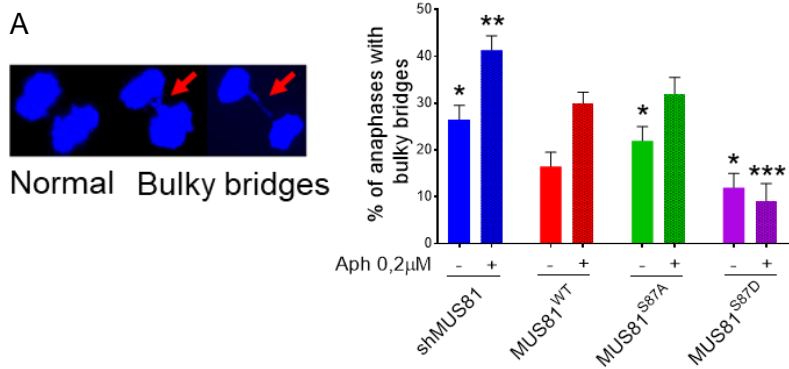
6. Regulated phosphorylation of MUS81 at Serine 87 is essential to prevent accumulation of genome instability

Downregulation of MUS81 induces mitotic defects and accumulation of bulky anaphase bridges as a consequence of poor resolution of replication/recombination intermediates prior to mitosis (Garner et al., 2013; Matos, Blanco, & West, 2013a). Our data suggest that S87 phosphorylation of MUS81 may affect function of the complex in mitosis. Hence, we analysed the presence of bulky anaphase bridges in cells expressing the wild-type MUS81 or the two S87 phosphomutants, exposed or not to a low-dose Aph (Fig. 30A). Under unperturbed cell growth, the number of anaphase cells with bulky chromatin bridges was found elevated, albeit modestly, in both MUS81-depleted cells and in cells expressing the unphosphorylatable S87A-MUS81 protein. In contrast, very few anaphases with bulky chromatin bridges were found in cells

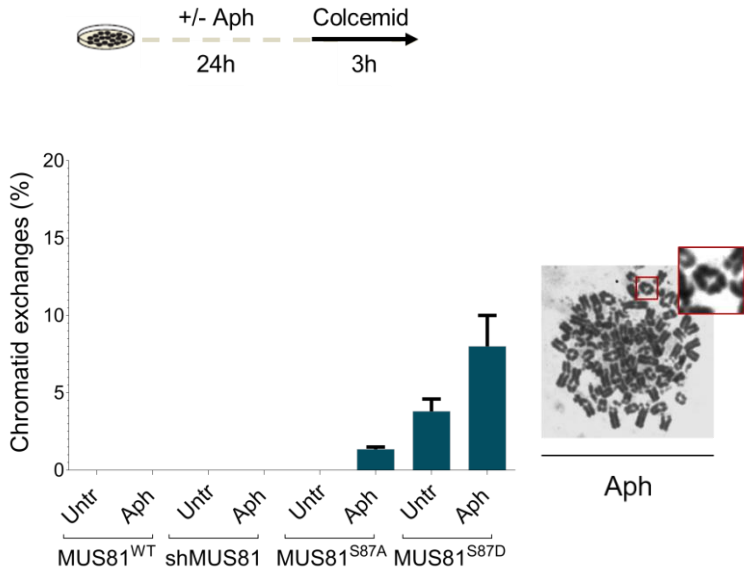
expressing the phosphomimic mutant of MUS81. In Aph-treated cells, the percentage of anaphases with bulky chromatin bridges was similar among cell lines, except those expressing the phosphomimic S87DMUS81mutant, which showed less anaphase bridges. These data support the functional role of S87 phosphorylation of MUS81 in mitosis. Nevertheless, deregulation of S87 phosphorylation causes DNA damage in S-phase being involved in premature formation of theMUS81/EME1/SLX4 complex. Hence, we investigated whether expression of the S87 unphosphorylable or phosphomimic MUS81mutant might undermine genome integrity. To this end, we analysed the number and type of chromosomal damage in metaphase spreads from cells treated or not with a low-dose Aph, which induces a mild replication stress that the MUS81 complex contributes to fix. As shown in Fig. 30B, mild replication stress increased the frequency of chromosome breakage in wild-type cells. As expected, the number of chromosome breaks detected on mild replication stress was slightly reduced upon MUS81 downregulation while, unexpectedly, it was only slightly enhanced by expression of the S87 unphosphorylable MUS81mutant. In contrast, the frequency of chromosome breakage

was significantly higher in cells expressing the S87D-MUS81 mutant already under unperturbed replication and increased further upon treatment with Aph. Interestingly, MUS81S87D cells also showed complex chromosome aberrations, such as chromatid exchanges and pulverized metaphases, which were otherwise absent in wild-type or MUS81S87A cells (Fig. 30C). The unscheduled targeting of replication forks by the MUS81 endonuclease triggered by chemical inhibition of WEE1 is sufficient to induce chromosome pulverization (Duda et al., 2016). As we show that S87 phosphorylation predominates on WEE1 inhibition (Fig. 28), we evaluated if chromosome pulverization observed in cells treated with the WEE1i might be modulated by the presence of the two S87 phosphomutants of MUS81. As reported in Fig. 30D, inhibition of WEE1 resulted in the appearance of pulverized metaphases in wild type cells, and this phenotype greatly increased in response to Aph. As expected, the percentage of pulverisation was significantly reduced in MUS81-depleted cells respect to the wild-type, especially after Aph treatment (Fig. 30D). Interestingly, WEE1i-dependent chromosome pulverisation was suppressed also by expression of the S87A-MUS81 mutant (Fig. 30D).

Conversely, MUS81S87D cells showed chromosome pulverization even in absence of WEE1i, and the phenotype was significantly enhanced in its presence, suggesting that pharmacological override of cell cycle control and unscheduled targeting of replication forks by the MUS81/EME1 complex act synergistically. Interestingly, while depletion of EME2 partially rescued the pulverization phenotype associated to inhibition of WEE1 in wild type cells it failed to modulate the pulverisation detected in MUS81S87D cells (Fig. 31A and B), confirming that expression of the phosphomimeticMUS81 mutant preferentially engages the MUS81/EME1 complex. Therefore, we conclude that phosphorylation of MUS81 S87 by CK2 is required to support function of the MUS81 complex during resolution of intermediates accumulating under mild replication stress, but also that loss of regulated phosphorylation strongly undermines genome integrity.



C



D

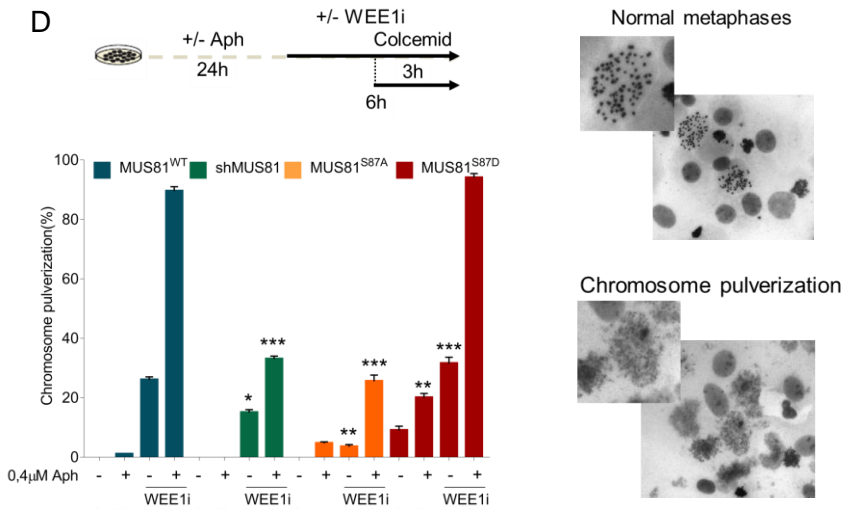


Figure 30 Regulated phosphorylation of MUS81 at S87 is essential to prevent accumulation of genome instability. (A) Analysis of the bulky anaphases bridges in MUS81 phosphomutants treated with a low-dose Aphidicolin (Aph). The graph shows the fractions of mitotic cells with bulky anaphase bridges. Error bars indicate SE; n=3 (>50 mitotic cells were analyzed in each population). Data are presented as mean \pm standard error (SE) from three independent experiments. *P < 0.5; **P < 0.1; ***P < 0.01, ANOVA test. Significance is reported compared to the wild-type. Representative images of single anaphases from the phosphomimetic MUS81 mutant are shown. Arrows indicate bridges. (B) Experimental scheme for evaluation of chromosomal aberrations is shown. Dot plot shows the number of chromosome aberrations per cell. Data are presented as means of three independent experiments. Horizontal black lines represent the mean \pm SE. (ns, not significant; **P < 0.01; ***P < 0.001; ****P < 0.0001 two-tailed Student's t test). Representative Giemsa-stained metaphases are given. Arrows in red indicate chromosomal aberrations. (C) Analysis of the frequency of metaphase spreads with chromatid exchanges in cells treated and processed as in (B). Bar graph shows the percentage of chromatid exchanges per metaphase cell. Data are presented as means of three independent experiments. Horizontal black lines represent the mean \pm SE. A representative Giemsa-stained metaphase with chromatid exchanges is given. (D) Experimental scheme for evaluation of chromosomal aberrations is shown. Bar graph shows the frequency of pulverized metaphases per metaphase cell. Data are presented as means of three independent experiments. Error bars representing standard errors are not shown or clarity but are <15 of the mean (*P < 0.5; **P < 0.01; ***P < 0.001; two-tailed

Student's t test). Representative Giemsa-stained metaphases are given for both normal and pulverized phenotype. Significance is reported compared to the wild-type.

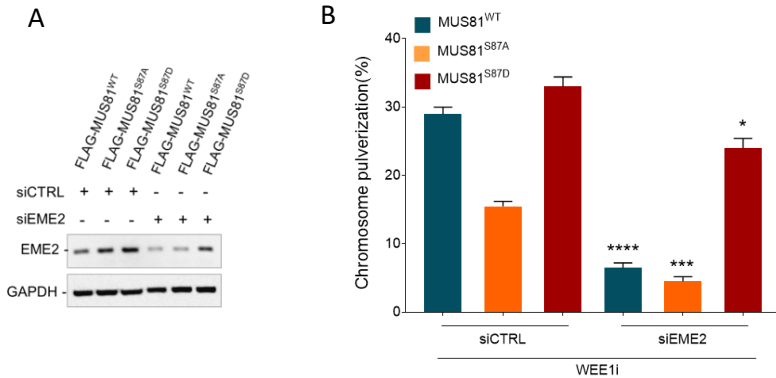


Figure 31 Depletion of EME2 does not prevents chromosome pulverization induced by expression of the S87 phosphomimetic MUS81 mutant. (A) Western blot of EME2 interference in MRC5SV40 complemented with MUS81WT and S87 phosphorylation mutant cells. Lamin B1 was used as loading control. B) Bar graph shows the frequency of pulverized metaphases per metaphase cell. Data are presented as means of three independent experiments. Error bars representing standard errors are not shown or clarity but are < 15 of the mean (*, $p < 0.5$ ** , $p < 0.01$; ***, $p < 0.001$; two-tailed Student's t test).

PART II

1.Regulation of the mitotic function of MUS81 by CK2 sustains viability in cells lacking BRCA2

Since we know that proliferation of BRCA2-deficient cells relies on the MUS81 complex to reduce replication stress in S-phase and to prevent detrimental consequences of under-replicated DNA in mitosis (Lai et al., 2017), we asked how much of the pro-survival role of the MUS81 complex depends on its mitotic function. To this aim, we took advantage from regulatory mutants of MUS81 that affect proper activation in the M-phase of the cell cycle by the CK2 kinase (Palma, Pugliese et al., 2018). MRC5 fibroblasts stably-depleted for MUS81 and complemented with the wild-type MUS81 (MUS81^{WT}), its CK2-unphosphorylable (MUS81^{S87A}) or CK2-phosphomimetic (MUS81^{S87D}) mutant were transfected with siRNA targeting BRCA2 (Fig.32A). Forty-eight hours after transfection, cells were seeded at low-density to analyse, by clonogenic assay, whether a loss of regulated MUS81 complex function in M-phase affected proliferation and viability in the absence of BRCA2. As expected, concomitant loss of MUS81 and BRCA2 caused a significant decrease in cell survival

compared to BRCA2 depletion alone (MUS81^{wt}) (Lai et al., 2017) (Fig. 32B-C). A less prominent decrease of cell proliferation was also observed in cells lacking BRCA2 and expressing MUS81^{S87A}, but not in cells expressing MUS81^{S87D} (Fig. 32B-C). To determine whether BRCA2 depletion affected S87MUS81 phosphorylation, we performed anti-pS87MUS81 immunofluorescence in asynchronous cultures of MUS81^{WT} cells (untr) or in cultures enriched in M-phase by nocodazole (NOC). Anti-pS87MUS81 immunofluorescence was coupled with EdU detection to identify any abnormal activation of the MUS81 complex in S-phase (Fig. 32D). As expected, MUS81 phosphorylation at S87 by CK2 was barely detectable in S-phase cells whereas it was abundant in Noc-arrested cells (Fig. 32D). Interestingly, depletion of BRCA2 did not induce any unscheduled phosphorylation of MUS81 at S87 in S-phase or increased its normal mitotic modification (Fig. 32D). Collectively these results confirm the important role of MUS81 in BRCA2-depleted cells and suggest that phosphorylation of S87 by CK2 is important to sustain proliferation in BRCA2 deficient cells.

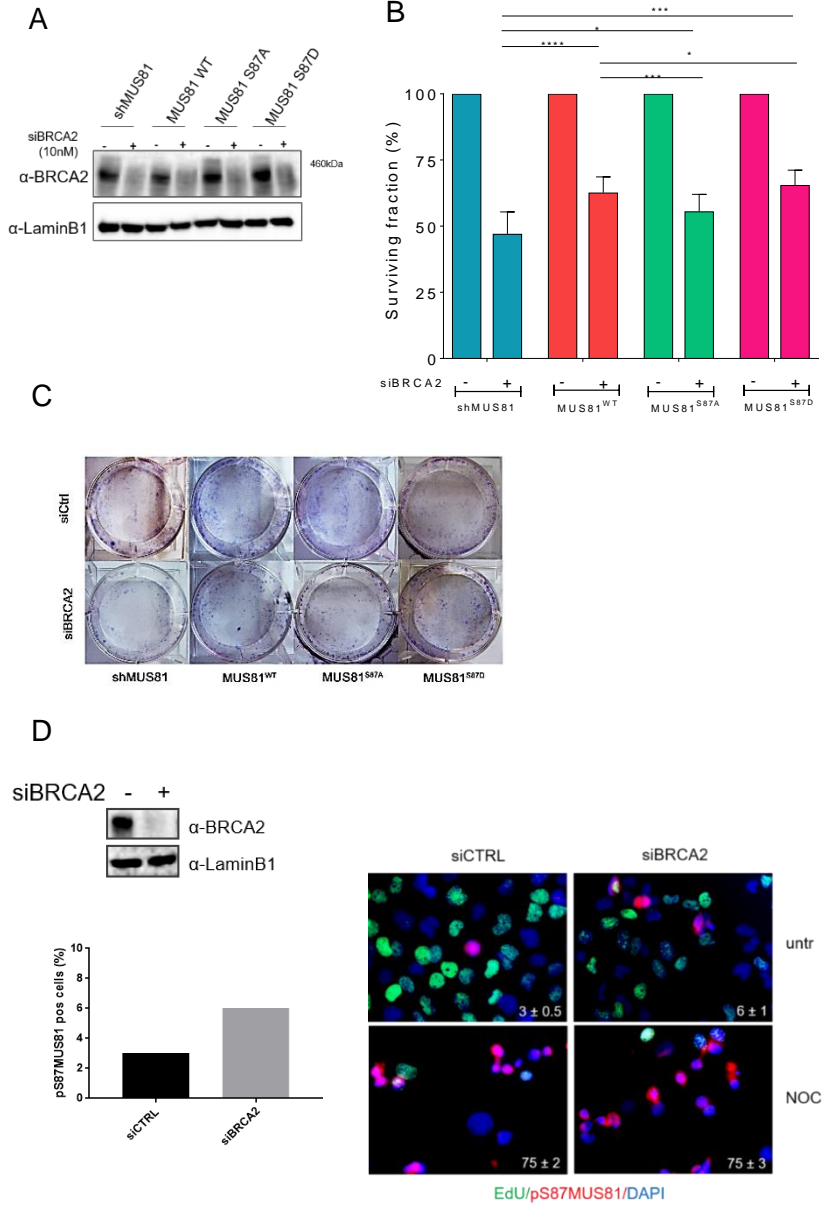


Figure 32 Regulation of the mitotic function of MUS81 by CK2 sustains viability in cells lacking BRCA2. (A) Analysis of protein depletion by Western blotting in MRC5 SV40 cells after transfection with control siRNAs or siBRCA2. Immunoblotting was performed 48 h after transfection using the indicated antibodies. Lamin B1 was used as loading control. (B) Cells treated as in A were plated 48h after transfection for clonogenic assay. Colonies were stained after 10-14 days. Error bars represented s.d. (n=4). *P<0.5, **** P<0.001, ANOVA test. (C) Representative images of GIEMSA stained colonies. (D) MUS81 phosphorylation by anti-pS87MUS81 immunofluorescence (red) was evaluated in MRC5 SV40 shMUS81 and MUS81 wild-type stably complemented cells transfected with siCTRL or siBRCA2 and previously exposed to a 30min EdU pulse to mark S-phase cells (green). Nuclei were depicted by DAPI staining (blue). Nocodazole (NOC) was used as control of cells accumulated in M-phase. The WB shows actual depletion levels, and images are representative of IF. The graph shows quantification of pS87MUS81 antibody signal intensities.

2. DNA damage in BRCA2-depleted cells correlates with phosphorylation status of S87-MUS81 and influence cell cycle progression

Our data show that abrogation of the mitotic function of the MUS81 complex through loss of CK2-dependent regulation of MUS81 is sufficient to reduce proliferation of BRCA2-deficient cells

recapitulating downregulation of MUS81 by RNAi. Since loss of BRCA2 induces accumulation of DNA breakage even under unperturbed cell growth and recent works demonstrate that DSBs formation after HU is prevented by MUS81 depletion in the absence of BRCA2 (Feng and Jasin 2017; Lemaçon et al. 2017b), we reasoned that BRCA2-deficient cells might require mitotic MUS81 function to induce DNA breaks for resolution of persistent replication intermediates. To this aim we performed neutral Comet assay to detect DSBs formation in shMUS81 cells complemented with the mitotic phosphomutants of MUS81 and depleted or not of BRCA2 (Fig. 33B). As expected, the analyses revealed few DSBs in cells depleted of MUS81 or in cells complemented with the wild-type MUS81 protein (Fig. 33B). Similarly, few DSBs were found in shMUS81 cells complemented with the S87A MUS81 mutant, whereas, a significant increase in the amount of DSBs was detected in cells expressing the S87D phosphomimetic mutant of MUS81 (Fig 33B). As expected, depletion of BRCA2 in wild-type cells increased the amount of DSBs, which were not detected in the shMUS81 cells (Fig. 33B). Interestingly, the increased formation of DSBs associated with

downregulation of BRCA2 was neither affected by loss of S87 MUS81 phosphorylation nor by its constitutive activation (Fig. 33B). To further investigate on the functional role of MUS81 phosphorylation at S87 in BRCA2-depleted cells we next analysed the level of H2AX phosphorylation, another diagnostic sign of DNA damage, by immunofluorescence. To discriminate between H2AX phosphorylation occurring in S-phase or in other phases of the cell cycle, we coupled anti- γ -H2AX immunofluorescence with detection of EdU incorporation. Consistently with what observed by neutral Comet assay, anti- γ -H2AX immunofluorescence confirmed that BRCA2 depletion increased DNA damage in wild-type cells (Fig. 33C). Although downregulation of MUS81 or the expression of MUS81^{S87A} resulted in low level of γ -H2AX-positive cells, the BRCA2-depletion surprisingly induced an accumulation of DNA damage especially in EdU-positive cells (Fig. 33C). By contrast, MUS81^{S87D} failed to further stimulate DNA damage in absence of BRCA2 but changed dramatically the ratio between the total number of γ -H2AX- and EdU/ γ -H2AX-positive cells (Fig. 33C). To evaluate whether DNA damage accumulation could lead to cell cycle defects,

we performed bivariate flow cytometry analysis of replicating cells pulse-labelled with 1h of BrdU (Fig. 34A). No overt difference in cell cycle was observed between the MUS81 mutant cell lines when BRCA2 was depleted (Fig. 34B). This result led us to investigate if concomitant BRCA2-depletion and abrogation of mitotic MUS81 function could affect progression from S to M-phase (S-M transition). To this end, we combined anti-pS10-H3 immunostaining with detection of EdU incorporation in S-phase cells (Fig. 34C). Depletion of BRCA2 halved the percentage of MUS81^{WT} cells entering mitosis from S-phase in the 8h chase period after pulse-labelling with EdU (Fig. 34D), confirming that loss of BRCA2 delays S-phase transit and/or induces accumulation in G2, to pause cell cycle for preserve genetic stability (Patel et al., 1998; Yu et al., 2000). In contrast, the delayed S-M transit induced by BRCA2 depletion did not occurred in absence of MUS81 or upon expression of the unphosphorylable S87A mutant (Fig. 34D). Surprising, a strongly-delayed S-M progression was apparent in MUS81^{S87D} cells and this phenotype was exacerbated after BRCA2-depletion (Fig. 34D). Altogether, these results support the idea that MUS81 activity in M-phase is required for a correct S-M

transition in BRCA2-deficient cells. Loss of MUS81 induces a replication fork progression defects in BRCA2-depleted cells (Lai et al., 2017). To determine whether increased DNA damage and delayed cell cycle progression observed in absence of MUS81 or upon expression of the unphosphorylable S87A mutant could correlate with defects in fork progression, we measured replication rates using DNA fibre assays. Ongoing forks were labelled using two consecutive IdU/CldU pulses of 15min to reduce the effect of fork degradation on replication tract length. Indeed, under our experimental conditions, depletion of BRCA2 did not significantly affect the length of replication tracks (Fig. 34E). According to previous studies (Sarbjana et al., 2014; Lai et al. 2017), MUS81 depletion had no effect on fork progression if BRCA2 is present, while its depletion combined with that of BRCA2 resulted in shorter replication track lengths (Fig. 34E). Of note, although expression of each MUS81 phosphorylation mutant did not significantly alter the replication track length compared with cells expressing wild-type MUS81, concomitant depletion of BRCA2 reduced replication track lengths in the presence of the unphosphorylable S87A mutant (Fig. 34E). Surprisingly, this did not

happen in the MUS81^{S87D}, in which the depletion of BRCA2 failed to influence fork velocity. These results indicate that concomitant loss of MUS81 or its mitotic phosphorylation at S87 can enhance greatly DNA damage in the absence of BRCA2, which seems unrelated to DSBs processing, but possibly linked with reduced fork velocity and inability to slowdown S-M transition.

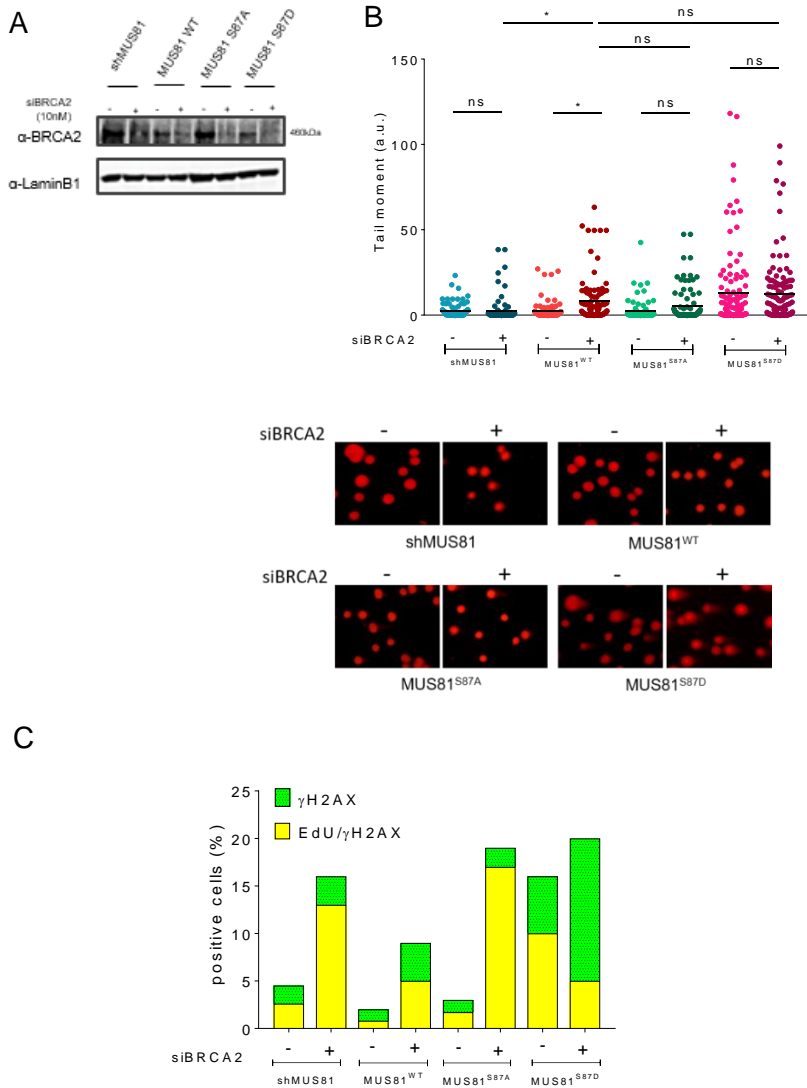


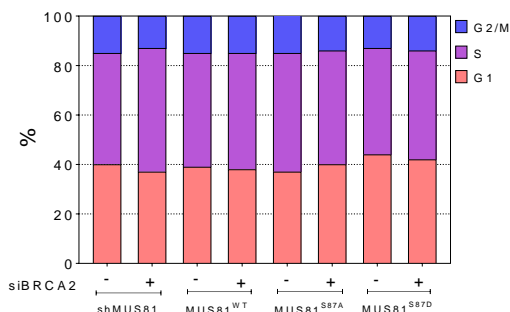
Figure 33 DNA damage in BRCA2-depleted cells correlates with phosphorylation status of S87-MUS81. (A) Analysis of protein depletion by Western blotting in MRC5

SV40 cells after transfection with control siRNAs (siCtrl) or siBRCA2. Immunoblotting was assessed 48 h after transfection using the appropriate antibodies. Lamin B1 was used as loading control. (B) Formation of DSBs after BRCA2-depletion. Cells were transfected with a Ctrl siRNA or with a siRNA against BRCA and, 48h afetr DSBs were evaluated by neutral comet assay. Data are presented as mean±SEM from three independent experiments. Statistical analysis was performed by two-way ANOVA test: ns, not significant, *P≤0.5, **** P≤0.001. Representative images of Comets are presented in the panel. (C) Analysis of the level of DNA damage during replication. Cells in S-phase were labelled by an EdU pulse and the graph shows the percentage of EdU and anti-γ-H2AX positive cells.

A



B



(C) Experimental scheme used to study the S-M transition in MUS81 phosphorylation mutants after BRCA2-depletion and Nocodazole accumulation. (D) Immunofluorescence analysis of S-M progression. S-phase cells were labelled with EdU pulse, and released in nocodazole to accumulate mitosis as in (C). Cells accumulated in mitosis, depleted or not with siBRCA2, and immunostained using anti-EdU and pS10H3 antibodies. (E) Experimental scheme of dual labelling replication assay for DNA fibres. Red tract: CldU; green tract: IdU. Dot plot showing the IdU+CldU tract length (μm) of ongoing forks in single DNA fibres from MRC5 SV40-derived cells stably non expressing MUS81, MUS81 wild-type and the two phosphomimetic forms (S87A and S87D) depleted or not with siBRCA2. The length of the tract was measured in at least 100 well isolated DNA fibres from three independent experiments. Mean values are represented as horizontal black lines \pm SE (ns = not significant; $P > 0.05$; $**P < 0.01$; $***P < 0.001$; $****P < 0.0001$; ANOVA test).

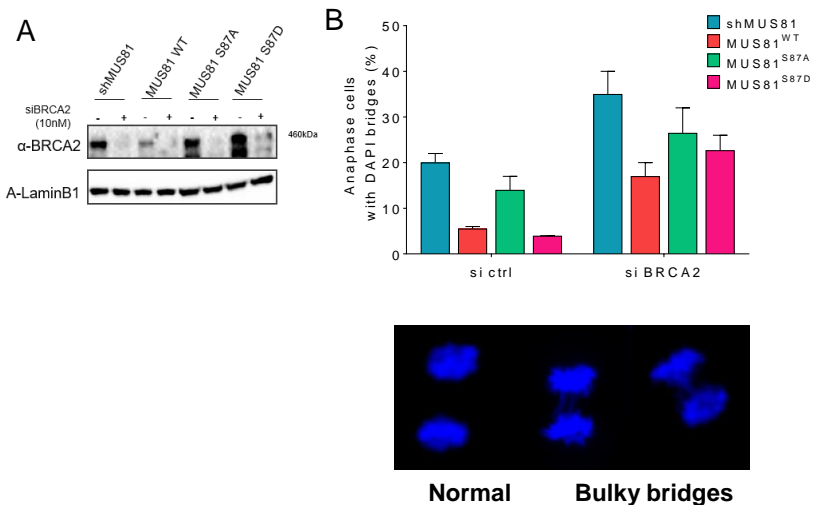
3. The absence of BRCA2 leads to formation of mitotic chromosome bridges in constitutive active MUS81 mutant

Since unresolved DNA and chromatin bridges during anaphase and telophase can induce cytokinesis defects, DNA segregation abnormalities might contribute to the cytokinetic defects in BRCA2 deficient cells (Choi et al., 2012; Daniels et al., 2004; Mondal et al., 2013). We recently demonstrated the important functional role of S87

phosphorylation in mitosis for the resolution of intermediates at under-replicated regions (Palma, Pugliese et al., 2018). Thus, we want to test whether S87MUS81 and BRCA2-depletion could impact on chromosome segregation. As expected, quantification of DAPI-positive anaphase bridges revealed that MUS81 inactivation in BRCA2-depleted cells led to a higher percentage of cells with DAPI-positive bridges compared to BRCA2 depletion alone (Fig. 35A). In agreement with our previous data (Palma, Pugliese et al., a 2018), the number of bulky bridges was found higher in both shMUS81 and MUS81^{S87A} cells and, notably, this phenotype was exacerbated when BRCA2 was depleted (Fig. 35B). Interestingly, a higher number of anaphase cells with chromatin bridges were found also in the phosphomimic mutant of MUS81 after BRCA2 depletion. Of note, the increase of DAPI-positive anaphase bridges after BRCA2 depletion was less in cells depleted of MUS81 or expressing the S87A unphosphorylatable mutant than in cells expressing the wild-type or phosphomimetic MUS81 protein. The elevated levels of DAPI-positive bridges suggested possible cytokinesis-related defects. To test this hypothesis, we analysed the frequency of multinucleated cells in

BRCA2-deficient cells expressing the wild-type MUS81 or its mitotic regulatory mutants by anti- α -tubulin immunofluorescence. A general increase in the frequency of multinucleated cells was seen in cells expressing the S87 phosphomutants of MUS81 or in cells knocked-down for MUS81 (Fig. 35C-D). In the absence of BRCA2, the number of multinucleated cells increased further in wild-type or in shMUS81 cells while it was marginally affected in MUS81^{S87A} or MUS81^{S87D} cells (Fig. 35C-D). This indicates that loss of MUS81 or its mitotic function is required to counteract cytokinesis failure in BRCA2-deficient cells although a MUS81 deregulated activity is sufficient to increase segregation defects *per se*. Since defective resolution of replication intermediates correlates with persisting DNA damage in the next cell cycle, we next analysed the accumulation of 53BP1 nuclear bodies (NBs) in Cyclin-A-negative G1 cells after immunostaining in cells expressing the wild-type form of MUS81 or its S87 phosphorylation mutants and BRCA2-depleted. Interestingly, and consistently with Lai and colleagues (Lai et al., 2017), the number of 53BP1-positive G1 cells increased after BRCA2-depletion in cells expressing the wild-type MUS81 but also in MUS81-deficient cells or

in the S87A-MUS81 mutant (Fig. 35E). Surprisingly, the constitutively active MUS81 mutant, MUS81-S87D, presented a reduced number of 53BP1 NBs upon BRCA2 depletion as compared with the control-depleted cells (Fig. 35E). Therefore, these results indicate that when mitotic activity of MUS81 is deregulated, the absence of BRCA2 worsens the levels of chromosome mis-segregation. However, BRCA2-depletion only minimally affects the persistence of DNA lesions or under-replicated regions observed in the unphosphorylatable MUS81 mutant.



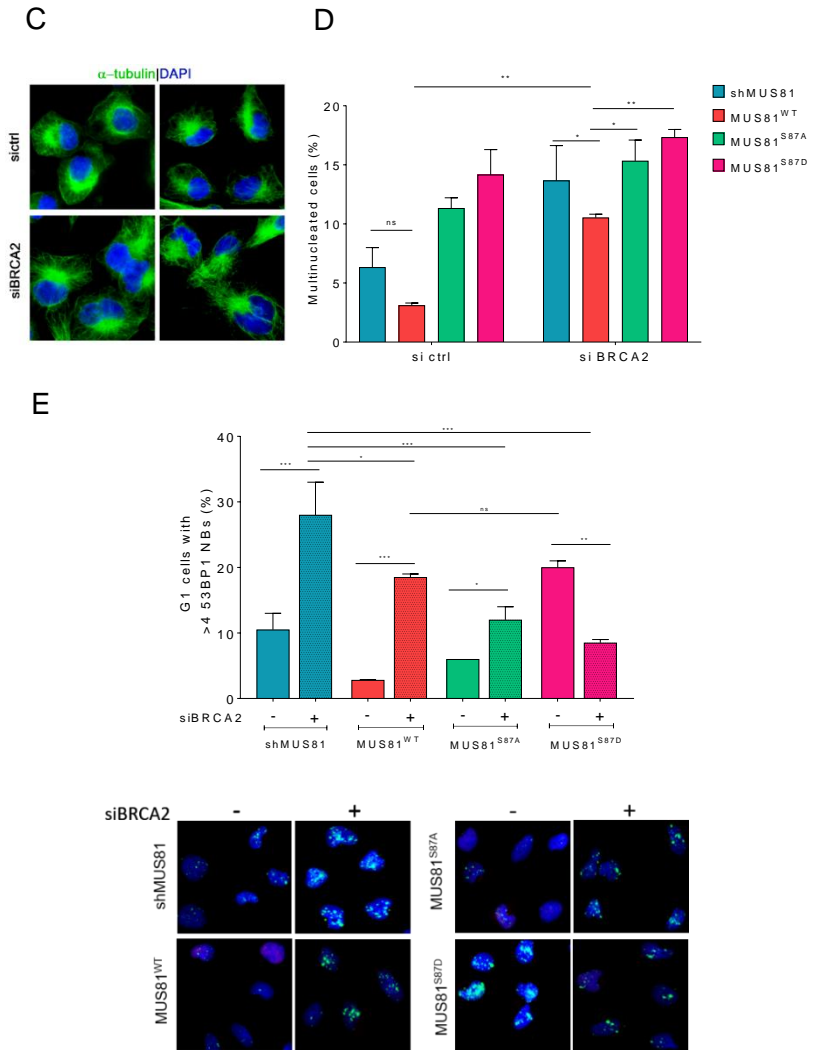


Figure 35 The absence of BRCA2 leads to formation of mitotic chromosome bridges in constitutive active MUS81 mutant. (A) Control of protein depletion by Western blotting in MRC5 SV40 cells after transfection with control siRNAs or siBRCA2.

Immunoblotting was performed using the relevant antibodies. Lamin B1 was used as loading control. (B) Analysis of the bulky anaphases bridges in MUS81 phosphomutants transfected or not with siBRCA2. The graph shows the fractions of mitotic cells with bulky anaphase bridges. Error bars indicate SE; n=3(>50 mitotic cells were analyzed in each population). Data are presented as mean±standard error (SE) from three independent experiments. *P< 0.5; **P< 0.1; ***P<0.01, ANOVA test. Significance is reported compared to the wild-type. Representative images of single anaphases from the phosphomimetic MUS81 mutant are shown. Arrows indicate bridges. (C) MUS81 phosphomimetic mutants were transfected with control or BRCA2. Representative images of cells stained with an α -tubulin antibody (green) after 48h after transfection are shown. DNA was counterstained with DAPI. (D) Quantification of the frequency of multinucleated cells in asynchronous cultures treated as in (C). Error bars represent s.d. (n=3). ns: non significant; *P<0.05; **P<0.01; ***P<0.001 (ANOVA-test). (E) Quantification of the frequency of cyclin A-negative G1 cells containing >4 53BP1 nuclear bodies. Representative image of fluorescence cells after 48h after transfection stained with anti-53BP1 (green) are shown in the panel, nuclear DNA was counterstained by DAPI. The graph shows quantification of the 53BP1-negative Cyclin A-cells. Data are mean values from three independent experiments. Statistical analysis was performed by Student's t-test. ns: not significant; *P<0.05; **P<0.01; ***P<0.001.

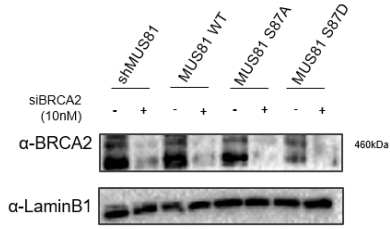
4. Different DNA repair pathways sensitize S87MUS81 phosphorylation mutant in BRCA2 deficient cells

Cells with impaired BRCA2 function and consequent HR deficiency are hypersensitive to cross-linking agents, such as cisplatin, and to poly(ADP-ribose) polymerase (PARP) inhibitors, which are being extensively explored as cancer therapeutics (Feng and Jasin 2017b; Bryant et al. 2005; Chan et al. 2011; Farmer et al. 2005; Murai et al. 2013). This profound hypersensitivity of BRCA2-mutant cells to PARP inhibitors has become an emerging therapeutic paradigm known as synthetic lethality. As loss of MUS81 or of its mitotic function reduced proliferation in BRCA2-depleted cells (Fig. 32B), we wanted to determine whether blocking MUS81 activation in mitosis would modify sensitivity to the PARP1i Olaparib. Therefore, we performed clonogenic survival assays in cells downregulated for MUS81 or expressing the wild-type form of MUS81 or its S87 phosphorylation mutants in absence of BRCA2. Treatment with Olaparib reduced cell survival in all cell lines but at different extent with cells downregulated of MUS81 or expressing the S87D mutant being the less sensitive (Fig. 36B). As expected, depletion of BRCA2

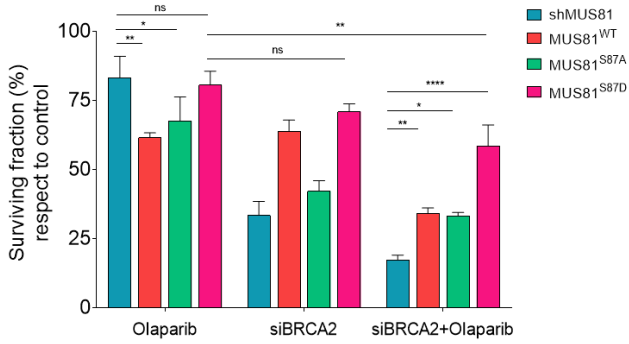
synergized with that of MUS81 or its mitotically-inactive mutant S87A. Interestingly, although concomitant depletion of BRCA2 and inhibition of PARP1 lead to further decrease of cell survival in wild-type MUS81 cells, the reduction of cell survival was less significant in absence of MUS81 or in MUS81^{S87A} cells. Surprisingly, expression of the constitutively-active S87D-MUS81 mutant abrogated Olaparib sensitivity associated to BRCA2-depletion. This striking phenotype prompted us to analyse further the effect of BRCA2-depletion in cells having a constitutively-active MUS81 protein. It was demonstrated that genetic ablation or inhibition of key components of pathways involved in DSBs repair such as alt-NHEJ suppressed aberrant phenotypes in BRCA2-depleted cells (Han et al.,2017). The phosphomimetic S87D MUS81 mutant generates spontaneous DNA damage in S-phase (Palma,Pugliese et al., 2018), which is apparently unaltered by BRCA2 deficiency (Fig. 33B-C). Since PARP1 inhibition should synergize with DNA damage left unrepaired by HR because of BRCA2 loss, we wondered whether inhibition of alt-NHEJ by the ligaseI/III inhibitor L67 (Chen et al., 2009) affected clonogenic cell survival of BRCA2-depleted cells expressing the different MUS81 phosphomutants.

As reported in Fig. 36C, concomitant BRCA2-depletion and L67 treatment resulted in a significant reduction in cellular viability in MUS81^{S87D} cells compared to BRCA2-depletion or L67 treatment alone. In contrast, we observed barely-significant differences in cells expressing wild-type MUS81 and a slight increase in the MUS81^{S87A} cells. Of note, the reduction in cell survival observed in MUS81^{S87D} cells depleted of BRCA2 after L67 treatment is comparable to that associated with Olaparib treatment in wild-type cells after BRCA2 down-regulation. These results suggest that MUS81^{S87D} may promote Olaparib resistance in BRCA2-deficient cells, indicating that the functionality of MUS81 complex affects sensitivity of BRCA2-deficient cells to Olaparib and suggest that the targeted inhibition of particular DNA repair pathways may be useful to exploit BRCA2-deficiency of human tumours and overcome resistance to PARPi.

A



B



C

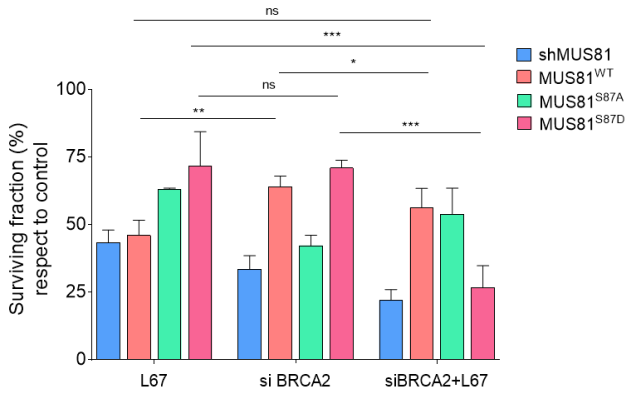


Figure 36 Different DNA repair pathways sensitize S87MUS81 phosphorylation mutant in BRCA2 deficient cells. (A) Western blotting analysis shows level of BRCA2 protein after transfection with siRNA. Lamin B1 was used as loading. (B) MRC5 SV40-derived cells stably depleted of MUS81 and complemented with MUS81 wild-type or the two phosphomimetic forms (S87A and S87D) were transfected with the indicated siRNAs or untransfected to perform clonogenic assay. Twenty-four hours later, cells were treated with 10 μ M olaparib (PARP inhibitor) and 24h after were plated at low cell density into 6-well plates. Cells were grown for 10 days, and colonies were stained. Data are presented as mean \pm SD (n=3). Statistical significance, *P<0.05; **P<0.01; ***P<0.001; ns: not significant) was calculated with Tukey multiple comparison test using one-way ANOVA. (C) Similar analyses were conducted treating cells after 24h after transfection with siBRCA2 with 0,5 μ M L67 inhibitor. Error bars represent s.d. (n=3). *P<0.05; **P<0.01; ***P<0.001; ns: not significant (ANOVA-test).

DISCUSSION

CK2 regulates S87 MUS81 phosphorylation in mitosis and after replication stress

The structure-specific endonuclease MUS81/EME1 plays important roles in the resolution of recombination intermediates, however, its function needs to be carefully regulated to avoid an unscheduled targeting intermediates during DNA replication, which may result in genome instability. Regulation of the MUS81 complex has been mostly investigated in yeast, and several publications demonstrated that cell cycle-dependent phosphorylation of the Mms4EME1 subunit by Cdc28CDK1 or Cdc5PLK1 ensures activation of the MUS81 complex in G2/M (Dehé et al., 2013; Gallo-Fernández et al., 2012; Matos et al., 2011a). In yeast, the MUS81 complex can be also regulated by checkpoint kinases in response to DNA damage (Dehé et al., 2013; Kai et al., 2005). In human cells, a cell cycle-dependent regulation of the MUS81 complex has been indirectly inferred from association with PLK1, and the presence of phosphorylated isoforms of EME1 in mitosis (Svendsen et al., 2010a; Wyatt et al., 2013). The functional role of such events and the identity of the targeted residues

are almost unknown, and only recently a mechanistic link between CDK1-dependent phosphorylation and activation of the human SLX4-MUS81-EME2 axis has been revealed (Duda, et al., 2016). However, in most cases, the phenotype associated with loss of MUS81 complex regulation has been deduced from inhibition of cell cycle-related kinases, such as CDK1 or PLK1, so that the observed effect may derive also from perturbation of cell cycle progression per se or from altered function of other targets. Here, we find that the biological function of the MUS81-EME1 complex in human cells is positively regulated by CK2, which phosphorylates Serine 87 (S87) of the MUS81 subunit in mitosis. Interestingly, phosphorylation at S87 increases from late G2 to prophase and disappears as soon as cells proceed to metaphase. Activation of the MUS81-EME1 complex during prophase or pro-metaphase has been hypothesised from interaction with its key partners using synchronised cells (Duda, et al., 2016). Our data on S87 phosphorylation confirm that the human MUS81-EME1 complex becomes active in late G2 and early mitosis and suggest that pS87MUS81 is excluded from chromatin in metaphase. Our findings also show that MUS81 S87 phosphorylation

is very low or undetectable in S-phase. The MUS81 complex (es) needs to be switched off during normal replication (Matos & West, 2014), and downregulation of S87 phosphorylation is consistent with the need to avoid adventitious targeting of replication intermediates. Although MUS81 can form distinct heterodimeric complexes with EME1 or EME2 (Pepe & West, 2014b), our data show that phosphorylation of S87 is mainly detected in the MUS81-EME1 complex. This is consistent with the MUS81-EME1 dimer being active in mitosis and suggests that different phosphorylation events may be involved in the regulation of specific MUS81 complexes. From this point of view, phosphorylation of the invariant subunit of the MUS81 heterodimers could be advantageous to direct association of MUS81 with EME1 or EME2, and to modulate endonucleolytic cleavage in vivo. From this point of view, although the amount of MUS81 in chromatin is unchanged by the S87 phosphorylation status, the different level of chromatin-associated EME1 or EME2 in the S87 phosphorylation mutants of MUS81 may reflect the ability to form different complexes. Experiments using inhibitors of cell cycle kinases provided clues about consequences of unscheduled activation

of the MUS81 complex on viability and chromosome stability in human cells (Duda et al., 2016; Forment et al., 2011; Matos et al., 2013a). Our findings clearly demonstrate that expression of a phosphomimic S87D-MUS81 mutant is detrimental to cell proliferation because of the generation of DSBs in S-phase cells. Interestingly, such unscheduled formation of DSBs in S-phase is largely prevented by ectopic expression of the bacterial RuvA protein. RuvA is a Holliday junction-binding protein, and its ectopic expression in human cells counteracts generation of DSBs by another structure-specific endonuclease, GEN1 (Malacaria, 2017b). Hence, from a mechanistic point of view, a mutation mimicking constitutive phosphorylation of MUS81 at S87 is sufficient to unleash targeting of HJ-like intermediates arising during normal replication and this is linked to generation of DNA damage. Much more interestingly, under unperturbed cell growth, expression of the S87D-MUS81 mutant results in a chromosome fragility phenotype, which is more marked than that observed in cells expressing the unphosphorylatable S87A-MUS81 form. In addition, cells expressing the phosphomimic S87D-MUS81 mutant not only have elevated number of chromosome breaks

and gaps, but also have a striking accumulation of radial chromosomes. Since the presence of radial chromosomes is associated with repair of DSBs at collapsed forks by NHEJ (Kasperek & Humphrey, 2011), unscheduled formation of DSBs by MUS81 complex in S-phase may engage end-joining repair in addition to homologous recombination, which may promote gross chromosomal rearrangements. In unperturbed cells, loss of the MUS81 complex function results in mitotic defects including accumulation of bulky anaphase bridges (Garner et al., 2013; Matos et al., 2013a). We show that cells expressing the S87A-MUS81 mutant recapitulate the high number of bulky anaphase bridges observed in cells depleted of MUS81, although they show few chromosome-breaks in metaphase. In contrast, expression of the phosphomimic S87D-MUS81 results in few bulky anaphase bridges, but in a striking chromosome fragility. Hence, formation of DSBs by an unscheduled function of the MUS81 complex during a normal S-phase is expected to be much more detrimental to genome stability of that associated with activation of the MUS81 complex at collapsed replication forks, while loss of resolution activity in early mitosis is better sustained, probably

because of backup activities (Franchitto et al., 2008; Murfuni et al., 2012; Murfuni et al., 2013a). Prolonged or pathological replication fork arrest has been associated to induction of MUS81-dependent DSBs (Hanada et al., 2007; Hengel et al., 2016; Murfuni et al., 2012; Murfuni et al., 2013a). Our data show that MUS81 S87 phosphorylation is low in cells treated with HU for 24 h, a condition known to promote MUS81 function at collapsed replication forks (Hanada et al., 2007), indicating distinct regulatory mechanisms of the human MUS81 complex during mild or persisting replication stress. However, we also provide evidence that CK2 inhibition reverts formation of MUS81-dependent DSBs after HU treatment. Hence, CK2-dependent phosphorylation on other residues of MUS81 or EME1/2 may be involved in regulating the MUS81 complex under different conditions, as reported in yeast (Dehé et al., 2013; Kai et al., 2005). Alternatively, CK2 may target other proteins required for MUS81 complex function under conditions of persisting replication stress. Interestingly, CK2 phosphorylates, among others, the RAD51 recombinase (Yata et al., 2012). Of note, RAD51 or RAD52 are involved in the formation of the MUS81 complex substrates at

demised replication forks (Hengel et al., 2016; Murfuni et al., 2013b). Clarifying this interesting point clearly goes beyond the scope of this work and deserves future investigations. In contrast to persisting or pathological replication stress, a mild condition of replication perturbation that does not arrest cells in S-phase can stimulate S87 phosphorylation of MUS81. Such mild condition of replication stress has been reported to trigger the function of the MUS81-EME1 complex to resolve intermediates at under-replicated regions, such as common fragile sites (Naim et al., 2013; Ying et al., 2013b). Our data on the cell cycle-specificity of MUS81 S87 phosphorylation suggest that this function of the MUS81 complex occurs post replication or in mitosis when common fragile sites loci might conclude their replication (Minocherhomji et al., 2015a). Strikingly, expression of the unphosphorylatable MUS81 S87A mutant enhances chromosomal damage in cells treated with low-dose Aph only slightly, while the presence of a phosphomimic MUS81 mutant dramatically increases the amount of chromosome breakage and radial chromosomes after a mild replication stress. Hence, as in untreated cells, the phenotype deriving from unscheduled targeting of perturbed replication forks by

the MUS81 complex predominates over that resulting from loss of function in G2/M. Our experiments indicate that phosphorylation of MUS81 S87 is important to establish a correct interaction between MUS81 and SLX4. SLX4 is a versatile scaffold involved in recruitment of multiple endonucleases (Muñoz et al., 2009; Svendsen et al., 2010b). In particular, activation of MUS81/EME1 in mitotic cells requires association with SLX4 through a region localized in the first 90 aminoacids of MUS81 (Duda et al., 2016; Nair et al., 2014; Wyatt et al., 2013). Interestingly, deletion of the SLX4-interacting region of MUS81 broadens substrate specificity, allowing the complex to target much more easily also replication intermediates at perturbed forks (Wyatt et al., 2017). Serine 87 is within the region interacting with SLX4 and its phosphorylation makes MUS81 more prone to associate with SLX4, providing a mechanistic explanation to the unscheduled targeting by the MUS81 S87D protein of HJ-like and possibly other branched intermediates during replication. It has been recently reported that inhibition of WEE1 licences association of MUS81/EME2 with SLX4 resulting in a wide chromosome instability in the form of pulverized metaphases (Duda, et al., 2016).

Interestingly, the dramatic effect of WEE1 inhibition on premature cell cycle progression and chromosome pulverization is completely prevented by the unphosphorylatable MUS81 S87A mutant, reinforcing the strong functional value of S87 phosphorylation. In our experimental conditions, however, depletion of EME2 substantially reduces but does not suppress WEE1i-associated phenotypes. In particular, expression of the S87D-MUS81 mutant induces a phenotype that is only minimally affected by EME2 depletion. As S87 phosphorylation occurs mainly in the MUS81/EME1 complex, it is conceivable that expression of the phosphomimic protein favours engagement of the MUS81/EME1 complex while, in wild-type cells, both complexes might contribute to the WEE1i-dependent phenotypes. Alternatively, the relative amount of each MUS81 complex may be cell-specific and affect also the genetic dependency of the WEE1i-dependent effects. Moreover, as WEE1-mediated promotion of MUS81/SLX4 interaction involves CDK1-dependent phosphorylation of SLX4 (Duda, et al., 2016), our data indicate that both the partners must be modified to promote a productive interaction. CK2 is a crucial kinase in mitosis, and is positively

regulated by CDK1 (22). From this point of view, human cells might have evolved a redundant regulatory mechanism to restrain MUS81 complex activity in late G2 and M phase. Indeed, elevated CDK1 level may directly contribute to activate the MUS81 complex phosphorylating EME1 (Mankouri et al., 2013), while, indirectly, may enhance activity of CK2 that, in turn, targets MUS81 licensing interaction with an already phosphorylated SLX4 (Fig. 37). This elaborate regulatory mechanism will allow cleavage of branched DNA intermediates during a narrow window at the beginning of mitosis, contributing to limit chromosome instability. Our results may also have strong implications for the onset of genome instability in cancer. Indeed, CK2 has been found overexpressed in many human tumours (Ruzzene & Pinna, 2010). Hence, it is tempting to speculate that in CK2-overexpressing cancer cells also the biological function of MUS81/EME1 may be elevated and contribute strongly to genome instability and, possibly, aggressiveness. Further studies will be needed to evaluate the status of MUS81 S87 in human tumours together with level and type of genome instability, in order to see if there is any correlation with the expression of CK2. Altogether, our

study provides the first mechanistic insight into the regulation of the human MUS81 complex, with functional implications on the consequences of deregulated processing of replication intermediates during unperturbed or minimally-perturbed DNA replication.

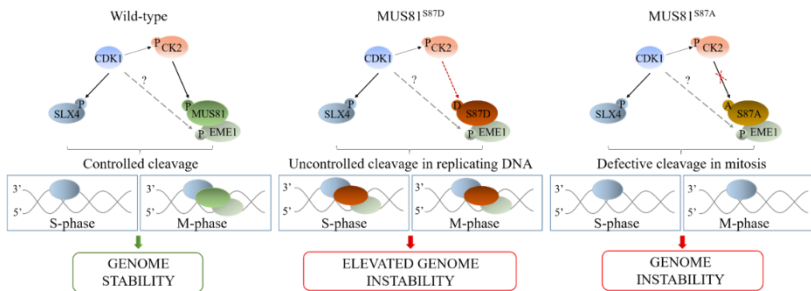


Figure 37 Summarizing model to illustrate the contribution of CK2-dependent phosphorylation to the MUS81/EME1/SLX4 regulation.

A regulated mitotic function of MUS81 correlates with proliferation and chemosensitivity of BRCA2-deficient cells

The role of BRCA2 in HR has been a subject of active investigation for many years. HR repairs DNA lesions including DNA double-strand breaks (DSBs) using a homologous DNA sequence, typically the sister chromatid in mitotic cells. BRCA2 plays an essential role in this process by loading RAD51 recombinase onto single-stranded DNA formed at DSBs, where the RAD51 nucleoprotein filaments form and catalyze the subsequent strand invasion reaction (Feng & Jasin, 2017b). Fork protection is an additional BRCA2-mediated process that helps safeguard genomic integrity (Schlachter et al., 2011). Our findings reveal that S87-MUS81 phosphorylation is required for proliferation and to prevent DNA damage and segregation defects under unperturbed cell growth in BRCA2-deficient cells. In particular, it is worth noting that abrogation of S87-MUS81 phosphorylation recapitulates most of the phenotypes induced by MUS81 down-regulation in unperturbed BRCA2-deficient cells (Lai et al., 2017). Since abrogation of S87 phosphorylation of MUS81 by CK2 impairs the function of the MUS81 complex in mitosis but is unrelated with

that performed in S-phase (Palma, Pugliese et al., 2018), our data suggest that is the mitotic function of MUS81 to be more relevant for proliferation in the absence of BRCA2. Consistent with this, depletion of BRCA2 increases two-fold S87 phosphorylation, which occurs exclusively outside S-phase. Very recently, MUS81 has been involved in flap cleavage at stalled forks that undergo degradation in the absence of BRCA2 (Lemaçon et al., 2017b). As this S-phase-related function of MUS81 would take place after replication fork stalling, while requirement of mitotic function of MUS81 would take place under unperturbed cell growth, it is likely that loss of BRCA2 evokes at least two independent mechanisms in which the MUS81 complex participates, possibly through independent regulatory networks. Alternatively, it might be possible that loss of mitotic MUS81 regulation somehow requires BRCA2 function as a back-up and not *vice versa*. Two recent studies reported that MUS81 nuclease supports fork restart in the absence of BRCA2 by cleaving degraded forks to mediate fork restart (Lemaçon et al., 2017b; Rondinelli et al., 2017). Our data confirms that MUS81 provides a mechanism of replication stress tolerance in BRCA2-depleted cells but also show that

replication fork progression is affected in the absence of the mitotic phosphorylation of MUS81 at S87. Since S87 phosphorylation is undetectable in S-phase it may be possible that an impaired function of MUS81 in mitosis could lead to accumulation of DNA lesions or unprocessed intermediates in the subsequent S-phase, which requires BRCA2-dependent repair/processing. Indeed, loss of MUS81 or its S87 phosphorylation results in segregation defects and more 53BP1 NBs in the subsequent G1-phase (Palma, Pugliese et al., 2018; Naim et al. 2013; Ying et al. 2013c) and we also observe that depletion of BRCA2 leads to DNA damage accumulation in cells stably-depleted of MUS81 or in MUS81^{S87A} cells. Of note, the identity of the intermediate targeted by MUS81 complex at the demised fork is still uncertain (Malacaria et al., 2017a) and the increase of DNA damage that we have seen by γ -H2AX immunofluorescence seems not derive from processing of DSBs, as they are not affected by BRCA2 depletion. One possibility is that loss of mitotic function of MUS81 and BRCA2 could stimulate accumulation of single-strand DNA lesions at or behind the forks (Kolinjivadi et al., 2017). Interestingly, we show that loss of MUS81 or its mitotic regulation equally

abrogates the delayed S-M progression observed upon BRCA2-depletion. The enhanced DNA damage detected in S87MUS81-expressing cells when BRCA2 is depleted and the defective S-M delay would suggest that the mitotic function of MUS81 is needed to delay and deal with defects associated with BRCA2-depletion while, in turn, loss of MUS81 mitotic function increases the need for BRCA2 function in S-phase. Clarifying these interesting points deserves future investigation. Formation of anaphase bridges in BRCA2-deficient has been previously reported in mouse embryonic stem cells (Laulier et al., 2011). As expected, MUS81 inactivation in BRCA2-depleted cells led to a significantly higher percentage of cells with DAPI-positive bridges relative to BRCA2 depletion alone (Fig.35B). Strikingly, expression of the unphosphorylatable MUS81 S87A mutant enhances bulky bridges formation in cells treated with siBRCA2, while the absence of BRCA2 in phosphomimic MUS81 mutant increments DAPI-positive bridges formation relative to MUS81^{S87D} alone. Differently from what we demonstrate in cells treated with low-dose of Aph (Palma, Pugliese et al., 2018), in this context, when we depleted BRCA2, the phenotype arise from the failure to

phosphorylate MUS81 during S-phase predominates over that resulting from constitutive S87 phosphorylation. We have demonstrated that cells have evolved an elaborate regulatory mechanism that allow MUS81 S87 phosphorylation during a narrow window at the beginning of mitosis, but in absence of BRCA2 this control it could be lost and it is conceivable that S87 phosphorylation could limit chromosome instability. This observation could be consistent with the reduction formation of 53BP1 NBs in G1 cells in MUS81^{S87D} cells after BRCA2-depletion (Fig.35E). Loss of BRCA2 sensitizes cells to PARP1 inhibitors (Ding et al., 2016; Lord & Ashworth, 2016; Ying, Hamdy, & Helleday, 2012). Interestingly, while we observe that loss of S87 phosphorylation seems to synergize with PARP1 inhibition in BRCA2-depleted cells, constitutive phosphorylation of MUS81 at S87 confers resistance to PARP1 inhibitors. PARP1 inhibitors have been recently approved for treatment of BRCA-mutant breast and ovarian cancers, however, not all patients respond to this therapy and resistance to these novel drugs remains a major clinical problem (Pujade-Lauraine et al., 2017; Bouwman and Jonkers, 2014; Bitler et al., 2017; Lim and Tan, 2017).

Several mechanisms of chemoresistance in BRCA2-deficient cells have been identified and, rather than restoring normal recombination, these mechanisms result in stabilization of stalled replication forks (Clements et al., 2018). For instance, depletion of ZRANB3, HLTf or SMARCAL1 abolishes formation of the reversed fork structures targeted by the MRE11 nuclease and thus results in chemoresistance of BRCA2-deficient cells (Taglialatela et al., 2017). Inhibition of MRE11 (Schlacher et al., 2011; 2012), or of the RAD51 antagonist RADX (Dungrawala et al., 2017) can similarly rescue PARP1i sensitivity of BRCA2-deficient cells. Finally, inhibition of a parallel fork degradation pathway governed by the chromatin modifier EZH2 which recruits the nuclease MUS81 to stalled forks (Rondinelli et al., 2017), or channelling the processing stalled forks toward translesion synthesis-mediated lesion bypass rather than fork reversal (Guillemette et al., 2015), can also suppress chemosensitivity of BRCA2-deficient cells. Although unscheduled activation of MUS81 through the phosphomimetic S87D mutation counteracts anaphase-bridge in mitosis, it induces DSBs in S-phase (Palma, Pugliese et al., 2018). Thus, it is conceivable that the S87D-MUS81 mutant rescues

PARPi sensitivity by cleaving stalled forks before fork reversal or immediately after bypassing the need for BRCA2-dependent fork protection. Formation of DSBs at replication forks, however, would call for enhanced HR and, thus, enhanced BRCA2 activation, making MUS81^{S87D} cells sensitive to loss of BRCA2. However, this is not the case and MUS81^{S87D} cells show wild-type sensitivity to concomitant depletion of BRCA2 (see Fig.36B). The higher resistance of MUS81^{S87D} cells to concomitant siBRCA2 and treatment with Olaparib suggest that MUS81^{S87D} may promote Olaparib resistance in BRCA2-deficient cells through activation of other DNA repair pathways. DSBs formed in S-phase can be repaired also by NHEJ and alt-NHEJ (Hartlerode & Scully, 2009; Polo & Jackson, 2011). The alternative end-joining may act on resected DNA ends, which likely form in S-phase because of elevated activity of CDK1/2 (Bonetti, Colombo, Clerici, & Longhese, 2018), and its function requires Ligase I/III (Chen et al. 2009; Simsek et al. 2011). Interestingly, we find that MUS81^{S87D} cells depleted of BRCA2 are extremely sensitive to the Ligase I/III inhibitor L67 (Kasckow et al., 2013). In speculation, phosphomimic mutant forms of MUS81 activity could avail the

alt-NHEJ pathway to repair DSBs and preserve cell viability in cells lacking BRCA2. Another hypothesis is that, in BRCA2-depleted cells, the unscheduled regulation of MUS81 at S87 could result in processing of different types of DNA substrates not only during S-phase leading to activation of backup repair pathway such as Alt-NHEJ. The molecular mechanism behind our observation is not still clear and object of our future studies. Of note, recent studies have shown that BRCA1/2-deficient tumors upregulate Polθ-mediated alternative end-joining (alt-NHEJ) repair as a survival mechanism (Kais et al., 2016), suggesting that deregulation of MUS81 function might be exploited in target therapy and as a biomarker for therapeutic selection. Combining the data presented in this second part of my thesis, we propose a model when the correlation between BRCA2 and MUS81 in preserve genome stability is strengthened by S87 phosphorylation. Most importantly, according with our results, the resistance of BRCA2-depleted cells expressing MUS81^{S87D} to PARPi but extreme sensitivity to Ligase I/III inhibition could be used as a potential biomarker for therapy of PARPi-resistant tumours having elevated levels of MUS81 activation. Since we demonstrate that CK2

phosphorylates MUS81 at Serine 87 (Palma, Pugliese et al., 2018) and CK2 is often over-expressed in tumours (Ruzzene & Pinna, 2010), also MUS81-S87 phosphorylation levels could be up-regulated. Hence, the understanding of the status of CK2 and consequent S87MUS81 in BRCAness human tumours may disclose better perspectives of prevention and novel therapeutic strategies.

ACKNOWLEDGEMENTS

I would like to thank my group leaders Dr. Pietro Pichierri and Dr.ssa Anna Paola Franchitto who contributed so much to my scientific growth. Thank you for the opportunity you gave me to do exciting research in the field of Molecular Biology. They have sent me their experience in this field and they have always believed in my capacity.

I want to thank all members of Genome stability groups for their collaboration, support and critical advice, in particular to Dr.ssa Anita Palma who contributed to this work with some experiments.

My gratitude goes to my family for their constant and unconditional support, through the duration of my studies.

This dissertation would not be finished without the support, encouragement and help of many people who I appreciate.

REFERENCES

- Abraham, J., Lemmers, B., Hande, M. P., Moynahan, M. E., Chahwan, C., Ciccio, A., Hakem, R. (2003). Eme1 is involved in DNA damage processing and maintenance of genomic stability in mammalian cells. *EMBO Journal*, 22(22), 6137–6147. <http://doi.org/10.1093/emboj/cdg580>
- Abraham, R. T. (2001). cell cycle checkpoint signaling through the ATM and ATR kinases.pdf. *Genes & Development*, 15, 2177–2196. <http://doi.org/10.1101/gad.914401>.DNA
- Alexandrov, L. B., Nik-Zainal, S., Wedge, D. C., Aparicio, S. A. J. R., Behjati, S., Biankin, A. V., Stratton, M. R. (2013). Signatures of mutational processes in human cancer. *Nature*, 500(7463), 415–421. <http://doi.org/10.1038/nature12477>
- Ammazzalorso, F., Pirzio, L. M., Bignami, M., Franchitto, A., & Pichierri, P. (2010). ATR and ATM differently regulate WRN to prevent DSBs at stalled replication forks and promote replication fork recovery. *The EMBO Journal*, 29(18), 3156–

3169. <http://doi.org/10.1038/emboj.2010.205>

Andersen, S. L., Bergstralh, D. T., Kohl, K. P., Jeannine, R., Moore, C. B., & Sekelsky, J. (2009). *Drosophila* MUS312 and the vertebrate ortholog BTBD12 interact with DNA structure-specific endonucleases in DNA repair and recombination, *35*(1), 128–135.

<http://doi.org/10.1016/j.molcel.2009.06.019.Drosophila>

Bastin-Shanower, S. a, Fricke, W. M., Mullen, J. R., & Brill, S. J. (2003). The mechanism of Mus81-Mms4 cleavage site selection distinguishes it from the homologous endonuclease Rad1-Rad10. *Molecular and Cellular Biology*, *23*(10), 3487–3496. <http://doi.org/10.1128/MCB.23.10.3487>

Baumann, C., Körner, R., Hofmann, K., & Nigg, E. A. (2007). PICH, a Centromere-Associated SNF2 Family ATPase, Is Regulated by Plk1 and Required for the Spindle Checkpoint. *Cell*, *128*(1), 101–114. <http://doi.org/10.1016/j.cell.2006.11.041>

Beck, H., Sofie, M., Larsen, Y., Patzke, S., Holmberg, C., Mejlvang, J., Nielsen, O. (2012). Cyclin-Dependent Kinase Suppression

by WEE1 Kinase Protects the Genome through Control of Replication Initiation and Nucleotide Consumption, *32*(20), 4226–4236. <http://doi.org/10.1128/MCB.00412-12>

Bhowmick, R., Minocherhomji, S., & Hickson, I. D. (2016a).

RAD52 Facilitates Mitotic DNA Synthesis Following Replication Stress. *Molecular Cell*, *64*(6), 1117–1126. <http://doi.org/10.1016/j.molcel.2016.10.037>

Bitler, B. G., Watson, Z. L., Wheeler, L. J., & Behbakht, K. (2017).

PARP inhibitors: Clinical utility and possibilities of overcoming resistance. *Gynecologic Oncology*, *147*(3), 695–704. <http://doi.org/10.1016/j.ygyno.2017.10.003>

Bizard Anna H. and Hickson Ian D. (2014). The dissolution of

double Holliday junctions. *Cold Spring Harbor Perspectives in Biology*, *6*(7), a016477.

<http://doi.org/10.1101/cshperspect.a016477>

Blais, V., Gao, H., Elwell, C. a, Boddy, M. N., Gaillard, P.-H. L.,

Russell, P., & McGowan, C. H. (2004). RNA interference inhibition of Mus81 reduces mitotic recombination in human

cells. *Molecular Biology of the Cell*, 15(2), 552–562.

<http://doi.org/10.1091/mbc.E03>

Blanco, M. G., & Matos, J. (2015). Hold your horSSEs: Controlling structure-selective endonucleases MUS81 and Yen1/GEN1.

Frontiers in Genetics, 6(JUL), 1–11.

<http://doi.org/10.3389/fgene.2015.00253>

Boddy, M. N., Gaillard, P. H. L., McDonald, W. H., Shanahan, P., Yates, J. R., & Russell, P. (2001). Mus81-Eme1 are essential components of a Holliday junction resolvase. *Cell*, 107(4), 537–548.

Boddy, M. N., Lopez-Girona, a, Shanahan, P., Interthal, H., Heyer, W. D., & Russell, P. (2000). Damage tolerance protein Mus81 associates with the FHA1 domain of checkpoint kinase Cds1.

Molecular and Cellular Biology, 20(23), 8758–8766.

<http://doi.org/10.1128/MCB.20.23.8758-8766.2000>

Bonetti, D., Colombo, C. V., Clerici, M., & Longhese, M. P. (2018). Processing of DNA ends in the maintenance of genome stability. *Frontiers in Genetics*, 9(SEP), 1–11.

<http://doi.org/10.3389/fgene.2018.00390>

Bournique, E., Dall'Osto, M., Hoffmann, J. S., & Bergoglio, V. (2018). Role of specialized DNA polymerases in the limitation of replicative stress and DNA damage transmission. *Mutation Research - Fundamental and Molecular Mechanisms of Mutagenesis*, 808(August 2017), 62–73.

<http://doi.org/10.1016/j.mrfmmm.2017.08.002>

Bouwman, P., & Jonkers, J. (2014). Molecular pathways: How can BRCA-mutated tumors become resistant to PARP inhibitors? *Clinical Cancer Research*, 20(3), 540–547.

<http://doi.org/10.1158/1078-0432.CCR-13-0225>

Branzei, D., & Foiani, M. (2005). The DNA damage response during DNA replication. *Current Opinion in Cell Biology*, 17(6), 568–575. <http://doi.org/10.1016/j.ceb.2005.09.003>

Branzei, D., & Foiani, M. (2010). Maintaining genome stability at the replication fork. *Nature Reviews. Molecular Cell Biology*, 11(3), 208–219. <http://doi.org/10.1038/nrm2852>

- Bryant, H. E., Schultz, N., Thomas, H. D., Parker, K. M., Flower, D., Lopez, E., Helleday, T. (2005). Specific killing of BRCA2-deficient tumours with inhibitors of poly(ADP-ribose) polymerase. *Nature*, *434*(7035), 913–917.
<http://doi.org/10.1038/nature03443>
- Byun, T. S., Pacek, M., Yee, M. C., Walter, J. C., & Cimprich, K. A. (2005). Functional uncoupling of MCM helicase and DNA polymerase activities activates the ATR-dependent checkpoint. *Genes and Development*, *19*(9), 1040–1052.
<http://doi.org/10.1101/gad.1301205>
- Cannavo, E., & Cejka, P. (2014). Sae2 promotes dsDNA endonuclease activity within Mre11-Rad50-Xrs2 to resect DNA breaks. *Nature*, *514*(7520), 122–125.
<http://doi.org/10.1038/nature13771>
- Castor, D., Nair, N., Déclais, A. C., Lachaud, C., Toth, R., Macartney, T. J., Rouse, J. (2013). Cooperative control of holliday junction resolution and DNA Repair by the SLX1 and MUS81-EME1 nucleases. *Molecular Cell*, *52*(2), 221–233.

<http://doi.org/10.1016/j.molcel.2013.08.036>

Cerrato, A., Morra, F., & Celetti, A. (2016). Use of poly ADP-ribose polymerase [PARP] inhibitors in cancer cells bearing DDR defects: The rationale for their inclusion in the clinic. *Journal of Experimental and Clinical Cancer Research*, *35*(1), 1–13. <http://doi.org/10.1186/s13046-016-0456-2>

Chan, K. L., North, P. S., & Hickson, I. D. (2007). BLM is required for faithful chromosome segregation and its localization defines a class of ultrafine anaphase bridges. *EMBO Journal*, *26*(14), 3397–3409. <http://doi.org/10.1038/sj.emboj.7601777>

Chan, N., Pires, I. M., Bencokova, Z., Coackley, C., Luoto, K. R., Bhogal, N., ... Bristow, R. G. (2011). Europe PMC Funders Group Contextual Synthetic Lethality of Cancer Cell Kill Based on the Tumor Microenvironment, *70*(20), 8045–8054. <http://doi.org/10.1158/0008-5472.CAN-10-2352.Contextual>

Chan, Y. W., & West, S. C. (2014). Spatial control of the GEN1 Holliday junction resolvase ensures genome stability. *Nature Communications*, *5*, 1–11. <http://doi.org/10.1038/ncomms5844>

Chapman, J. R., & Jackson, S. P. (2008). Phospho-dependent interactions between NBS1 and MDC1 mediate chromatin retention of the MRN complex at sites of DNA damage. *EMBO Reports*, 9(8), 795–801. <http://doi.org/10.1038/embor.2008.103>

Chaudhury, I., & Koepp, D. M. (2016). Recovery from the DNA replication checkpoint. *Genes*, 7(11).
<http://doi.org/10.3390/genes7110094>

Chaudhury, I., Sareen, A., Raghunandan, M., & Sobeck, A. (2013). FANCD2 regulates BLM complex functions independently of FANCI to promote replication fork recovery. *Nucleic Acids Research*, 41(13), 6444–6459.
<http://doi.org/10.1093/nar/gkt348>

Chen, S. H., Jody L. Plank, Smaranda Willcox, Jack D. Griffith, T. H. (2014). Top3 α is required during the convergent migration step of double holliday junction dissolution. *PLoS ONE*, 9(1), 0–5. <http://doi.org/10.1371/journal.pone.0083582>

Chen, X. B., Melchionna, R., Denis, C. M., Gaillard, P. H. L., Blasina, A., Van de Weyer, I., McGowan, C. H. (2001). Human

Mus81-associated endonuclease cleaves Holliday junctions in vitro. *Molecular Cell*, 8(5), 1117–1127.

Chen, X., Zhong, S., Zhu, X., Dziegielewska, B., Ellenberger, T., Gerald, M., Tomkinson, A. E. (2009). Rational Design of Human DNA Ligase Inhibitors that Target Cellular DNA Replication and Repair. *Cancer Research*, 68(9), 7–25.
<http://doi.org/10.1158/0008-5472.CAN-07-6636>.Rational

Chen X., Hengyao N., Woo-Hyun C., Zhu Z., Alma P., Eun Y. S., Sang E.L., Patrick S., and G. I. (2015). Cell cycle regulation of DNA double-strand break end resection by Cdk1-dependent Dna2 phosphorylation. *Nature Structural and Molecular Biology*, 91(2), 165–171.
<http://doi.org/10.1016/j.chemosphere.2012.12.037>.Reactivity

Choi, E., Park, P. G., Lee, H. O., Lee, Y. K., Kang, G. H., Lee, J. W., Lee, H. (2012). BRCA2 Fine-Tunes the Spindle Assembly Checkpoint through Reinforcement of BubR1 Acetylation. *Developmental Cell*, 22(2), 295–308.
<http://doi.org/10.1016/j.devcel.2012.01.009>

- Ciccia, A., & Elledge, S. J. (2010). The DNA damage response: making it safe to play with knives. *Molecular Cell*, *40*(2), 179–204. <http://doi.org/10.1016/j.molcel.2010.09.019>
- Ciccia, A., Ling, C., Coulthard, R., Yan, Z., Xue, Y., Meetei, A. R., West, S. C. (2007). Identification of FAAP24, a Fanconi Anemia Core Complex Protein that Interacts with FANCM. *Molecular Cell*, *25*(3), 331–343. <http://doi.org/10.1016/j.molcel.2007.01.003>
- Clements, K. E., Thakar, T., Nicolae, C. M., Liang, X., Wang, H.-G., & Moldovan, G.-L. (2018). Loss of E2F7 confers resistance to poly-ADP-ribose polymerase (PARP) inhibitors in BRCA2-deficient cells. *Nucleic Acids Research*, *46*(17), 8898–8907. <http://doi.org/10.1093/nar/gky657>
- Copsey, A., Tang, S., Jordan, P. W., Blitzblau, H. G., Newcombe, S., Chan, A. C. Ho, Hoffmann, E. (2013). Smc5/6 Coordinates Formation and Resolution of Joint Molecules with Chromosome Morphology to Ensure Meiotic Divisions. *PLoS Genetics*, *9*(12). <http://doi.org/10.1371/journal.pgen.1004071>

- Crasta, K., Ganem, N. J., Dagher, R., Lantermann, A. B., Ivanova, E. V., Pan, Y., Pellman, D. (2012). DNA breaks and chromosome pulverization from errors in mitosis. *Nature*, 482(7383), 53–58. <http://doi.org/10.1038/nature10802>
- Daniels, M. J., Wang, Y., Lee, M. Y., & Venkitaraman, A. R. (2004). Abnormal cytokinesis in cells deficient in the breast cancer susceptibility protein BRCA2. *Science*, 306(5697), 876–879. <http://doi.org/10.1126/science.1102574>
- Davis, A., & Chen, D. (2013). DNA double strand break repair via non-homologous end-joining. *Translational Cancer Research*, 2(3), 130–43. <http://doi.org/10.3978/j.issn.2218-676X.2013.04.02.DNA>
- Dehé, P.-M., Coulon, S., Scaglione, S., Shanahan, P., Takedachi, A., Wohlschlegel, J. a, Gaillard, P.-H. L. (2013). Regulation of Mus81-Eme1 Holliday junction resolvase in response to DNA damage. *Nature Structural & Molecular Biology*, 20(5), 598–603. <http://doi.org/10.1038/nsmb.2550>
- Dehé, P. M., & Gaillard, P. H. L. (2017). Control of structure-

specific endonucleases to maintain genome stability. *Nature Reviews Molecular Cell Biology*, 18(5), 315–330.

<http://doi.org/10.1038/nrm.2016.177>

Ding, X., Chaudhuri, A. R., Callen, E., Pang, Y., Biswas, K., Klarmann, K. D., Sharan, S. K. (2016). Synthetic viability by BRCA2 and PARP1/ARTD1 deficiencies. *Nature Communications*, 7(May).

<http://doi.org/10.1038/ncomms12425>

Domínguez-kelly, R., Martín, Y., Koundrioukoff, S., Tanenbaum, M. E., Smits, V. A. J., Medema, R. H., Freire, R. (2011). Wee1 controls genomic stability during replication by regulating the Mus81-Eme1 endonuclease, *194*(4).

<http://doi.org/10.1083/jcb.201101047>

Duda, H., Arter, M., Blanco, M. G., Altmeyer, M., Matos Correspondence, J., Gloggnitzer, J., Matos, J. (2016). A Mechanism for Controlled Breakage of Under-replicated Chromosomes during Mitosis. *Developmental Cell*, 39, 740–755. <http://doi.org/10.1016/j.devcel.2016.11.017>

- Dungrawala, H., Bhat, K. P., Le Meur, R., Chazin, W. J., Ding, X., Sharan, S. K., Cortez, D. (2017). RADX Promotes Genome Stability and Modulates Chemosensitivity by Regulating RAD51 at Replication Forks. *Molecular Cell*, 67(3), 374–386.e5. <http://doi.org/10.1016/j.molcel.2017.06.023>
- Ehmsen, K. T., & Heyer, W. D. (2008). *Saccharomyces cerevisiae* Mus81-Mms4 is a catalytic, DNA structure-selective endonuclease. *Nucleic Acids Research*, 36(7), 2182–2195. <http://doi.org/10.1093/nar/gkm1152>
- Eid, W., Steger, M., El-Shemerly, M., Ferretti, L. P., Peña-Díaz, J., König, C., Ferrari, S. (2010). DNA end resection by CtIP and exonuclease 1 prevents genomic instability. *EMBO Reports*, 11(12), 962–968. <http://doi.org/10.1038/embor.2010.157>
- Farmer, H., McCabe, N., Lord, C. J., Tutt, A. N. J., Johnson, D. A., Richardson, T. B., Ashworth, A. (2005). Targeting the DNA repair defect in BRCA mutant cells as a therapeutic strategy. *Nature*, 434(7035), 917–921. <http://doi.org/10.1038/nature03445>

Fekairi, S., Scaglione, S., Chahwan, C., Taylor, E. R., Coulon, S., Dong, M., Gaillard, P. L. (2010). NIH Public Access, *138*(1), 78–89. <http://doi.org/10.1016/j.cell.2009.06.029>. Human

Feng, W., & Jasin, M. (2017). Homologous Recombination and Replication Fork Protection: BRCA2 and More! *Cold Spring Harbor Symposia on Quantitative Biology*, *82*, 329–338. <http://doi.org/10.1101/sqb.2017.82.035006>

Forment, J. V., Blasius, M., Guerini, I., & Jackson, S. P. (2011). Structure-specific DNA endonuclease mus81/eme1 generates DNA damage caused by chk1 inactivation. *PLoS ONE*, *6*(8). <http://doi.org/10.1371/journal.pone.0023517>

Fortini, P., Pascucci, B., Parlanti, E., D'Errico, M., Simonelli, V., & Dogliotti, E. (2003). The base excision repair: Mechanisms and its relevance for cancer susceptibility. *Biochimie*, *85*(11), 1053–1071. <http://doi.org/10.1016/j.biochi.2003.11.003>

Franchin, C., Borgo, C., Zaramella, S., Cesaro, L., Arrigoni, G., Salvi, M., & Pinna, L. A. (2017). Exploring the CK2 paradox: Restless, dangerous, dispensable. *Pharmaceuticals*, *10*(1), 1–8.

<http://doi.org/10.3390/ph10010011>

Franchitto, A., & Pichierri, P. (2014). Replication fork recovery and regulation of common fragile sites stability. *Cellular and Molecular Life Sciences*, 71(23), 4507–4517.

<http://doi.org/10.1007/s00018-014-1718-9>

Franchitto, A., Pirzio, L. M., Prosperi, E., Sapora, O., Bignami, M., & Pichierri, P. (2008). Replication fork stalling in WRN-deficient cells is overcome by prompt activation of a MUS81-dependent pathway. *Journal of Cell Biology*, 183(2), 241–252.

<http://doi.org/10.1083/jcb.200803173>

Fricke, W. M., Bastin-Shanower, S. a., & Brill, S. J. (2005).

Substrate specificity of the *Saccharomyces cerevisiae* Mus81-Mms4 endonuclease. *DNA Repair*, 4(2), 243–251.

<http://doi.org/10.1016/j.dnarep.2004.10.001>

Friedberg, E. C., Aguilera, A., Gellert, M., Hanawalt, P. C., Hays, J.

B., Lehmann, A. R., ... Wood, R. D. (2006). DNA repair: From molecular mechanism to human disease. *DNA Repair*, 5(8),

986–996. <http://doi.org/10.1016/j.dnarep.2006.05.005>

Froget, B., Lambert, S., & Baldacci, G. (2008). Cleavage of Stalled Forks by Fission Yeast Mus81 / Eme1 in Absence of DNA Replication Checkpoint, *19*(February), 445–456.
<http://doi.org/10.1091/mbc.E07>

Fu, H., Martin, M. M., Regairaz, M., Huang, L., You, Y., Lin, C. M., ... Aladjem, M. I. (2015). The DNA repair endonuclease Mus81 facilitates fast DNA replication in the absence of exogenous damage. *Nature Communications*, *6*.
<http://doi.org/10.1038/ncomms7746>

Fugger, K., Mistrik, M., Hickson, I. D., Sørensen, C. S., Fugger, K., Mistrik, M., Sørensen, C. S. (2015). Article FBH1 Catalyzes Regression of Stalled Replication Forks. *CellReports*, *10*(10), 1749–1757. <http://doi.org/10.1016/j.celrep.2015.02.028>

Gadaleta, M. C., & Noguchi, E. (2017). Regulation of DNA replication through natural impediments in the eukaryotic genome. *Genes*, *8*(3). <http://doi.org/10.3390/genes8030098>

Gallo-Fernández, M., Saugar, I., Ortiz-Bazán, M. Á., Vázquez, M. V., & Tercero, J. A. (2012). Cell cycle-dependent regulation of

the nuclease activity of Mus81-Eme1/Mms4. *Nucleic Acids Research*, 40(17), 8325–8335.

<http://doi.org/10.1093/nar/gks599>

Gao Hui, Xiao-Bo Chen, and C. H. M. (2003). Mus81 Endonuclease Localizes to Nucleoli and to Regions of DNA Damage in Human S-phase Cells. *Molecular Biology of the Cell*, 15(April), 3751–3737. <http://doi.org/10.1091/mbc.E03>

Garner, E., Kim, Y., Lach, F. P., Kottemann, M. C., & Smogorzewska, A. (2013). Human GEN1 and the SLX4-Associated Nucleases MUS81 and SLX1 Are Essential for the Resolution of Replication-Induced Holliday Junctions. *Cell Reports*, 5(1), 207–215. <http://doi.org/10.1016/j.celrep.2013.08.041>

Ge, X. Q., Jackson, D. A., & Blow, J. J. (2007). Dormant origins licensed by excess Mcm2-7 are required for human cells to survive replicative stress. *Genes and Development*, 21(24), 3331–3341. <http://doi.org/10.1101/gad.457807>

George-Lucian Moldovan and Alan D. D'Andrea. (2012). To the

rescue: The Fanconi Anemia genome stability pathway salvages replication forks. *Cancer Cell*, 22(1), 5–6.

<http://doi.org/10.1016/j.ccr.2012.06.006>.To

Guillemette, S., Serra, R. W., Peng, M., Hayes, J. A.,

Konstantinopoulos, P. A., Green, M. R., Cantor, S. B. (2015).

Resistance to therapy in BRCA2 mutant cells due to loss of the nucleosome remodeling factor CHD4. *Genes and Development*, 29(5), 489–494. <http://doi.org/10.1101/gad.256214>.114

Han, J., Ruan, C., Huen, M. S. Y., Wang, J., Xie, A., Fu, C., ...

Huang, J. (2017). BRCA2 antagonizes classical and alternative nonhomologous end-joining to prevent gross genomic instability. *Nature Communications*.

<http://doi.org/10.1038/s41467-017-01759-y>

Hanada, K., Budzowska, M., Davies, S. L., van Drunen, E.,

Onizawa, H., Beverloo, H. B., ... Kanaar, R. (2007). The structure-specific endonuclease Mus81 contributes to replication restart by generating double-strand DNA breaks.

Nature Structural & Molecular Biology, 14(11), 1096–1104.

<http://doi.org/10.1038/nsmb1313>

Hartlerode, A. J., & Scully, R. (2009). Mechanisms of double-strand break repair in somatic mammalian cells. *Biochemical Journal*, 423(2), 157–168. <http://doi.org/10.1042/BJ20090942>

Hartung, F., Suer, S., Bergmann, T., & Puchta, H. (2006). The role of AtMUS81 in DNA repair and its genetic interaction with the helicase AtRecQ4A. *Nucleic Acids Research*, 34(16), 4438–4448. <http://doi.org/10.1093/nar/gkl576>

Helleday, T. (2003). Pathways for mitotic homologous recombination in mammalian cells. *Mutation Research - Fundamental and Molecular Mechanisms of Mutagenesis*, 532(1–2), 103–115. <http://doi.org/10.1016/j.mrfmmm.2003.08.013>

Heller, R. C., & Marians, K. J. (2005). The disposition of nascent strands at stalled replication forks dictates the pathway of replisome loading during restart. *Molecular Cell*, 17(5), 733–743. <http://doi.org/10.1016/j.molcel.2005.01.019>

Heller, R. C., & Marians, K. J. (2006). Replisome assembly and the direct restart of stalled replication forks. *Nature Reviews Molecular Cell Biology*, 7(12), 932–943.

<http://doi.org/10.1038/nrm2058>

Hengel, S. R., Malacaria, E., Da Silva C., L. F., Bain, F. E., Diaz, A., Koch, B. G., Spies, M. (2016). Small-molecule inhibitors identify the RAD52-ssDNA interaction as critical for recovery from replication stress and for survival of BRCA2 deficient cells. *ELife*, 5(JULY), 1–30. <http://doi.org/10.7554/eLife.14740>

Heyer, W. (2015). Regulation of Recombination and Genomic Maintenance. *Cold Spring Harbor Perspectives in Biology*, 1–22.

Hills, S. A., & Diffley, J. F. X. (2014). DNA replication and oncogene-induced replicative stress. *Current Biology*, 24(10), R435–R444. <http://doi.org/10.1016/j.cub.2014.04.012>

Hoeijmakers, J. H. (2001). Genome maintenance mechanisms for preventing cancer. *Nature*, 411, 366–374.

<http://doi.org/10.1038/35077232>

- Holland, A. J., & Cleveland, D. W. (2012). Chromoanagenesis and cancer: Mechanisms and consequences of localized, complex chromosomal rearrangements. *Nature Medicine*, *18*(11), 1630–1638. <http://doi.org/10.1038/nm.2988>
- Huen, M. S. Y., & Chen, J. (2008). The DNA damage response pathways: At the crossroad of protein modifications. *Cell Research*, *18*(1), 8–16. <http://doi.org/10.1038/cr.2007.109>
- Huertas, P., & Jackson, S. P. (2009). Human CtIP Mediates Cell Cycle Control of DNA End Resection and Double Strand Break Repair^[S]. *The Journal of Biological Chemistry*, *284*(14), 9558–9565. <http://doi.org/10.1074/jbc.M808906200>
- Interthal, H., & Heyer, W. D. (2000). MUS81 encodes a novel helix-hairpin-helix protein involved in the response to UV- and methylation-induced DNA damage in *Saccharomyces cerevisiae*. *Molecular and General Genetics*, *263*(5), 812–827. <http://doi.org/10.1007/s004380000241>
- Ip, S. C. Y., Rass, U., Blanco, M. G., Flynn, H. R., Skehel, J. M., & West, S. C. (2008). Identification of Holliday junction

resolvases from humans and yeast. *Nature*, 456(7220), 357–361. <http://doi.org/10.1038/nature07470>

Jackson, S. P., & Bartek, J. (2010). The DNA-damage response in human biology and disease. *Nature*, 461(7267), 1071–1078. <http://doi.org/10.1038/nature08467>.

Jasin, M., & Rothstein, R. (2013). Repair of strand breaks by homologous recombination. *Cold Spring Harbor Perspectives in Biology*, 5, 1–19. <http://doi.org/10.1101/cshperspect.a012740>

Jinxue He, Xi Kang, Yuxin Yin, K.S. Clifford Chao, and W. H. S. (2016). PTEN Regulates DNA Replication Progression and Stalled Fork Recovery. *Nature Communications*, 91(2), 165–171. <http://doi.org/10.1016/j.chemosphere.2012.12.037>.Reactivity

Kai, M., Boddy, M. N., Russell, P., & Wang, T. S. F. (2005). Replication checkpoint kinase Cds1 regulates Mus81 to preserve genome integrity during replication stress. *Genes and Development*, 19(8), 919–932. <http://doi.org/10.1101/gad.1304305>

- Kais Zeina, Beatrice Rondinelli, Amie Holmes, Colin O’Leary, David Kozono, Alan D. D’Andrea, and R. C. (2016). FANCD2 maintains fork stability in BRCA1/2-deficient tumors and promotes alternative end-joining DNA repair. *Cell Reports*, 165(2), 255–269. <http://doi.org/10.1016/j.trsl.2014.08.005>.The
- Kaliraman, V., Mullen, J. R., Fricke, W. M., Bastin-shanower, S. a, & Brill, S. J. (2001). Functional overlap between Sgs1 – Top3 and the Mms4 – Mus81 endonuclease. *Genes & Development*, 15, 2730–2740. <http://doi.org/10.1101/gad.932201.age>
- Kasckow, J., Felmet, K., Appelt, C., Thompson, R., Rotondi, A., & Haas, G. (2013). Targeting abnormal DNA double strand break repair in tyrosine kinase inhibitor-resistant chronic myeloid leukemias. *Oncogene*, 32(14), 1784–1793. <http://doi.org/10.3371/CSRP.KAFE.021513>.Telepsychiatry
- Kasperek, T. R., & Humphrey, T. C. (2011). DNA double-strand break repair pathways, chromosomal rearrangements and cancer. *Seminars in Cell and Developmental Biology*, 22(8), 886–897. <http://doi.org/10.1016/j.semcdb.2011.10.007>

Kersten, K., de Visser, K. E., van Miltenburg, M. H., & Jonkers, J. (2017). Genetically engineered mouse models in oncology research and cancer medicine. *EMBO Molecular Medicine*, 9(2), 137–153. <http://doi.org/10.15252/emmm.201606857>

Khakhar, R. R., Cobb, J. A., Bjergbaek, L., Hickson, I. D., & Gasser, S. M. (2003). RecQ helicases: multiple roles in genome maintenance. *Trends in Cell Biology*, 13(9), 493–501. [http://doi.org/10.1016/S0962-8924\(03\)00171-5](http://doi.org/10.1016/S0962-8924(03)00171-5)

Kim, S. (2005). Protein kinase CK2 interacts with Chk2 and phosphorylates Mre11 on serine 649. *Biochemical and Biophysical Research Communications*, 331, 247–252. <http://doi.org/10.1016/j.bbrc.2005.03.162>

Kolinjivadi, A. M., Sannino, V., de Antoni, A., Técher, H., Baldi, G., & Costanzo, V. (2017). Moonlighting at replication forks – a new life for homologous recombination proteins BRCA1, BRCA2 and RAD51. *FEBS Letters*, 591(8), 1083–1100. <http://doi.org/10.1002/1873-3468.12556>

Kowalczykowski, S. C. (2015). An Overview of the Molecular

Mechanisms of Recombinational DNA Repair. *Cold Spring Harbor Perspectives in Biology*, 7(11), a016410.

<http://doi.org/10.1101/cshperspect.a016410>

Kowalski, M., Przybyłowska, K., Rusin, P., Olszewski, J., Morawiec-Sztandera, A., Bielecka-Kowalska, A., ... Majsterek, I. (2009). Genetic polymorphisms in DNA base excision repair gene XRCC1 and the risk of squamous cell carcinoma of the head and neck. *Journal of Experimental & Clinical Cancer Research*, 28(1), 37. <http://doi.org/10.1186/1756-9966-28-37>

Lai, X., Broderick, R., Bergoglio, V., Zimmer, J., Badie, S., Niedzwiedz, W., Tarsounas, M. (2017). MUS81 nuclease activity is essential for replication stress tolerance and chromosome segregation in BRCA2-deficient cells. *Nature Communications*, 8(May). <http://doi.org/10.1038/ncomms15983>

Laulier, C., Cheng, A., & Stark, J. M. (2011). The relative efficiency of homology-directed repair has distinct effects on proper anaphase chromosome separation. *Nucleic Acids Research*,

39(14), 5935–5944. <http://doi.org/10.1093/nar/gkr187>

Lemaçon, D., Jackson, J., Quinet, A., Brickner, J. R., Li, S., Yazinski, S., Vindigni, A. (2017a). MRE11 and EXO1 nucleases degrade reversed forks and elicit MUS81-dependent fork rescue in BRCA2-deficient cells. *Nature Communications*, 8(1). <http://doi.org/10.1038/s41467-017-01180-5>

Leng, X.-F., Chen, M.-W., Xian, L., Dai, L., Ma, G.-Y., & Li, M.-H. (2012). Combined analysis of mRNA expression of ERCC1, BAG-1, BRCA1, RRM1 and TUBB3 to predict prognosis in patients with non-small cell lung cancer who received adjuvant chemotherapy. *Journal of Experimental & Clinical Cancer Research*, 31(1), 25. <http://doi.org/10.1186/1756-9966-31-25>

Lengsfeld B. M., Alison J. Rattray, Venugopal Bhaskara, Rodolfo Ghirlando, A. T. T. P. (2007). Sae2 is an endonuclease that processes hairpin DNA cooperatively with the Mre11/Rad50/Xrs2 complex. *Molecular Cell*, 33(11), 1212–1217. <http://doi.org/10.1016/j.dci.2009.07.003>. Characterization

Lim, J. S. J., & Tan, D. S. P. (2017). Understanding resistance

mechanisms and expanding the therapeutic utility of PARP inhibitors. *Cancers*, 9(8), 1–14.

<http://doi.org/10.3390/cancers9080109>

Lopes, M., Cotta-Ramusino, C., Pelliccioli, a, Liberi, G., Plevani, P., Muzi-Falconi, M., Foiani, M. (2001). The DNA replication checkpoint response stabilizes stalled replication forks. *Nature*, 412(6846), 557–561.

Lopes, M., Foiani, M., & Sogo, J. M. (2006). Multiple mechanisms control chromosome integrity after replication fork uncoupling and restart at irreparable UV lesions. *Molecular Cell*, 21(1), 15–27. <http://doi.org/10.1016/j.molcel.2005.11.015>

Lord, C. J., & Ashworth, A. (2012). The DNA damage response and cancer therapy. *Nature*, 481(7381), 287–294.

<http://doi.org/10.1038/nature10760>

Lord, C. J., & Ashworth, A. (2016). BRCAness revisited. *Nature Reviews Cancer*, 16(2), 110–120.

<http://doi.org/10.1038/nrc.2015.21>

- Lukas, C., Savic, V., Bekker-Jensen, S., Doil, C., Neumann, B., Pedersen, R. S., Lukas, J. (2011). 53BP1 nuclear bodies form around DNA lesions generated by mitotic transmission of chromosomes under replication stress. *Nature Cell Biology*, *13*(3), 243–253. <http://doi.org/10.1038/ncb2201>
- Makharashvili, N., Tubbs, A. T., Yang, S., Wang, H., Zhou, Y., Deshpande, R. A., Paull, T. T. (2014). Catalytic and non-catalytic roles of the CtIP endonuclease in double-strand break end resection, *54*(6), 1022–1033. <http://doi.org/10.1016/j.molcel.2014.04.011>. Catalytic
- Malacaria, E., Franchitto, A., & Pichierri, P. (2017a). SLX4 prevents GEN1-dependent DSBs during DNA replication arrest under pathological conditions in human cells. *Scientific Reports*, *7*(March), 1–14. <http://doi.org/10.1038/srep44464>
- Mankouri, H. W., Huttner, D., & Hickson, I. D. (2013). How unfinished business from S-phase affects mitosis and beyond. *The EMBO Journal*, *32*(20), 2661–71. <http://doi.org/10.1038/emboj.2013.211>

Matos, J., Blanco, M. G., Maslen, S., Skehel, J. M., & West, S. C. (2011a). Regulatory control of the resolution of DNA recombination intermediates during meiosis and mitosis. *Cell*, *147*(1), 158–172. <http://doi.org/10.1016/j.cell.2011.08.032>

Matos, J., Blanco, M. G., & West, S. C. (2013a). Cell-cycle kinases coordinate the resolution of recombination intermediates with chromosome segregation. *Cell Reports*, *4*(1), 76–86. <http://doi.org/10.1016/j.celrep.2013.05.039>

Matos, J., & West, S. C. (2014). Holliday junction resolution: regulation in space and time. *DNA Repair*, *19*, 176–81. <http://doi.org/10.1016/j.dnarep.2014.03.013>

Meggio, F., & Pinna, L. a. (2003). One-thousand-and-one substrates of protein kinase CK2? *The FASEB Journal : Official Publication of the Federation of American Societies for Experimental Biology*, *17*(3), 349–368. <http://doi.org/10.1096/fj.02-0473rev>

Mehta, A., & Haber, J. E. (2014). Sources of DNA Double-Strand Breaks and Models of Rec. *Cold Spring Harbor Perspectives in*

Biology, 6, 1–19. <http://doi.org/10.1101/cshperspect.a016428>

Minocherhomji, S., & Hickson, I. D. (2014). Structure-specific endonucleases: guardians of fragile site stability. *Trends in Cell Biology*, 24(5), 321–327. <http://doi.org/10.1016/j.tcb.2013.11.007>

Minocherhomji, S., Ying, S., Bjerregaard, V. A., Bursomanno, S., Aleliunaite, A., Wu, W., ... Hickson, I. D. (2015c). Replication stress activates DNA repair synthesis in mitosis. *Nature*, 528(7581), 286–290. <http://doi.org/10.1038/nature16139>

Miotto, B., Chibi, M., Xie, P., Koundrioukoff, S., Moolman-Smook, H., Pugh, D., Defossez, P. A. (2014). The RBBP6/ZBTB38/MCM10 Axis Regulates DNA Replication and Common Fragile Site Stability. *Cell Reports*, 7(2), 575–587. <http://doi.org/10.1016/j.celrep.2014.03.030>

Mondal, G., Rowley, M., Guidugli, L., Wu, J., Pankratz, V. S., & Couch, F. J. (2012). BRCA2 localization to the midbody by Filamin A regulates CEP55 signaling and completion of cytokinesis. *Developmental Cell*, 23(1), 137–152.

<http://doi.org/10.1016/j.devcel.2012.05.008.BRCA2>

Mullen, J. R., Kaliraman, V., Ibrahim, S. S., & Brill, S. J. (2001).

Requirement for three novel protein complexes in the absence of the Sgs1 DNA helicase in *Saccharomyces cerevisiae*.

Genetics, 157(1), 103–118.

Muñoz, I. M., Hain, K., Déclais, A. C., Gardiner, M., Toh, G. W.,

Sanchez-Pulido, L., ... Rouse, J. (2009). Coordination of Structure-Specific Nucleases by Human SLX4/BTBD12 Is Required for DNA Repair. *Molecular Cell*, 35(1), 116–127.

<http://doi.org/10.1016/j.molcel.2009.06.020>

Murai, J., Huang, S. N., Das, B. B., Renaud, A., Zhang, Y.,

Doroshov, J. H., ... Pommier, Y. (2012). Differential trapping of PARP1 and PARP2 by clinical PARP inhibitors. *Cancer Research*, 72(21), 5588–5599. <http://doi.org/10.1158/0008-5472.CAN-12-2753>. Differential

Differential

Murfuni, I., Basile, G., Subramanyam, S., Malacaria, E., Bignami,

M., Spies, M., Pichierri, P. (2013a). Survival of the Replication Checkpoint Deficient Cells Requires MUS81-RAD52 Function,

9(10). <http://doi.org/10.1371/journal.pgen.1003910>

Murfuni, I., Nicolai, S., Baldari, S., Crescenzi, M., Bignami, M., Franchitto, a, & Pichierri, P. (2012). The WRN and MUS81 proteins limit cell death and genome instability following oncogene activation. *Oncogene*, 32(5), 610–620.
<http://doi.org/10.1038/onc.2012.80>

Müge Öğrünç and Aziz Sancar. (2003). Identification and Characterization of Human MUS81-MMS4 Structure Specific Endonuclease. *Journal of Biological Chemistry*, 278(919), 1–21.

Naim, V., Wilhelm, T., Debatisse, M., & Rosselli, F. (2013). ERCC1 and MUS81-EME1 promote sister chromatid separation by processing late replication intermediates at common fragile sites during mitosis. *Nature Cell Biology*, 15(8), 1008–15.
<http://doi.org/10.1038/ncb2793>

Nair, N., Castor, D., Macartney, T., & Rouse, J. (2014). Identification and characterization of MUS81 point mutations that abolish interaction with the SLX4 scaffold protein. *DNA*

Repair, 24, 131–137.

<http://doi.org/10.1016/j.dnarep.2014.08.004>

Newman, M., Murray-Rust, J., Lally, J., Rudolf, J., Fadden, A., Knowles, P. P., ... McDonald, N. Q. (2005). Structure of an XPF endonuclease with and without DNA suggests a model for substrate recognition. *The EMBO Journal*, 24(5), 895–905.

<http://doi.org/10.1038/sj.emboj.7600581>

Ohouo, P. Y., Bastos de Oliveira, F. M., Almeida, B. S., & Smolka, M. B. (2010). DNA damage signaling recruits the Rtt107-Slx4 scaffolds via Dpb11 to Mediate replication stress response. *Molecular Cell*, 39(2), 300–306.

<http://doi.org/10.1016/j.molcel.2010.06.019>

Ölmezer, G., Levikova, M., Klein, D., Falquet, B., Fontana, G. A., Cejka, P., & Rass, U. (2016). Replication intermediates that escape Dna2 activity are processed by Holliday junction resolvase Yen1. *Nature Communications*, 7.

<http://doi.org/10.1038/ncomms13157>

Osman, F., & Whitby, M. C. (2007). Exploring the roles of Mus81-

Eme1/Mms4 at perturbed replication forks. *DNA Repair*, 6, 1004–1017. <http://doi.org/10.1016/j.dnarep.2007.02.019>

Özer, Ö., & Hickson, I. D. (2018). Pathways for maintenance of telomeres and common fragile sites during DNA replication stress. *Open Biology*, 8(4), 180018. <http://doi.org/10.1098/rsob.180018>

Palma, A., Pugliese, G. M., Murfunì, I., Marabitti, V., Malacaria, E., Rinalducci, S., Sanchez, M., Zolla, L., Franchitto, A., Pichierri, P. (2018). Phosphorylation by CK2 regulates MUS81/EME1 in mitosis and after replication stress. *Nucleic Acids Research*, (April), 1–16. <http://doi.org/10.1093/nar/gky280>

Patel, K. J., Yu, V. P. C. C., Lee, H., Corcoran, A., Thistlethwaite, F. C., Evans, M. J., Venkitaraman, A. R. (1998). Involvement of Brca2 in DNA repair. *Molecular Cell*, 1(3), 347–357. [http://doi.org/10.1016/S1097-2765\(00\)80035-0](http://doi.org/10.1016/S1097-2765(00)80035-0)

Pepe, A., & West, S. C. (2014a). MUS81-EME2 promotes replication fork restart. *Cell Reports*, 7(4), 1048–55. <http://doi.org/10.1016/j.celrep.2014.04.007>

- Pepe, A., & West, S. C. (2014c). Substrate specificity of the MUS81-EME2 structure selective endonuclease. *Nucleic Acids Research*, *42*(6), 3833–45. <http://doi.org/10.1093/nar/gkt1333>
- Petermann, E., Orta, M. L., Issaeva, N., Schultz, N., & Helleday, T. (2010). Hydroxyurea-Stalled Replication Forks Become Progressively Inactivated and Require Two Different RAD51-Mediated Pathways for Restart and Repair. *Molecular Cell*, *37*, 492–502. <http://doi.org/10.1016/j.molcel.2010.01.021>
- Petr Cejka, Jody L. Plank, Csanad Z. Bachrati, Ian D. Hickson, and S. C. K. (2010). Rmi1 stimulates decatenation of double Holliday junctions during dissolution by Sgs1–Top3. *Nature Structural and Molecular Biology*, *17*(11), 29–39. <http://doi.org/10.1016/j.artmed.2015.09.007.Information>
- Pfander, B., & Matos, J. (2017a). Control of Mus81 nuclease during the cell cycle. *FEBS Letters*, *591*(14), 2048–2056. <http://doi.org/10.1002/1873-3468.12727>
- Pichierri, P., Franchitto, A., Mosesso, P., & Palitti, F. (2001). Werner’s syndrome protein is required for correct recovery

after replication arrest and DNA damage induced in S-phase of cell cycle. *Molecular Biology of the Cell*, 12(8), 2412–21.

<http://doi.org/10.1091/MBC.12.8.2412>

Polo, S., & Jackson, S. (2011). Dynamics of DNA damage response proteins at DNA breaks: a focus on protein modifications.

Genes & Development, 25(5), 409–33.

<http://doi.org/10.1101/gad.2021311.critical>

Princz, L. N., Gritenaite, D., & Pfander, B. (2015). The Slx4-Dpb11 scaffold complex: Coordinating the response to replication fork stalling in S-phase and the subsequent mitosis. *Cell Cycle*,

14(4), 488–494. <http://doi.org/10.4161/15384101.2014.989126>

Princz, L. N., Wild, P., Bittmann, J., Aguado, F. J., Blanco, M. G.,

Pfander, B., & Matos, J. (2017). Dbf 4 -dependent kinase and the Rtt 107 scaffold promote Mus 81 -Mms 4 resolvase

activation during mitosis, 36(5), 664–678.

<http://doi.org/10.15252/embj.201694831>

Pujade-Lauraine, E., Ledermann, J. A., Selle, F., GebSKI, V., Penson,

R. T., Oza, A. M., Vergote, I. (2017). Olaparib tablets as

maintenance therapy in patients with platinum-sensitive, relapsed ovarian cancer and a *BRCA1/2* mutation (SOLO2/ENGOT-Ov21): a double-blind, randomised, placebo-controlled, phase 3 trial. *The Lancet Oncology*, 18(9), 1274–1284. [http://doi.org/10.1016/S1470-2045\(17\)30469-2](http://doi.org/10.1016/S1470-2045(17)30469-2)

Raghunandan, M., Chaudhury, I., Kelich, S. L., Hanenberg, H., & Sobeck, A. (2015). FANCD2, FANCI and BRCA2 cooperate to promote replication fork recovery independently of the Fanconi Anemia core complex. *Cell Cycle*, 14(3), 342–353. <http://doi.org/10.4161/15384101.2014.987614>

Regairaz, M., Zhang, Y. W., Fu, H., Agama, K. K., Tata, N., Agrawal, S., Pommier, Y. (2011). Mus81-mediated DNA cleavage resolves replication forks stalled by topoisomerase I-DNA complexes. *Journal of Cell Biology*, 195(5), 739–749. <http://doi.org/10.1083/jcb.201104003>

Rondinelli, B., Gogola, E., Yücel, H., Duarte, A. A., Van De Ven, M., Van Der Sluijs, R., D’Andrea, A. D. (2017). EZH2 promotes degradation of stalled replication forks by recruiting

MUS81 through histone H3 trimethylation. *Nature Cell Biology*, 19(11), 1371–1378. <http://doi.org/10.1038/ncb3626>

Rowlands, H., Dhavarasa, P., Cheng, A., & Yankulov, K. (2017). Forks on the run: Can the stalling of DNA replication promote epigenetic changes? *Frontiers in Genetics*, 8(JUN), 1–15. <http://doi.org/10.3389/fgene.2017.00086>

Roy, R., Chun, J., & Powell, S. N. (2016). BRCA1 and BRCA2: different roles in a common pathway of genome protection. *Nat Rev Cancer*, 12(1), 68–78. <http://doi.org/10.1038/nrc3181>.BRCA1

Ruzzene, M., & Pinna, L. A. (2010). Addiction to protein kinase CK2: A common denominator of diverse cancer cells? *Biochimica et Biophysica Acta - Proteins and Proteomics*, 1804(3), 499–504. <http://doi.org/10.1016/j.bbapap.2009.07.018>

Saintigny, Y., Makienko, K., Swanson, C., Emond, J., Monnat, R. J., & Emond, M. J. (2002). Homologous Recombination Resolution Defect in Werner Syndrome Homologous Recombination Resolution Defect in Werner Syndrome.

Molecular and Cellular Biology, 22(20), 6971–6978.

<http://doi.org/10.1128/MCB.22.20.6971>

Sarbajna, S., Davies, D., & West, S. C. (2014). Roles of SLX1-SLX4, MUS81-EME1, and GEN1 in avoiding genome instability and mitotic catastrophe. *Genes and Development*, 28, 1124–1136. <http://doi.org/10.1101/gad.238303.114>

Sarbajna, S., & West, S. C. (2014). Holliday junction processing enzymes as guardians of genome stability. *Trends in Biochemical Sciences*, 39(9), 409–419. <http://doi.org/10.1016/j.tibs.2014.07.003>

Schlacher, K. (2011). Double-Strand Break Repair Independent Role For BRCA2 In Blocking Stalled Replication Fork Degradation By MRE11. *Cell*, 145(4), 529–542. <http://doi.org/10.1016/j.cell.2011.03.041>. Double-Strand

Schwartz, E. K., Wright, W. D., Ehmsen, K. T., Evans, J. E., Stahlberg, H., & Heyer, W.-D. (2012). Mus81-Mms4 Functions as a Single Heterodimer To Cleave Nicked Intermediates in Recombinational DNA Repair. *Molecular and Cellular*

Biology, 32(15), 3065–3080.

<http://doi.org/10.1128/MCB.00547-12>

Scalfani, R. A., & Holzen, T. M. (2007). Cell Cycle Regulation of DNA Replication. *Annual Review of Genetics*, 41(1), 237–280.

<http://doi.org/10.1146/annurev.genet.41.110306.130308>

Segurado, M., & Diffley, J. (2008). Separate roles for the DNA damage checkpoint protein kinases in stabilizing DNA replication forks. *Genes & Development*, 1816–1827.

<http://doi.org/10.1101/gad.477208.tion>

Atsushi, S., Moiani, D., Arvai, A. S., Jefferson S.P., Perry, S. M., Harding, Genoio, M., Maity, R., Van Rossum-Fikkert, S., Kertokalio, A., Romoli, F., Ismail, A., Ismalaj, E., Petricci, E., Matthew, J. N., Robe and J. A. T. (2014). DNA Double Strand Break Repair Pathway Choice Is Directed by Distinct MRE11 Nuclease Activities. *Molecular Cell*, 53(1), 7–18.

<http://doi.org/10.1016/j.molcel.2013.11.003.DNA>

Shimura, T., Torres, M. J., Martin, M. M., Rao, V. A., Katsura, M., Miyagawa, K., & Aladjem, M. I. (2008). Bloom's syndrome

helicase and Mus81 are required to induce transient double-strand DNA breaks in response to DNA replication stress, *375*(4), 1152–1164.

<http://doi.org/10.1016/j.jmb.2007.11.006>.Bloom

Simsek, D., Brunet, E., Wong, S. Y. W., Katyal, S., Gao, Y., McKinnon, P. J., Jasin, M. (2011). DNA ligase III promotes alternative nonhomologous end-joining during chromosomal translocation formation. *PLoS Genetics*, *7*(6), 1–11.

<http://doi.org/10.1371/journal.pgen.1002080>

Sogo, J. M., Lopes, M., & Foiani, M. (2002). Fork reversal and ssDNA accumulation at stalled replication forks owing to checkpoint defects. *Science*, *297*(5581), 599–602.

<http://doi.org/10.1126/science.1074023>

Sotiriou, S. K., Kamileri, I., Lugli, N., Evangelou, K., Da-Ré, C., Huber, F., Halazonetis, T. D. (2016). Mammalian RAD52 Functions in Break-Induced Replication Repair of Collapsed DNA Replication Forks. *Molecular Cell*, *64*(6), 1127–1134.

<http://doi.org/10.1016/j.molcel.2016.10.038>

- Spycher, C., Miller, E. S., Townsend, K., Pavic, L., Morrice, N. A., Janscak, P., Stucki, M. (2008). Constitutive phosphorylation of MDC1 physically links the MRE11-RAD50-NBS1 complex to damaged chromatin. *Journal of Cell Biology*, 181(2), 227–240.
<http://doi.org/10.1083/jcb.200709008>
- Stracker T. H. and Petrini J. H. J. (2011). The MRE11 complex: starting from the ends. *Nature Reviews. Molecular Cell Biology*, 12(12), 1385–1395.
<http://doi.org/10.2217/nmm.12.167>.Gene
- Strauss, B., Harrison, A., Coelho, P. A., Yata, K., Zernicka-Goetz, M., & Pines, J. (2018). Cyclin B1 is essential for mitosis in mouse embryos, and its nuclear export sets the time for mitosis. *Journal of Cell Biology*, 217(1), 179–193.
<http://doi.org/10.1083/jcb.201612147>
- Svendsen, J. M., Smogorzewska, A., Sowa, M. E., Connell, B. C. O., Gygi, S. P., Elledge, S. J., & Harper, J. W. (2010a). NIH Public Access. *DNA Repair*, 138(1), 63–77.
<http://doi.org/10.1016/j.cell.2009.06.030>.Mammalian

- Symington, L. S. (2014). End Resection at Double-Strand Breaks: Mechanism and Regulation Lorraine. *Microbiological Reviews*, 52(June), 291–315.
- Szakai, B., & Branzei, D. (2013). Premature Cdk1/Cdc5/Mus81 pathway activation induces aberrant replication and deleterious crossover. *EMBO Journal*, 32(8), 1155–1167.
<http://doi.org/10.1038/emboj.2013.67>
- Taglialatela, A., Alvarez, S., Leuzzi, G., Sannino, V., Ranjha, L., Huang, J. W., Ciccina, A. (2017). Restoration of Replication Fork Stability in BRCA1- and BRCA2-Deficient Cells by Inactivation of SNF2-Family Fork Remodelers. *Molecular Cell*, 68(2), 414–430.e8. <http://doi.org/10.1016/j.molcel.2017.09.036>
- Técher, H., Koundrioukoff, S., Carignon, S., Wilhelm, T., Millot, G. A., Lopez, B. S., Debatisse, M. (2016). Signaling from Mus81-Eme2-Dependent DNA Damage Elicited by Chk1 Deficiency Modulates Replication Fork Speed and Origin Usage. *Cell Reports*, 1–14. <http://doi.org/10.1016/j.celrep.2015.12.093>
- Van, C., Yan, S., Michael, W. M., Waga, S., & Cimprich, K. A.

(2010). Continued primer synthesis at stalled replication forks contributes to checkpoint activation. *Journal of Cell Biology*, *189*(2), 233–246. <http://doi.org/10.1083/jcb.200909105>

Wehrkamp-Richter, S., Hyppa, R. W., Prudden, J., Smith, G. R., & Boddy, M. N. (2012). Meiotic DNA joint molecule resolution depends on Nse5-Nse6 of the Smc5-Smc6 holocomplex. *Nucleic Acids Research*, *40*(19), 9633–9646. <http://doi.org/10.1093/nar/gks713>

West, S. C., Blanco, M. G., Chan, Y. W., Matos, J., Sarbajna, S., & Wyatt, H. D. M. (2016). Resolution of recombination intermediates: Mechanisms and regulation. *Cold Spring Harbor Symposia on Quantitative Biology*, *80*, 103–109. <http://doi.org/10.1101/sqb.2015.80.027649>

Whitby, M. C., Osman, F., & Dixon, J. (2003). Cleavage of model replication forks by fission yeast Mus81-Eme1 and budding yeast Mus81-Mms4. *Journal of Biological Chemistry*, *278*(9), 6928–6935. <http://doi.org/10.1074/jbc.M210006200>

Wild, P., & Matos, J. (2016). Cell cycle control of DNA joint

molecule resolution. *Current Opinion in Cell Biology*, 40, 74–80. <http://doi.org/10.1016/j.ceb.2016.02.018>

Williams, R. S., Moncalian, G., Williams, J. S., Yamada, Y., Limbo, O., Shin, D. S., John, A. (2008). Mre11 Dimers Coordinate DNA End Bridging and Nuclease Processing in Double-Strand-Break Repair. *October*, 135(1), 97–109. <http://doi.org/10.1016/j.cell.2008.08.017>.Mre11

Woodward, A. M., Göhler, T., Luciani, M. G., Oehlmann, M., Ge, X., Gartner, A., Blow, J. J. (2006). Excess Mcm2-7 license dormant origins of replication that can be used under conditions of replicative stress. *Journal of Cell Biology*, 173(5), 673–683. <http://doi.org/10.1083/jcb.200602108>

Wyatt, H. D. M., Laister, R. C., Martin, S. R., Arrowsmith, C. H., & West, S. C. (2017). The SMX DNA Repair Tri-nuclease. *Molecular Cell*, 65(5), 848–860.e11. <http://doi.org/10.1016/j.molcel.2017.01.031>

Wyatt, H. D. M., Sarbajna, S., Matos, J., & West, S. C. (2013). Coordinated actions of SLX1-SLX4 and MUS81-EME1 for

holliday junction resolution in human cells. *Molecular Cell*, 52(2), 234–247. <http://doi.org/10.1016/j.molcel.2013.08.035>

Wyatt, H. D. M., & West, S. C. (2017). SMX makes the cut in genome stability. *Oncotarget*, 8(61), 102765–102766. <http://doi.org/10.18632/oncotarget.22420>

Yang, Y., Xie, Y., & Xian, L. (2013). Breast cancer susceptibility gene 1 (BRCA1) predict clinical outcome in platinum- and taxal-based chemotherapy in non-small-cell lung cancer (NSCLC) patients: a system review and meta-analysis. *Journal of Experimental & Clinical Cancer Research*, 32(1), 15. <http://doi.org/10.1186/1756-9966-32-15>

Yata, K., Lloyd, J., Maslen, S., Bleuyard, J. Y., Skehel, M., Smerdon, S. J., & Esashi, F. (2012). Plk1 and CK2 Act in Concert to Regulate Rad51 during DNA Double Strand Break Repair. *Molecular Cell*, 45(3), 371–383. <http://doi.org/10.1016/j.molcel.2011.12.028>

Yde, C. W., Olsen, B. B., Meek, D., Watanabe, N., & Guerra, B. (2008). The regulatory beta-subunit of protein kinase CK2

regulates cell-cycle progression at the onset of mitosis.

Oncogene, 27(37), 4986–4997.

<http://doi.org/10.1038/onc.2008.146>

Ying, S., Hamdy, F. C., & Helleday, T. (2012). Mre11-dependent degradation of stalled DNA replication forks is prevented by BRCA2 and PARP1. *Cancer Research*, 72(11), 2814–2821. <http://doi.org/10.1158/0008-5472.CAN-11-3417>

Ying, S., Minocherhomji, S., Chan, K. L., Palmai-Pallag, T., Chu, W. K., Wass, T., Hickson, I. D. (2013a). MUS81 promotes common fragile site expression. *Nature Cell Biology*, 15(8), 1001–7. <http://doi.org/10.1038/ncb2773>

Yu, V. P. C. C., Koehler, M., Steinlein, C., Schmid, M., Hanakahi, L. A., Van Gool, A. J., Venkitaraman, A. R. (2000). Gross chromosomal rearrangements and genetic exchange between nonhomologous chromosomes following BRCA2 inactivation. *Genes and Development*, 14(11), 1400–1406. <http://doi.org/10.1101/gad.14.11.1400>

Zeman, M. K., & Cimprich, K. A. (2014). Causes and consequences

of replication stress. *Nature Cell Biology*, 16(1).

Zhang, B. N., Bueno Venegas, A., Hickson, I. D., & Chu, W. K. (2018). DNA replication stress and its impact on chromosome segregation and tumorigenesis. *Seminars in Cancer Biology*, (April), 0–1. <http://doi.org/10.1016/j.semcancer.2018.04.005>

Zhang R., Sagar S., Qin Y., Steven P. L., Nozomu Y., Bradsher J., Blais, V., McGowan, C. H., and C. C. H. (2005). BLM Helicase Facilitates Mus81 Endonuclease Activity in Human Cells. *Cancer Research*, 65(7), 2526–2531. <http://doi.org/10.1158/0008-5472.CAN-04-2421>

Zhu, W., Ukomadu, C., Jha, S., Senga, T., Dhar, S. K., Wohlschlegel, J. and Dutta, A. (2007). Mcm10 and And-1 / CTF4 recruit DNA polymerase α to chromatin for initiation of DNA replication. *Genes & Development*, 2288–2299. <http://doi.org/10.1101/gad.1585607.Mcm10>

